

UC Davis

Research reports

Title

Development of Performance-Based Specifications for Asphalt Rubber Binder: Phase 2g
Additional Testing of Five Plant-Sampled Binders and RHMA G Mixes

Permalink

<https://escholarship.org/uc/item/1qb0924p>

Authors

Jones, David
Rizvi, Hashim
Brotschi, Julian

Publication Date

2023

DOI

10.7922/G2QF8R64

Development of Performance-Based Specifications for Asphalt Rubber Binder: Phase 2g Additional Testing of Five Plant-Sampled Binders and RHMA-G Mixes

Authors:

David Jones, Hashim Rizvi, and Julian Brotschi

California Department of Resources, Recycling and Recovery:
Characterization of Rubberized Binders for Performance Grade and Rubber Content

PREPARED FOR:

California Department of Resources, Recycling & Recovery
1001 I St.
Sacramento, CA, 95814

PREPARED BY:

University of California
Pavement Research Center
UC Davis and UC Berkeley



TECHNICAL REPORT DOCUMENTATION PAGE

1. REPORT NUMBER UCPRC-RR-2020-08	2. GOVERNMENT ASSOCIATION NUMBER	3. RECIPIENT'S CATALOG NUMBER
4. TITLE AND SUBTITLE Development of Performance-Based Specifications for Asphalt Rubber Binder: Phase 2g Testing of Five Plant-Sampled Binders and RHMA-G Mixes		5. REPORT PUBLICATION DATE January 2023
		6. PERFORMING ORGANIZATION CODE
7. AUTHOR(S) David Jones (ORCID 0000-0002-2938-076X) Hashim Rizvi (ORCID 0000-0002-2529-0724) Julian Brotschi (ORCID 0000-0002-1752-2898)		8. PERFORMING ORGANIZATION REPORT NO. UCPRC-RR-2020-08 UCD-ITS-RR-20-110
		10. WORK UNIT NUMBER
9. PERFORMING ORGANIZATION NAME AND ADDRESS University of California Pavement Research Center Department of Civil and Environmental Engineering, UC Davis 1 Shields Avenue Davis, CA 95616		11. CONTRACT OR GRANT NUMBER DRR16145
		13. TYPE OF REPORT AND PERIOD COVERED Research Report
12. SPONSORING AGENCY AND ADDRESS California Department of Resources, Recycling and Recovery 1001 I St Sacramento, CA 95814		14. SPONSORING AGENCY CODE
15. SUPPLEMENTAL NOTES doi:10.7922/G2QF8R64		
16. ABSTRACT <p>The work discussed in this interim report is part of a larger study, funded by the California Department of Transportation, with the objective of developing and recommending testing procedures and criteria for performance-based specifications of asphalt rubber binders used in gap-graded and open-graded mixes using current Superpave performance grade (PG) equipment. Work covered the testing of five plant-produced binders, the base binders used to produce them, and the gap-graded rubberized hot mix asphalt mixes produced with them. The following important observations from the binder rheology tests were made:</p> <ul style="list-style-type: none"> • Although the low-temperature performance grades appeared to be reasonable, the high-temperature grades appeared to be unrealistically high, while the intermediate-temperature grades appeared to be potentially lower than anticipated when compared to the base binders. • A comparison of the concentric cylinder and parallel plate (3 mm gap) geometries indicated that the results between the two geometries are different and are likely to be higher than the precision and bias of the individual procedures. Precision and bias statements for these procedures had not been developed at the time of preparing this report. • Consistent trends in results were observed between high-temperature PG/true grade, ΔT_C, and non-recoverable creep compliance at 3.2 kPa. • Observations from previous testing and during this phase of the study indicated that incompletely digested rubber particles—which have different sensitivities to temperature, aging, and applied stress and strain than the base asphalt binder—appeared to have a dominant influence on results and caused variability between results, regardless of the testing geometry used. Considering these incompletely digested particles as part of a homogenous binder may therefore not be appropriate when determining performance grades. Work is continuing in Phase 3 of this study to adjust testing procedures to account for the influence that these incompletely digested particles have on results. <p>The proposed modifications to short- and long-term aging procedures (i.e., rolling thin film oven and pressure aging vessel) and to the bending beam rheometer specimen preparation procedures developed in Phase 2 are considered to be more aligned with the original intent of the tests and will likely reduce the variability between replicate specimens during testing.</p> <p>Preliminary test results indicate that Fourier transformed infrared spectroscopy is a potentially valid method for quantifying rubber content in rubber-modified binders.</p>		
17. KEYWORDS asphalt rubber binder, AR binder, performance grade		18. DISTRIBUTION STATEMENT No restrictions. This document is available to the public through the National Technical Information Service, Springfield, VA 22161
19. SECURITY CLASSIFICATION (of this report) Unclassified	20. NUMBER OF PAGES 110	21. PRICE None


Reproduction of completed page authorized

UCPRC ADDITIONAL INFORMATION

1. DRAFT STAGE Final	2. VERSION NUMBER 1
3. PARTNERED PAVEMENT RESEARCH CENTER STRATEGIC PLAN ELEMENT NUMBER CR-AR Binder	4. CALRECYCLE TASK NUMBER DRR16145
5. CALRECYCLE TECHNICAL LEAD AND REVIEWER(S) Nathan Gauff	6. FHWA NUMBER N/A
7. PROPOSALS FOR IMPLEMENTATION None	

8. RELATED DOCUMENTS None

9. VERSION UPDATES None

10. LABORATORY ACCREDITATION The UCPRC laboratory is accredited by AASHTO re:source for the tests listed in this report	
--	---

11. SIGNATURES					
D. Jones FIRST AUTHOR	J.T. Harvey TECHNICAL REVIEW	C. Fink EDITOR	J.T. Harvey PRINCIPAL INVESTIGATOR	N. Gauff CALRECYCLE TECH. LEAD	N. Gauff CALRECYCLE CONTRACT MANAGER

Reproduction of completed page authorized

DISCLAIMER STATEMENT

This document is disseminated in the interest of information exchange. The contents of this report reflect the views of the authors who are responsible for the facts and accuracy of the data presented herein. The contents do not necessarily reflect the official views or policies of the State of California or the Federal Highway Administration. This publication does not constitute a standard, specification, or regulation. This report does not constitute an endorsement by the Department of any product described herein.

PROJECT OBJECTIVES

The work discussed in this report is part of a larger study, funded by the California Department of Transportation, with the objective of developing and recommending testing procedures and criteria for performance-based specifications of asphalt rubber binders. This objective will be achieved through completion of the following tasks:

1. Evaluate the rheological properties of laboratory- and plant-produced asphalt rubber binders at high and intermediate temperatures using both parallel plate and concentric cylinder geometries.
2. Evaluate and refine short- and long-term aging procedures for asphalt rubber binders.
3. Evaluate low-temperature rheological properties of asphalt rubber binders.
4. Evaluate the relationship between the rheological properties of asphalt rubber binders and mix performance in terms of rutting, fatigue cracking, and low-temperature cracking.
5. Recommend performance-related specification criteria for asphalt rubber binders.

This report provides the results of testing five plant-produced binders and the gap-graded rubberized hot mix asphalt mixes produced with them, as part of Task 4.

ACKNOWLEDGEMENTS

The University of California Pavement Research Center acknowledges the following individuals and organizations who contributed to the project:

- Nathan Gauff and William Heung, CalRecycle
- The California Department of Transportation
- The UCPRC laboratory operations team

EXECUTIVE SUMMARY

Introduction

The work discussed in this interim report is part of a larger study, funded by the California Department of Transportation (Caltrans), with the objective of developing and recommending testing procedures and criteria for performance-based specifications of asphalt rubber binders used in gap-graded and open-graded mixes using current Superpave performance grade (PG) equipment. Work covered the testing of five plant-produced binders and the gap-graded rubberized hot mix asphalt mixes produced with them.

Testing Summary

Rheology Testing

Rheology testing to determine the high-, intermediate-, and low-temperature performance grades and multiple stress creep recovery (MSCR) of five plant-produced asphalt rubber binders using the testing procedures developed in Phase 2 of a comprehensive study for Caltrans on the development of performance-based specifications for asphalt rubber binder was undertaken to test the procedures. The following important observations from the tests were made:

- Testing in this phase of the study provided results that were consistent with those obtained during preliminary testing in Phase 2e of the larger study.
- Although the low-temperature performance grades appeared to be reasonable, the high-temperature grades appeared to be unrealistically high, while the intermediate-temperature grades appeared to be potentially lower than anticipated, when compared to the base binders.
- A comparison of the concentric cylinder and parallel plate (3 mm gap) geometries indicated that the results between the two geometries are different and are likely to be higher than the precision and bias of the individual procedures. Precision and bias statements for these procedures had not been developed at the time of preparing this report.
- Consistent trends in results were observed between high temperature PG/true grade, Delta T_C , and non-recoverable creep compliance at 3.2 kPa.
- Observations in Phase 2e and during this phase of the study indicated that incompletely digested rubber particles appeared to have a dominant influence on results and caused variability between results, regardless of the testing geometry used. Considering these incompletely digested particles as part of a homogenous binder may therefore not be appropriate when determining performance grades.

Mix Testing

Mix testing was undertaken to assess rutting and cracking performance in relation to performance grading to determine whether the rheology testing approaches provide properties that are representative of likely field performance. A comparison of binder and mix test results did not show any consistent trends across all five binders. However, the following trends between some results were observed:

- Rutting test result rankings (flow number and cycles to 5% permanent axial strain) were consistent with the binder high temperature PG result rankings.
- Flexibility index rankings (highest to lowest) were consistent with Delta T_c (lowest to highest) and non-recoverable creep compliance (highest to lowest). Flexibility index results (highest to lowest) also corresponded with mix rutting results (lowest to highest) as expected (i.e., cracking and rutting results are opposite).
- Beam fatigue rankings did not match any binder testing rankings. However, excluding the binder and mix results from one “outlier,” the mix fatigue life and binder m-value rankings were the same for the other four binders/mixes.

Rubber Content Determination

Limited exploratory testing was conducted to assess the use of Fourier-transform infrared (FTIR) spectroscopy to determine rubber content in rubber modified binders. One base binder with eight different crumb rubber modifier (CRM) contents, ranging from 2.5% to 35% by weight of the base binder, were tested in unaged and PAV-aged condition. Extender oil alone and base binder modified with extender oil only were also tested to determine the potential influence of extender oil on the results. A known styrene-butadiene rubber (SBR, 75% butadiene and 25% styrene) signature was used to identify the presence of CRM.

In both aging conditions, the SBR signature values increased with increasing rubber dosage. Values for the PAV-aged binders were notably higher than those for the unaged binders, indicating that aging will influence values over time. The results indicate that FTIR is a potentially valid method for quantifying rubber content in rubber modified binders.

Conclusions

Incompletely digested rubber particles—which have different sensitivities to temperature, aging, and applied stress and strain than the base asphalt binder—appear to dominate the binder rheology test results, leading to what appears to be unrealistic performance grades. Work is

continuing in Phase 3 of this study to adjust testing procedures to account for the influence that these incompletely digested particles have on results.

The proposed modifications to short- and long-term aging procedures (i.e., rolling thin film oven and pressure aging vessel) and to the BBR specimen preparation procedures developed in Phase 2 are considered to be more aligned with the original intent of the tests and will likely reduce the variability between replicate specimens during testing.

Recommendations

No recommendations for implementation are warranted at this stage of the study. Phase 3 is investigating the extent to which incompletely digested rubber particles might affect performance grading results along with testing procedures to overcome the problems. This phase is focusing on removal of larger incompletely digested particles from the binder by sieving or centrifuging and then testing the binders following standard performance grading procedures using parallel plate geometry with either 1 mm or 2 mm gaps. Results after removal of particles larger than 250, 500, and 850 μm are being compared with unprocessed binders tested with concentric cylinder and parallel plate with 3 mm gap geometries. The five asphalt rubber binders tested in this phase of the study are being retested in Phase 3 to assess the removal of larger incompletely digested rubber particles on performance grades.

Blank page

TABLE OF CONTENTS

EXECUTIVE SUMMARY	v
LIST OF TABLES	xi
LIST OF FIGURES	xi
LIST OF ABBREVIATIONS	xiii
TEST METHODS CITED IN THE TEXT	xv
CONVERSION FACTORS	xvii
1. INTRODUCTION	1
1.1 Background	1
1.1.1 Use of Rubberized Asphalt Concrete	1
1.1.2 Production of Rubber-Modified Binders.....	1
1.1.3 Crumb Rubber Modifier Production	2
1.1.4 Current Caltrans Asphalt Rubber Binder Specifications	3
1.2 Problem Statements	4
1.3 Project Objectives	6
1.4 Measurement Units	9
2. SUMMARY OF PHASE 2 RESEARCH	11
2.1 Introduction	11
2.2 Phase 1: DSR Testing Geometries.....	11
2.3 Phase 2a: Short- and Long-Term Aging Procedures	12
2.4 Phase 2b: Bending Beam Rheometer Specimen Preparation Procedures.....	15
2.5 Phase 2c: Intermediate-Temperature Testing.....	15
2.6 Phase 2d: Multiple Stress Creep Recovery Testing.....	15
2.7 Phase 2e: Rheology Testing on Plant-Produced Binders	16
2.8 Phase 2f: Performance Testing on Plant-Produced Mixes.....	18
2.9 Conclusions	19
2.10 Recommendations	19
3. TESTING PLANS	21
3.1 Introduction	21
3.2 Base Binder Testing.....	21
3.3 Asphalt Rubber Binder Testing.....	21
3.3.1 Crumb Rubber Particle Size Distribution.....	21
3.3.2 Rheology Testing	21
3.4 RHMA-G Mix Testing	22
3.4.1 Performance Testing Specimen Preparation	23
3.4.2 Mix Testing Details	23
4. BINDER TESTING	27
4.1 Introduction	27
4.2 Rubber Gradations	27
4.3 High-Temperature Testing	27
4.3.1 Base Binders	28
4.3.2 Asphalt Rubber Binders	28
4.4 Intermediate Temperature Testing.....	32

4.4.1	Base Binders	33
4.4.2	Asphalt Rubber Binders	33
4.5	Low-Temperature Testing	36
4.5.1	Base Binders	36
4.5.2	Asphalt Rubber Binders	37
4.6	Multiple Stress Creep Recovery Testing	41
4.6.1	Base Binders	41
4.6.2	Asphalt Rubber Binders	41
4.7	Discussion	43
5.	MIX TESTING	45
5.1	Introduction	45
5.2	Specimen Air-Void Contents	45
5.3	Mix Stiffness: AMPT Dynamic Modulus.....	46
5.4	Mix Stiffness: Flexural Modulus	46
5.5	Rutting Performance: Unconfined Repeated Load Triaxial	47
5.6	Cracking Performance: Four-Point Bending Beam Fatigue.....	49
5.7	Cracking Performance: Semicircular Bend	51
5.8	Discussion	52
6.	DETERMINATION OF RUBBER CONTENT IN ASPHALT RUBBER BINDERS	55
6.1	Introduction	55
6.2	Methodology.....	55
7.	CONCLUSIONS AND RECOMMENDATIONS	57
7.1	Introduction	57
7.2	Testing Summary.....	57
7.2.1	Rheology Testing	57
7.2.2	Mix Testing	58
7.2.3	Rubber Content Determination	58
7.3	Conclusions	58
7.4	Recommendations	59
	REFERENCES	61
	APPENDIX A: BINDER TEST RESULTS	63
	APPENDIX B: MIX TEST RESULTS	83

LIST OF TABLES

Table 1.1: Caltrans Specifications for Asphalt Rubber Binder Constituents	3
Table 1.2: Asphalt Rubber Binder Reaction Design Profile	4
Table 1.3: Caltrans Specifications for Asphalt Rubber Binder Quality Control and Acceptance	4
Table 3.1: Tests Performed on Plant-Produced Mixes	22
Table 4.1: Rubber Gradations Used in Plant-Produced Binders	27
Table 4.2: High-Temperature Grade and True Grade Results.....	27
Table 4.3: Intermediate-Temperature Grade and True Grade Results.....	33
Table 4.4: Low-Temperature Grade and True Grade Results	37
Table 4.5: Rankings of Select Binder Testing Results.....	44
Table 5.1: Dynamic Modulus Master Curve Parameters	46
Table 5.2: Flexural Modulus Master Curve Parameters	47
Table 5.3: Ranking of Cracking Test Results	52
Table 5.4: Rankings of Select Binder and Mix Testing Results.....	53

LIST OF FIGURES

Figure 1.1: Flowchart of project tasks/phases.....	8
Figure 4.1: Base binder high-temperature grade and true grade.....	29
Figure 4.2: Base binder unaged high-temperature.	29
Figure 4.3: Base binder RTFO-aged high-temperature.....	29
Figure 4.4: AR binder high-temperature grade and true grade.....	29
Figure 4.5: AR binder high temperature (unaged): Concentric cylinder.....	30
Figure 4.6: AR binder high temperature (unaged): Parallel plate.....	30
Figure 4.7: AR binder high temperature (RTFO-aged): Concentric cylinder.	30
Figure 4.8: AR binder high temperature (RTFO-aged): Parallel plate.	30
Figure 4.9: AR binder high temperature (unaged): Difference between DSR geometries.....	31
Figure 4.10: AR binder high temperature (RTFO-aged): Difference between DSR geometries. ...	31
Figure 4.11: AR binder high temperature (unaged): Difference in mid-point $G^*/\sin(\delta)$	31
Figure 4.12: AR binder high temperature (RTFO-aged): Difference in mid-point $G^*/\sin(\delta)$	31
Figure 4.13: Base binder intermediate-temperature performance grade and true grade.	34
Figure 4.14: Base binder intermediate temperature.....	34
Figure 4.15: AR binder intermediate-temperature performance grade and true grade.	34
Figure 4.16: AR binder intermediate temperature: Concentric cylinder.	35
Figure 4.17: AR binder intermediate temperature: Parallel plate.....	35
Figure 4.18: AR binder intermediate temperature: Difference between DSR geometries.....	35
Figure 4.19: AR binder intermediate temperature: Difference in mid-point $G^*\times\sin(\delta)$	35
Figure 4.20: Base binder: Low-temperature performance grade and true grade.	38
Figure 4.21: Base binder: Low-temperature stiffness.	38
Figure 4.22: Base binder: Low-temperature m-value.....	38
Figure 4.23: AR binder: Low-temperature performance grade and true grade.....	39
Figure 4.24: AR binder: Low-temperature stiffness.	39

Figure 4.25: AR binder: Low-temperature m-value.....	39
Figure 4.26: Delta T _c of base and asphalt rubber binders.	40
Figure 4.27: Base binder: Average percent recovery at 64°C.	42
Figure 4.28: Base binder: Non-recoverable creep compliance at 64°C.	42
Figure 4.29: AR binder: Average percent recovery at 64°C.	42
Figure 4.30: AR binder: Non-recoverable creep compliance at 64°C.	42
Figure 5.1: Specimen air-void contents.	45
Figure 5.2: Dynamic shear modulus master curves.....	46
Figure 5.3: Flexural dynamic modulus master curves.	47
Figure 5.4: Cumulative permanent axial strain versus number of cycles (52°C).....	48
Figure 5.5: Average flow number (52°C).	49
Figure 5.6: Number of cycles to 1, 3, and 5% permanent axial strain.	49
Figure 5.7: Fatigue regression models.....	50
Figure 5.8: Calculated fatigue life at 200, 300, 400, and 600 μstrain.	50
Figure 5.9: Semicircular bend fracture energy.	51
Figure 5.10: Semicircular bend flexibility index.....	51
Figure 6.1: Typical wave form of FTIR data and butadiene band location.....	55
Figure 6.2: Area under the curve calculation for the butadiene signature of AR binders.	56

LIST OF ABBREVIATIONS

AASHTO	American Association of State Highway and Transportation Officials
AMPT	Asphalt mix performance tester
AR	Asphalt rubber
ASTM	American Society for Testing and Materials
BBR	Bending beam rheometer
CalRecycle	California Department of Resources Recycling and Recovery
Caltrans	California Department of Transportation
CC	Concentric cylinder
CRM	Crumb rubber modifier
CT	Caltrans test
DGAC	Dense-graded asphalt concrete
DSR	Dynamic shear rheometer
E^*	Dynamic modulus
FI	Flexibility index
FTIR	Fourier Transformed Infrared Spectroscopy
G^*	Complex shear modulus
G_f	Fracture energy
Gmb	Bulk specific gravity
GTR	Ground tire rubber
HMA	Hot mix asphalt
J_{NR}	Non-recoverable creep compliance
LVDT	Linear variable displacement transducer
MSCR	Multiple stress creep recovery
PAV	Pressurized aging vessel
PG	Performance grade
PM	Polymer modified
PP	Parallel plate
RAC	Rubberized asphalt concrete
RAP	Recycled asphalt pavement
RHMA-G	Gap-graded rubberized hot mix asphalt
RHMA-O	Open-graded rubberized hot mix asphalt
RTFO	Rolling thin-film oven
SCB	Semicircular bend
SBR	Styrene-butadiene rubber
TR	Tire rubber modified
UCPRC	University of California Pavement Research Center
δ	Phase angle

Blank page

TEST METHODS CITED IN THE TEXT

AASHTO

- M 320 Standard Specification for Performance-Graded Asphalt Binder
- M 332 Standard Specification for Performance-Graded Asphalt Binder Using Multiple Stress Creep Recovery (MSCR) Test
- R 28 Standard Practice for Accelerated Aging of Asphalt Binder Using a Pressurized Aging Vessel (PAV)
- TP 124 Provisional Standard Method of Test for Determining the Fracture Potential of Asphalt Mixtures Using Semicircular Bend Geometry (SCB) at Intermediate Temperature
- T 166 Standard Method of Test for Bulk Specific Gravity (Gmb) of Compacted Hot Mix Asphalt (HMA) Using Saturated Surface-Dry Specimens
- T 240 Standard Method of Test for Effect of Heat and Air on a Moving Film of Asphalt (Rolling Thin-Film Oven Test)
- T 269 Standard Method of Test for Percent Air Voids in Compacted Dense and Open Asphalt Mixtures
- T 313 Standard Method of Test for Determining the Flexural Creep Stiffness of Asphalt Binder Using the Bending Beam Rheometer
- T 315 Standard Method of Test for Determining the Rheological Properties of Asphalt Binder Using a Dynamic Shear Rheometer
- T 321 Standard Method of Test for Determining the Fatigue Life of Compacted Asphalt Mixtures Subjected to Repeated Flexural Bending
- T 331 Bulk Specific Gravity (Gmb) and Density of Compacted Hot Mix Asphalt (HMA) Using Automatic Vacuum Sealing Method
- T 378 Standard Method of Test for Determining the Dynamic Modulus and Flow Number for Asphalt Mixtures Using the Asphalt Mixture Performance Tester (AMPT)

ASTM

- D8 Standard Terminology Relating to Materials for Roads and Pavements
- D36 Standard Test Method for Softening Point of Bitumen (Ring-and-Ball Apparatus)
- D92 Standard Test Method for Flash and Fire Points by Cleveland Open Cup Tester
- D217 Standard Test Methods for Cone Penetration of Lubricating Grease
- D297 Standard Test Methods for Rubber Products—Chemical Analysis
- D445 Standard Test Method for Kinematic Viscosity of Transparent and Opaque Liquids (and Calculation of Dynamic Viscosity)
- D2007 Standard Test Method for Characteristic Groups in Rubber Extender and Processing Oils and Other Petroleum-Derived Oils by the Clay-Gel Absorption Chromatographic Method
- D5329 Standard Test Methods for Sealants and Fillers, Hot-Applied, for Joints and Cracks in Asphalt Pavements and Portland Cement Concrete Pavements
- D7741 Standard Test Method for Measurement of Apparent Viscosity of Asphalt-Rubber or Other Asphalt Binders by Using a Rotational Handheld Viscometer

Caltrans CT

- 208 Method of Test for Apparent Specific Gravity of Fine Aggregates
- 385 Method of Test for Sampling and Testing Crumb Rubber Modifier
- 388 Method of Test for Sampling and Reheating Asphalt Rubber Binder Field Samples Prior to Viscosity Testing in Accordance to ASTM D 7741

CONVERSION FACTORS

SI* (MODERN METRIC) CONVERSION FACTORS				
APPROXIMATE CONVERSIONS TO SI UNITS				
Symbol	When You Know	Multiply By	To Find	Symbol
Length				
in.	inches	25.40	millimeters	mm
ft.	feet	0.3048	meters	m
yd.	yards	0.9144	meters	m
mi.	miles	1.609	kilometers	km
Area				
in ²	square inches	645.2	square millimeters	mm ²
ft ²	square feet	0.09290	square meters	m ²
yd ²	square yards	0.8361	square meters	m ²
ac.	acres	0.4047	hectares	ha
mi ²	square miles	2.590	square kilometers	km ²
Volume				
fl. oz.	fluid ounces	29.57	milliliters	mL
gal.	gallons	3.785	liters	L
ft ³	cubic feet	0.02832	cubic meters	m ³
yd ³	cubic yards	0.7646	cubic meters	m ³
Mass				
oz.	ounces	28.35	grams	g
lb.	pounds	0.4536	kilograms	kg
T	short tons (2,000 pounds)	0.9072	metric ton	t
Temperature (exact degrees)				
°F	Fahrenheit	(F-32)/1.8	Celsius	°C
Forces and Pressure or Stress				
lbf	poundforce	4.448	newtons	N
lbf/in ²	poundforce per square inch	6.895	kilopascals	kPa
APPROXIMATE CONVERSIONS FROM SI UNITS				
Symbol	When You Know	Multiply By	To Find	Symbol
Length				
mm	millimeters	0.03937	inches	in.
m	meters	3.281	feet	ft.
m	meters	1.094	yards	yd.
km	kilometers	0.6214	miles	mi.
Area				
mm ²	square millimeters	0.001550	square inches	in ²
m ²	square meters	10.76	square feet	ft ²
m ²	square meters	1.196	square yards	yd ²
ha	hectares	2.471	acres	ac.
km ²	square kilometers	0.3861	square miles	mi ²
Volume				
mL	milliliters	0.03381	fluid ounces	fl. oz.
L	liters	0.2642	gallons	gal.
m ³	cubic meters	35.31	cubic feet	ft ³
m ³	cubic meters	1.308	cubic yards	yd ³
Mass				
g	grams	0.03527	ounces	oz.
kg	kilograms	2.205	pounds	lb.
t	metric ton	1.102	short tons (2,000 pounds)	T
Temperature (exact degrees)				
°C	Celsius	1.8C+32	Fahrenheit	°F
Force and Pressure or Stress				
N	newtons	0.2248	poundforce	lbf
kPa	kilopascals	0.1450	poundforce per square inch	lbf/in ²

* SI is the abbreviation for the International System of Units. Appropriate rounding should be made to comply with Section 4 of ASTM E380. (Revised March 2021)

Blank page

1. INTRODUCTION

1.1 Background

1.1.1 Use of Rubberized Asphalt Concrete

Each year the United States generates nearly 300 million scrap tires, the approximate equivalent of one passenger car tire per person per year (1). Most of these tires end up in landfills, with the consequent environmental impacts. One tire disposal solution grinds the tires into crumbs that are incorporated into asphalt binders used to produce rubberized asphalt concrete (RAC), which includes gap- and open-graded rubberized hot mix asphalt (RHMA-G and RHMA-O, respectively). RAC is commonly used in California, Arizona, Texas, Florida, and New Jersey. Successful, documented use of this material has created growing interest in many other states (2,3).

The maximum allowable crumb rubber particle size in asphalt rubber binders differs among the states (e.g., California and Arizona specify rubber particles passing the #8 [2.36 mm] sieve, while Florida limits the maximum size to that passing the #30 [5 mm] sieve). Crumb rubber particle size in asphalt rubber chip seal applications is typically limited to that passing the #18 (1 mm) sieve to prevent clogging of binder spray nozzles.

In addition to recognizing the environmental benefits of recycling tires into asphalt concrete, research has also shown that RAC, when used in overlays, has better resistance to the fatigue and reflective cracking caused by traffic and exposure to temperature extremes than conventional dense-graded asphalt concrete (DGAC). Studies have also shown that half-thickness RAC used in overlays on cracked pavement can typically provide the same reflective cracking life as full thickness DGAC overlays (4-6).

1.1.2 Production of Rubber-Modified Binders

In California, crumb rubber from scrap tires is generally added to asphalt binder in a so-called wet process. Wet-process rubber-modified binder can be produced at an asphalt plant, at a nearby distribution center (field blending), or at a supplier's terminal or a refinery (terminal blending). Two forms of modified binder are currently produced: *asphalt rubber binder* and *tire rubber-modified binder*:

- Asphalt rubber (AR) binders, by ASTM definition, must contain 15% or more rubber by weight of the binder. California Department of Transportation (Caltrans) specifications require 18% to 22%. The rubber particles have a coarse gradation (between 250 μm and 2.36 mm), and extender oils are often used to promote digestion. Larger particles are typically not fully digested into the binder.
- Tire rubber-modified (TR) binders typically contain less than 10% rubber, and the rubber particles are usually smaller than 250 μm . These binders have characteristics similar to those of polymer-modified binders and can be characterized accordingly using existing Superpave performance-grading procedures (AASHTO M 320). In California, these binders must meet Caltrans PG-M modified binder specifications.

The significant differences in the constituents and production procedures of asphalt rubber binders result in a product very different from unmodified asphalt binders and therefore different approaches are required to test and characterize them.

The Superpave PG procedures (AASHTO M 320) were developed for asphalt binders that contain no additives or particles and are therefore often inappropriate for testing asphalt rubber binders. Consequently, current quality control testing of asphalt rubber binders is limited to rotational viscosity (Haake) and cone penetration. For this reason, it is generally agreed that alternative binder grading procedures consistent with Superpave PG procedures are needed to characterize asphalt rubber binders. The research discussed in this report contributes to the development of these performance grading procedures for wet-process asphalt rubber binders.

1.1.3 Crumb Rubber Modifier Production

Crumb rubber modifier (CRM) (also known as *ground tire rubber* [GTR]) is produced by grinding waste tires. The two main methods used are *ambient grinding* and *cryogenic fracturing*. In the ambient grinding process, the scrap tires are cut into small pieces and then shredded and ground at ambient temperature into small crumbs. The ambient grinding method results in irregular-shaped rubber particles with rough surfaces. In cryogenic fracturing, the cut scrap tire pieces are frozen with liquid nitrogen and then fractured into small crumbs. Cryogenic fracturing usually results in cubical-shaped rubber particles with smooth surfaces. The CRM used to produce asphalt rubber binders in California is primarily derived from ambient grinding.

1.1.4 Current Caltrans Asphalt Rubber Binder Specifications

Current Caltrans specifications for the constituents of asphalt rubber binder, the asphalt rubber binder reaction design profile, and the criteria for quality control and acceptance are summarized in Table 1.1, Table 1.2, and Table 1.3, respectively. Asphalt rubber binder quality is characterized based on rotational viscosity (Haake), cone penetration, resilient properties, and softening properties. The asphalt rubber binder must meet the specified limits in Table 1.3 after at least 45 minutes of reaction time between the asphalt binder and the crumb rubber.

According to the ASTM D8 test method, a minimum of 15% CRM by weight of the asphalt binder is required to meet the definition of asphalt rubber binder. However, Caltrans specifications require a CRM content between 18% and 22% by weight of the base binder, of which 25% must be natural rubber. An extender oil must be added at a rate of 2% to 6% by weight of the base asphalt binder to facilitate the reaction between the asphalt binder and rubber particles.

Current Caltrans specifications also require crumb rubber particles finer than 2.36 mm (100% passing the #8 sieve). Cryogenic grinding is only permitted as a first step for the separation of metals and fibers, after which larger rubber particles are ground at ambient temperatures to meet the required sizes.

Table 1.1: Caltrans Specifications for Asphalt Rubber Binder Constituents

Component	Characteristic	Test Method	Value
Base asphalt binder	Viscosity, $m^2/s (\times 10^{-6})$ at 100°C	ASTM D445	$X \pm 3^a$
	Flash point, Cleveland Open Cup (°C)	ASTM D92	>207
	Asphaltenes (% by mass)	ASTM D2007	<0.1
	Aromatics (% by mass)	ASTM D2007	>55
Crumb rubber modifier ^b	Scrap tire crumb rubber gradation (% passing #8 sieve)	CT 385	100
	High natural rubber gradation (% passing #10 sieve)	CT 385	100
	Wire in CRM (% max.)	CT 385	0.01
	Fabric in CRM (% max.)	CT 385	0.05
	CRM particle length (in. max.) ^c	—	3/16
	CRM specific gravity ^c	CT 208	1.1–1.2
	Natural rubber content in high natural rubber (%) ^c	ASTM D297	40.0–48.0

^a The symbol “X” is the proposed extender oil viscosity. “X” must be from 19 to 36. A change in “X” requires a new asphalt rubber binder design.

^b CRM must be ground and granulated at ambient temperature. If the steel and fiber are cryogenically separated, this must occur before grinding and granulating. If cryogenically produced, CRM particles must be large enough to be ground or granulated and must not pass through the grinder or granulator.

^c Test at mix design and for certificate of compliance.

Table 1.2: Asphalt Rubber Binder Reaction Design Profile

Characteristic	Test Method	Minutes of Reaction ^{a,b}							Value
		45	60	90	120	240	360	1440	
Cone penetration @77°F (0.10 mm)	ASTM D217	X				X		X	25–70
Resilience @ 77°F (% rebound)	ASTM D5329	X				X		X	>18
Field softening point (°F)	ASTM D36	X				X		X	125–165
Viscosity @ 375°F, (centipoise)	ASTM D7741 ^c	X	X	X	X	X	X	X	1,500–4,000

^a Six hours (360 minutes) after CRM addition, the oven temperature is reduced to 275°F for 16 hours. After the 16-hour (1,320-minute) cool down after CRM addition, the binder is reheated to the reaction temperature expected during production for sampling and testing at 24 hours (1,440 minutes).

^b “X” denotes required testing.

^c Sample prepared according to CT 388.

Table 1.3: Caltrans Specifications for Asphalt Rubber Binder Quality Control and Acceptance

Characteristic	Test Purpose	Test Method	Value	
			Minimum	Maximum
Cone penetration @77°F (0.10 mm)	Acceptance	ASTM D217	25	70
Resilience @ 77°F (% rebound)	Acceptance	ASTM D5329	18	—
Field softening point (°F)	Acceptance	ASTM D36	125	165
Viscosity @ 375°F (centipoise)	Quality control	ASTM D7741 ^a	1,500	4,000

^a Sample prepared according to CT 388.

For each Caltrans project, asphalt rubber binder producers must propose a design and profile for the binder that will be used. The proposed design must specify the materials to be used, including base binder, extender oil, and crumb rubber. The asphalt rubber binder profile serves as a production quality indicator and is not used as a performance specification. The profile illustrates the characteristics of the binder over a 24-hour (1,440-minute) reaction period.

1.2 Problem Statements

A number of limitations to the current asphalt rubber binder specification have been identified through a review of the literature and discussions with stakeholders (3). These include the following:

- The current Caltrans specification for wet-process asphalt rubber binders focuses mainly on measuring viscosity at the plant using a handheld rotational viscometer. Temperature control requirements during testing are limited, which can influence results given that asphalt binder properties are highly influenced by temperature. While viscosity is an important parameter for the pumpability and workability of the binder and ultimately of the mix, it does not directly relate to the in-service performance of the binder within a rubberized asphalt concrete mix or a rubberized asphalt surface treatment. Additionally, due to the particulate phase of these binders, viscosity measurements alone lack sufficient accuracy to completely describe their complex behavioral and performance properties.

- Although cone penetration grading and resilience properties do provide a means to evaluate the stiffness and resilience of asphalt rubber binders, the Superpave performance grading testing procedure moved away from these tests because they have several limitations, including the following:
 - + They are empirical tests that measure a binder's viscous and elastic properties, but the tests do not necessarily correlate with field performance.
 - + The tests only measure a binder's properties at a single intermediate temperature and thereby fail to provide an accurate indication of its properties at typical high and low service temperatures, or of its temperature susceptibility (change of stiffness with change of temperature).
 - + The tests do not address the effects of short-term aging (during mixing and compaction) and long-term aging (during service life) on binder properties.
- Softening point generally indicates the phase change temperature of binders and may not be sufficient for comprehensive performance/rheological characterization.
- Rheological testing using a dynamic shear rheometer (DSR) and a bending beam rheometer (BBR) is now considered standard practice for evaluating performance-related characteristics of unmodified, polymer-modified, and tire rubber-modified asphalt binders. However, the standard parallel plate geometry used in a DSR test is potentially inappropriate for measuring the properties of asphalt rubber binders produced per Caltrans specifications. When an asphalt rubber binder is tested in a DSR using parallel plate geometry with a 1 mm or 2 mm gap, incompletely digested rubber particles can contact both the top and bottom plates and interfere with the torque and strain measurements. This interference results in the rheology of the rubber particles dominating the measurement and potentially providing misleading information about the rheology of the blended asphalt rubber binder as a whole. A potential consequence of this misleading information can be the choice/use of an inappropriate binder for a given climatic region. According to AASHTO T 315 (Standard Method of Test for Determining the Rheological Properties of Asphalt Binder Using a Dynamic Shear Rheometer), the gap size between the plates should be at least four times the maximum particle size to provide reliable results (i.e., an 8 mm gap, with correspondingly adjusted plate diameter, would be required for 2.0 mm [#10] crumb rubber particles). However, the maximum gap size recommended by rheologists is about 5 mm, to ensure a satisfactory linear shear rate through the asphalt binder sample sandwiched between the plates. Although increasing the gap size is a potential solution for dealing with the larger rubber particle sizes, this increase can introduce other problems, such as poor repeatability, unacceptable temperature gradients, difficulty in trimming the specimen, uncontrollable edge effects, and potentially misleading results. When testing with parallel plate geometry, the modulus of the asphalt binder is proportional to the sample radius to the power of four. Consequently, a 2%

reduction in radius due to incorrect trimming implies a potential 16% reduction in the measured modulus.

- Other limitations of the current performance grading testing procedures when testing asphalt rubber binders include the following:
 - + Rubber particles do not age in the same way or to the same extent as asphalt binders.
 - + Short-term aging in a rolling thin-film oven (RTFO) does not uniformly coat the bottle with the specified sample size (i.e., asphalt content is between 18% and 22% less because of the rubber) and at the current testing temperature because the asphalt rubber binder is more viscous, and it is difficult to remove the aged binder from the bottle.
 - + Long-term aging of asphalt rubber binder in a pressurized aging vessel (PAV) does not uniformly coat the pan with the specified sample size.
 - + Low-temperature testing of asphalt rubber specimens in the BBR using current specimen preparation procedures is questionable, since the viscous, particulate-rich binders are difficult to pour into the specimen preparation mold. The test method and interpretation of its results also need to be studied in greater detail to confirm their appropriateness for testing asphalt rubber binder.
- The actual grading limits developed for unmodified and polymer-modified asphalt binders may not be appropriate asphalt rubber binder performance indicators as they may not reflect the contribution of the binder rheology in terms of the rutting, fatigue, and low-temperature cracking performance of RAC mixes.

To resolve these issues, there is a need for alternative testing configurations and procedures that can better evaluate the performance characteristics of field-blended wet-process asphalt rubber binders using the same or similar Superpave PG parameters as for unmodified, polymer-modified (PM) and tire rubber-modified (TR) asphalt binders are needed. These alternate methods can then be used to establish performance-based contract acceptance criteria for the production of asphalt rubber binders, which will in turn lead to more reliable performance in the field.

1.3 Project Objectives

The work discussed in this report is part of a larger study, funded by Caltrans, with the objective of developing and recommending testing procedures and criteria for performance-based specifications of asphalt rubber binders used in gap- and open-graded mixes using current Superpave PG equipment. This objective will be met by completing the following tasks in a series

of phases (Figure 1.1). Work that had been completed at the time of preparing this report is noted.

1. Review relevant literature on the topic. Contact DSR equipment manufacturers and discuss test requirements and alternative geometries. (Completed in Phase 1 [3].)
2. Collect samples of asphalt binder, crumb rubber particles, and extender oil for laboratory preparation of asphalt rubber binders. On completion of initial screening tests, identify completed and current projects where asphalt rubber binder samples can be collected for additional testing. Prepare laboratory-conditioned samples for testing with a DSR. (Completed in Phase 1 [3].)
3. Evaluate the use and ability of the alternative concentric cylinder DSR geometry to provide realistic and repeatable results for unmodified, polymer-modified (PM), and tire rubber-modified (TR) binders that are comparable to results from the same tests using conventional parallel plate geometries. The performance of these binders is routinely measured with parallel plate geometry in terms of the Superpave performance grading system. (Completed in Phase 1a [3].)
4. Compare the abilities of the parallel plate and concentric cylinder geometries for testing asphalt rubber binder containing crumb rubber particles of various sizes, and evaluate the effects of different crumb rubber particles and asphalt rubber binder properties on test results. (Completed in Phase 1b [3].)
5. Evaluate and refine short- and long-term aging procedures for asphalt rubber binders. (Completed in Phase 2a [3].)
6. Evaluate and refine specimen preparation procedures for low-temperature testing of asphalt rubber binders in a BBR. (Completed in Phase 2b [3].)
7. Evaluate whether the concentric cylinder geometry is appropriate for intermediate-temperature and multiple stress creep recovery (MSCR) testing. (Preliminary testing on this task was completed in Phase 2c and Phase 2d [3]. Additional testing is in progress as part of Phase 3 and will be documented in a later report.)
8. Evaluate the high-, intermediate-, and low-temperature rheological properties of field-sampled asphalt rubber binders using the refined procedures developed in Tasks 1 through 7, and interpret the test results in conjunction with results from tests on field-sampled gap-graded mixes prepared with the same binders. (Preliminary testing was completed in Phase 2e for the plant-produced binders and in Phase 2f for the gap-graded mixes [3]. Additional testing includes the five binders and mixes discussed in this report and a further 20 binders discussed in the Phase 3 [Caltrans] report.)
9. Suggest provisional performance grading criteria and provisional contract acceptance criteria for wet-process asphalt rubber binders. (This task is dependent on results from all previous tasks and will be documented in a later report.)

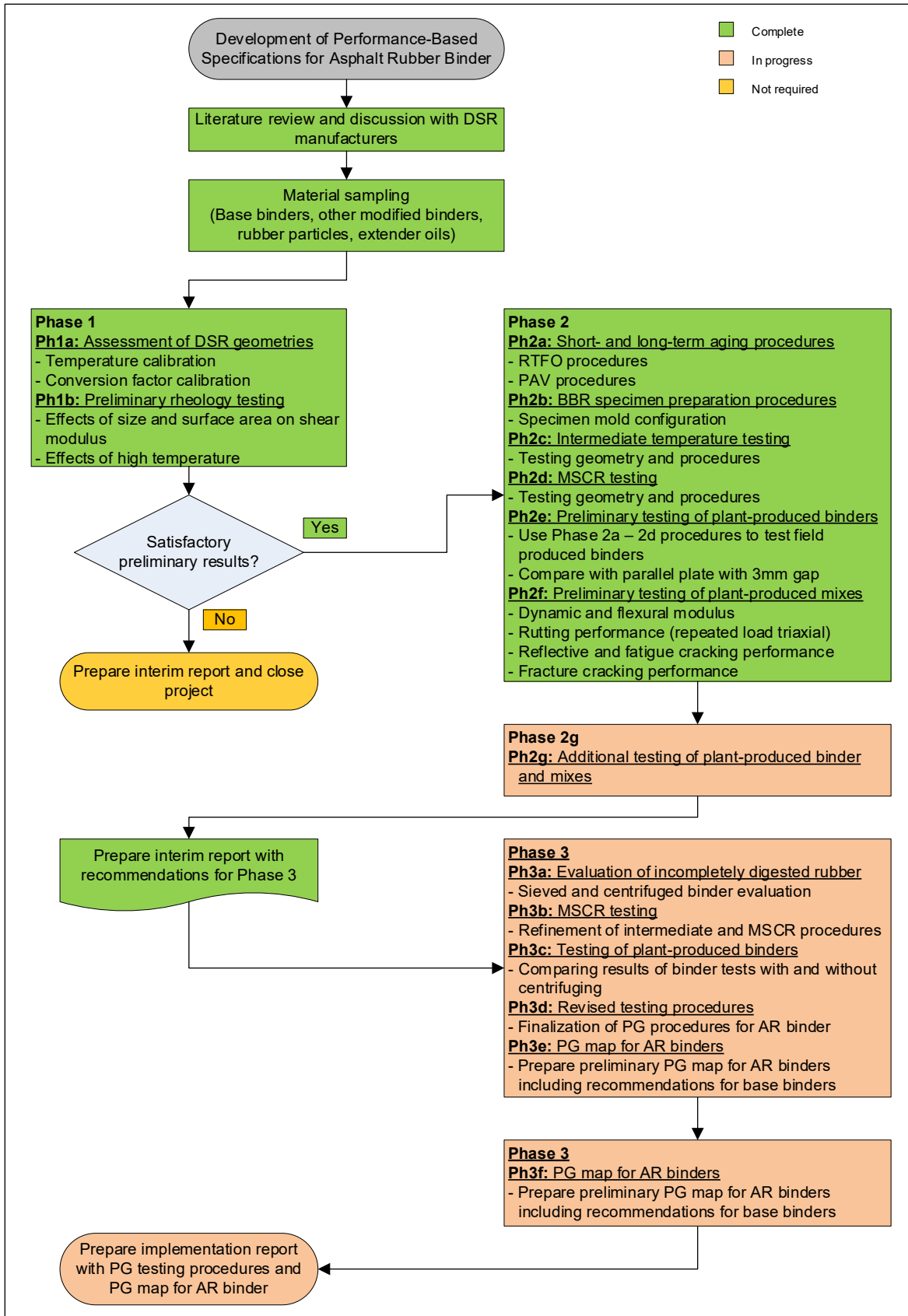


Figure 1.1: Flowchart of project tasks/phases.

10. Prepare provisional procedures for conducting the recommended tests and interpreting the test results. (Documented in the Phase 2 report [3]. Interpretation of results will be documented in a later report.)
11. Prepare reports documenting this research effort, with recommendations for specification language and, if required, recommendations for further research to validate the provisional performance grading and contract acceptance criteria.

This interim report provides the results of testing five plant-produced binders and the gap-graded rubberized hot mix asphalt mixes produced with them, as part of Item 8 in the above list.

Although this study focuses on testing asphalt rubber binders used in gap- and open-graded mixes, the results are relevant for asphalt rubber binders used in chip seals and other surface treatments. However, to prevent clogging of spray nozzles, the maximum rubber particle size used in these applications is typically limited to that passing the #18 (1 mm) sieve, which is considerably smaller than the #8 (2.36 mm) maximum size used in binders used in gap- and open-graded mixes.

1.4 Measurement Units

Although Caltrans has returned to the use of US standard measurement units, metric units have always been used by the UCPRC in the design and layout of test tracks and for the laboratory, accelerated wheel load testing, field measurements, and data storage. The Superpave performance grading system is a metric standard and uses metric units. In this report, both English and metric units (provided in parentheses after the English units) are provided in the general discussion. Metric units are used in the reporting of performance grading and mix test results. A conversion table is provided on page xviii.

Blank page

2. SUMMARY OF PHASE 2 RESEARCH

2.1 Introduction

The first two phases of a three-phase study to investigate test methods for measuring the performance properties of asphalt rubber binders produced according to Caltrans specifications were recently completed (3). The current method of rotational viscosity testing (Haake) used by Caltrans is deemed to be an insufficient measure for assessing the expected performance for asphalt rubber binders compared to the more rigorous testing requirements for unmodified, polymer-modified, and tire rubber-modified binders. The first phase of the study consisted of preliminary testing to compare two different dynamic shear rheometer (DSR) geometries, with a goal to make recommendations about whether to adopt similar testing procedures for asphalt rubber binders to supplement those currently used for unmodified and other modified binders. The second phase of the study investigated short- and long-term aging procedures, developed revised specimen preparation procedures for bending beam rheometer (BBR) testing, and conducted preliminary investigations into the use of the two DSR geometries for intermediate-temperature testing and multiple stress creep recovery (MSCR) testing. Three asphalt rubber binders, and loose mixtures produced with them, were sampled from three different field projects to assess the binder testing procedures developed and to relate the tested properties to expected field performance. This report covers Phase 2g, which entailed the testing of five additional asphalt rubber binders and the gap-graded rubberized asphalt (RHMA-G) mixes produced with them.

2.2 Phase 1: DSR Testing Geometries

The high temperature properties of unmodified and other modified asphalt binders are typically measured in tests that use a DSR with parallel plate geometry, with the gap size between the plates dependent on the size of any particulates in the binder. A 2.0 mm gap size is considered to be the maximum appropriate gap for testing asphalt binders to limit variability in results due to specimen trimming and binder flow at higher temperatures, provided that no particulates in the binder exceed the AASHTO/ASTM-recommended maximum particle size of 0.25 mm (or 250 μm [#60]). In addition, DSR manufacturers recommend that the gap between the plates should be at least four times the maximum particle size to provide reliable results. However,

Caltrans specifications allow crumb rubber particles up to 2.36 mm (passing the #8 sieve), which exceeds this maximum recommended size for parallel plate testing (i.e., an 8 mm gap, with correspondingly adjusted plate diameter, would be required for 2.0 mm [#10] particle sizes). Consequently, the appropriateness of the parallel plate geometry for testing asphalt rubber binders is questionable because the rheology of the large incompletely digested rubber particles may dominate the DSR results and give misleading performance parameters for the binder properties. Phase 1 of the study therefore assessed the concentric cylinder, an alternative geometry that can accommodate larger particles in the asphalt rubber binder. The two geometries were compared using unmodified, polymer-modified, tire rubber-modified (i.e., binders with no particulates), and wet-process asphalt rubber binders (binder containing incompletely digested rubber particles). Binders with no particles were tested with a 1 mm gap, while the asphalt rubber binders were tested with a 3 mm parallel plate gap (to better accommodate the incompletely digested rubber particles). Key findings from the work completed to date include the following:

- The results obtained from testing the same unmodified, polymer-modified, and tire rubber-modified binders with concentric cylinder and parallel plate geometries in a DSR showed that the two geometries produced results for the same binder that were statistically similar at a 95% confidence interval.
- The results obtained from testing asphalt rubber binders with three different crumb rubber particle size ranges (180 μm to 250 μm , 250 μm to 425 μm , and 425 μm to 850 μm [#40 to #20, #60 to #40, and #80 to #60, respectively]) showed a strong correlation between the two testing geometries for finer particle size ranges, but the correlations became weaker with increasing particle size. These weaker correlations in the larger size ranges were attributed in part to the increasing influence of the larger incompletely digested rubber particles in proximity of the plates. Strong correlations between the two geometries were also noted in the test results from assessments of the effects of extender oils and from tire-crushing methods (crushing at ambient versus cryogenic temperatures).

2.3 Phase 2a: Short- and Long-Term Aging Procedures

Phase 2a of the study investigated modifications to the AASHTO T 240 rolling thin film oven (RTFO) and AASHTO R 28 pressurized aging vessel (PAV) tests to make them more representative of the short- and long-term aging that asphalt rubber binders are subjected to during mix

production and during service life. Suggested modifications to the test procedures include the following:

- RTFO testing
 - + Preheating the bottles at 190°C for 10 minutes to improve the uniformity of the coating.
 - + Increasing the sample size from 35 g to 45 g to account for the rubber particles, to ensure that the specified amount of the base asphalt binder is tested, and to ensure that sufficient binder is available for rheology testing.
 - + Increasing the RTFO test temperature from 163°C to 190°C to better represent rubberized asphalt concrete mix production temperatures.
- PAV sample preparation
 - + Preheating the pans at 190°C for 10 minutes prior to pouring to facilitate more even spread of the binder to the required thickness.
 - + Increasing the sample size from 50 g to 63 g to account for the rubber particles, to ensure that the specified amount of the base asphalt binder is tested, and to ensure that sufficient binder from a single PAV test is available for rheology testing.
 - + Increasing the sample preparation temperature from 163°C to 190°C to be consistent with the temperature of the RTFO-aged binder.
 - + Altering the pouring procedure and agitating the pan during pouring to facilitate even spread of the binder to the required thickness.

Test results revealed the following:

- RTFO testing
 - + Complete coating of the bottle was achieved with the larger sample at the higher temperature. Although coating was satisfactory using the smaller sample at the higher temperature, insufficient material was produced for the desired rheology testing. Film thickness on the bottle was relatively even but marginally thicker than that measured during aging of conventional unmodified binders, with these results primarily attributed to the presence of incompletely digested rubber particles.
 - + Aging at 190°C increased the shear modulus of the asphalt rubber binder and reduced the phase angle, as expected. The true high temperature performance grade (PG) typically increased by about 6°C, which equates to a one-grade bump. Sample size and extender oil had limited effect on these parameters.
 - + Rubber particle size had a notable effect on all tests, which is consistent with findings from the literature.
 - + The measured carbonyl and sulfoxide indices for unaged and RTFO-aged binders showed clear trends with respect to the effect of aging temperature and sample size, as expected. Ongoing testing in Phase 3 will include a more detailed comparison of

laboratory- and plant-produced binders to determine whether the proposed revised aging procedure is representative of aging conditions during plant production, storage, transport to the project, and placement.

- + The butadiene index appears to increase with increasing rubber content and could be a useful potential indicator of the level of modification in asphalt rubber binders. This index also changed with increasing RTFO-aging temperature and the larger sample size, which implies that some rubber modification may have continued during aging.
- PAV preparation procedures
 - + Complete coating of the pan was achieved with the 63 g sample, and the average film thickness after pouring and after PAV aging met the requirements listed in AASHTO R 28.
 - + Following this method provides an additional 130 g of aged binder per PAV test compared to following the standard method (i.e., 10 pans of 63 g versus 10 pans of 50 g), which provides sufficient binder for both intermediate-temperature testing (using the concentric cylinder geometry) and low-temperature testing. This is considered to be an important advantage given that one PAV test takes 20 hours, excluding preparation time.
- Preliminary intermediate-temperature testing of PAV-aged binder
 - + No clear trends were observed from the preliminary intermediate-temperature test results on three binders for the different preparation procedures. Only two of the three binders could be tested due to torque limitations of the DSR. The results from one of the binders were consistent with expectations. PAV preparation procedures did not appear to have a significant effect on the test results of the second binder.
- Preliminary BBR testing
 - + No clear trends were observed from the stiffness testing results, with little variation observed between the different PAV preparation methods across the three binders tested when variation between replicates within each method were considered.
 - + The m-value did not appear to be significantly affected by PAV sample preparation method.

Although only limited DSR and BBR testing was conducted in this phase of the research, the modifications proposed above are considered to be appropriate in reflecting the original intent and mechanisms of the tests. Unfortunately, there is no documented procedure to verify the appropriateness of the procedures given that asphalt rubber binders cannot be effectively extracted and recovered from loose mix or core samples removed from highways.

2.4 Phase 2b: Bending Beam Rheometer Specimen Preparation Procedures

Phase 2b investigated modifications to the mold used to prepare BBR specimens. Pouring asphalt rubber binder into a standard BBR mold is very difficult given the mold's small opening and the viscosity and consistency of the binder. Modified molds that allow binder to be poured through a 12.5 mm opening (i.e., the width of the mold) instead of the standard 6.25 mm opening (i.e., the thickness of the specimen) improved the quality of the specimens in terms of dimension uniformity and absence of air bubbles. However, the specimen's wider surface area made trimming more challenging, and the specimen's rougher surface after trimming could influence the dimensions of the beam. Ongoing refinements to the trimming process are being investigated, along with the determination of new variance limits, to accommodate these inconsistencies.

BBR testing indicated that the mold configuration used to prepare beam specimens can affect the measured rheological properties of the binder and that the low-temperature performance grade could change if the modified configuration is used instead of the standard configuration. Results from the modified configuration appeared to be more consistent than those produced with the standard configuration.

2.5 Phase 2c: Intermediate-Temperature Testing

Preliminary intermediate-temperature test results indicated that the concentric cylinder geometry is potentially suitable for testing of asphalt rubber binders at intermediate temperatures. However, all testing in this phase of the study was conducted at 25°C, and the test setup will require more testing with a representative set of asphalt rubber binders to determine whether it is appropriate for determining actual intermediate-temperatures, and whether maximum torque ranges of the DSR are likely to be exceeded. Refinements to the testing geometry (e.g., different bob sizes) and testing procedures (e.g., different bob immersion depths) will also be investigated during planned additional testing in Phase 3.

2.6 Phase 2d: Multiple Stress Creep Recovery Testing

Preliminary multiple stress creep recovery (MSCR) test results indicated that the concentric cylinder geometry is also potentially suitable for testing this property of asphalt rubber binders. However, given that only limited testing was undertaken and that the results were somewhat

inconsistent, additional testing is required before any conclusions on the appropriateness of using the concentric cylinder geometry for MSCR testing can be drawn. This evaluation will continue in the next phase when field binders are tested.

2.7 Phase 2e: Rheology Testing on Plant-Produced Binders

Preliminary rheology testing to determine the high-, intermediate-, and low-temperature performance grades of three plant-produced asphalt rubber binders using the proposed testing procedures was undertaken to test the procedures. The following observations from the high temperature tests were made:

- Concentric cylinder
 - + An increase of four grades over the base binder was recorded for two of the asphalt rubber binders and an increase of five grades was recorded for the third.
 - + Mean true grade results showed that all three binders were relatively close and fell in a range between 91°C and 95°C.
 - + Variation in results of the three replicates in each test was small.
 - + The incompletely digested rubber particles clearly had a significant influence on the results when compared to the base binder.
 - + All results were higher than the maximum grade of 82°C listed in the AASHTO M 320 standard.
- Parallel plates with 3 mm gap
 - + The same grade increases recorded for the tests with the concentric cylinder were observed for the tests with the parallel plate.
 - + Mean true grade results showed that all three binders were relatively close and fell in a range between 92°C and 105°C, a range approximately 7°C higher than the concentric cylinder measurements.
 - + Variation in results of the three replicates for each binder was notably larger than the variation recorded when testing with the concentric cylinder.
- Difference between concentric cylinder and parallel plate
 - + For the unaged binders, $G^*/\sin(\delta)$ values measured with the parallel plate geometry were consistently higher than those determined from concentric cylinder measurements. Similar trends between the different binders were also apparent.
 - + For the RTFO-aged binders, $G^*/\sin(\delta)$ values determined with the parallel plate geometry were again considerably higher than those determined with the concentric cylinder for two of the three binders tested.

- Binder grade
 - + Testing with both geometries provided the same high-temperature grade despite the noted variations in test results discussed above.

The following observations from the low-temperature tests were made:

- Stiffness values were well below the AASHTO M 320 criteria for determining the low-temperature grade ($S \leq 300$) and, consequently, grades were dictated by the m-value (≥ 0.30). The presence of incompletely digested rubber particles and potential phase separation between these particles and the asphalt binder probably contributed to the low stiffness values.
- Although the acceptable ranges between two test results for the same unmodified binder as listed in AASHTO T 313 (7.2% for stiffness and 2.9% for m-value) were exceeded in most instances, the low-temperature grade of each tested binder remained the same. These larger differences between results were attributed in part to the rougher beam surfaces after trimming and to variation in the number, size, and degree of digestion of the rubber particles in each beam. Revised acceptance ranges for asphalt rubber binders will be suggested, if appropriate, after completion of further testing on additional plant-produced binders in Phase 3.
- The AASHTO M 320 procedure contains no recommendations for asphalt rubber binders. The minimum low-temperature grade in the standard table for conventional binders with a high-temperature grade equal to or greater than 76°C is -22°C, which was achieved for two of the tested binders. The low-temperature grade of the third binder did not differ from that of the base binder.
- Questions regarding other factors that may influence results, and specifically the variability between results, and that may require further investigation, include:
 - + Whether changes in the properties of the incompletely digested rubber particles occur at very low temperatures (i.e., in the range of glass transition)
 - + Whether different rubber particles (e.g., synthetic versus natural rubber) have different coefficients of thermal expansion
 - + Whether the properties of the rubber particles are in any way effected by the type of temperature control medium used in the BBR (i.e., ethanol for the testing discussed in this report).

A small study was conducted to determine the extent to which incompletely digested particles might affect performance-grading test results. This was achieved by comparing the results from the three plant-produced asphalt rubber binders with the results produced using the same binder but with all particles larger than 300 μm ($> \#50$ sieve) removed. Preliminary testing was limited

to the high-temperature grading only. Sieved binders were tested using a 25 mm parallel plate geometry with 2 mm gap according to the standard AASHTO T 315 method. The following observations were made:

- The high temperature performance grades of the sieved binders were consistently two grades lower than those determined for the unsieved binders, indicating that the incompletely digested particles had a significant influence on the test results.
- The percent decrease in $G^*/\sin(\delta)$ when comparing the sieved with the unsieved binders was significant.
- The correlation between the true performance grades of the two types of binders was strong, indicating that testing sieved binders in a standard parallel plate geometry may be an appropriate alternative to testing unsieved binders in the concentric cylinder geometry.

Given that the variability of incompletely digested rubber particles in asphalt rubber binder samples leads to considerable variability in high-, intermediate-, and low-temperature test results, testing sieved binders may be a more appropriate approach to performance grade testing of these binders, or at least for developing a relationship between test results from unsieved and sieved binders as a means to determine a representative PG grading for asphalt rubber binders. Sieved/centrifuged binders will therefore be included as part of the scheduled Phase 3 testing of additional plant-produced binders.

2.8 Phase 2f: Performance Testing on Plant-Produced Mixes

Preliminary mix testing was undertaken to assess rutting and cracking performance in relation to performance grading to determine whether the rheology testing approaches provide properties that are representative of likely field performance. The following observations were made based on the testing of three plant-produced gap-graded asphalt rubber mixes:

- The dynamic and flexural moduli results were similar for all three mixes and were consistent with those measured on other RHMA-G mixes.
- The initial rates of cumulative permanent deformation with increasing loading cycles were similar for the three mixes, but thereafter one mix appeared to be more susceptible to rutting than the other two. Similar trends were recorded in the flow number tests and in tests to determine the number of cycles to 3% and 5% permanent axial strain. Rankings in these tests were consistent with the true high-temperature grade results of the binders.
- Two of the mixes had similar fatigue life results that were somewhat lower than expected for RHMA-G mixes, when compared with other mixes recently tested at the UCPRC. The

remaining mix had a slightly higher fatigue life that was more consistent with other RHMA-G mixes tested.

- The semicircular beam flexibility index results showed the same ranking and trends as the beam fatigue results.

Given that only three plant-produced binders and the mixes produced with them were tested in this phase, the database of results was considered to be insufficient for in-depth analysis purposes. Additional plant-produced mixes were programmed for testing in Phase 2g (this report) and Phase 3.

2.9 Conclusions

Based on the results obtained from Phase 1 and Phase 2 testing, the concentric cylinder geometry appears to be a potentially appropriate alternative to the parallel plate geometry for quantifying the properties of asphalt rubber binders produced per Caltrans specifications, and specifically for assessing the performance properties of binders containing crumb rubber particles larger than 250 μm (particles retained on the #60 sieve). Additional testing of a larger number of binders, planned for Phase 2g (this report) and Phase 3 of the project, is required to confirm these initial findings. The concentric cylinder geometry requires a larger binder sample for testing, and it takes longer to complete than testing with the parallel plate geometry. Incompletely digested rubber particles, which have different sensitivities to temperature and applied stress and strain than the base asphalt binder, appear to dominate the test results, and this will need to be factored into the analyses and interpretation of rheology and mix performance test results. The proposed modifications to the short- and long-term aging procedures and to the BBR specimen preparation procedures are considered to be more aligned with the original intent of the tests and will likely reduce the variability between replicate specimens during testing.

2.10 Recommendations

Initial results from Phase 1 and Phase 2 support the continuation of testing to assess the appropriateness of using the concentric cylinder geometry to measure the performance properties of asphalt rubber binders that are produced according to Caltrans specifications using a wet process with crumb rubber particles larger than 0.25 mm (#60 mesh). This testing should

be in line with the original workplan and objectives prepared for this project, and work should continue to refine the testing procedures on additional plant-produced binders, assess the repeatability and reproducibility of measurements from any proposed test methods, and evaluate the applicability of the results to the actual performance properties of mixes produced with asphalt rubber binders. The potential influence of incompletely digested rubber particles dominating the results will need to be carefully considered in any testing and analysis procedures.

3. TESTING PLANS

3.1 Introduction

The testing plan included testing of five plant-produced asphalt rubber binders and the corresponding five-plant produced mixes sourced from asphalt plants supplying RHMA-G mix for overlay projects on five different California highways (BUT-162 [in Butte County], MER-33 [in Merced County], LAK-20 [in Lake County], INY-395 [in Inyo County], and IMP-111 [in Imperial County]). Samples of crumb rubber, base binder, asphalt rubber binder, and loose mix were collected from each plant. Projects were selected from those available to ensure statewide representation of climate, binders, aggregates, and asphalt plants.

3.2 Base Binder Testing

Base binder performance grade (PG) was verified.

3.3 Asphalt Rubber Binder Testing

3.3.1 Crumb Rubber Particle Size Distribution

Samples of waste tire rubber and high natural rubber were collected from all projects. Scrap tire and high natural rubber gradations were both checked to confirm that they met Caltrans specifications. Samples were mixed in a ratio of 75% waste tire rubber to 25% high natural rubber in line with Caltrans specifications. The gradation of the combined 200 g sample was then checked for reasonableness (Caltrans specifications do not require the reporting of a gradation of the combined rubber).

3.3.2 Rheology Testing

Binder testing followed the procedures developed in Phase 1 and Phase 2 of the study (3), summarized in Chapter 2. High-temperature tests (Phase 1 and Phase 2a), intermediate-temperature tests (Phase 2c), and multiple stress creep recovery tests (Phase 2d) included both concentric cylinder and parallel plate geometries. Difficulties with testing at intermediate temperatures with the concentric cylinder geometry were anticipated due to torque limitations of the equipment. Specimens for the low temperature tests were fabricated using the modified mold configuration (Phase 2b). Dynamic shear rheometer (DSR) geometries used for the different tests included the following:

- Concentric cylinder
 - + High-temperature tests: 29 mm diameter cup with 17 mm spindle and 6 mm gap between the spindle and cup edges
 - + Intermediate-temperature tests: 29 mm diameter cup with 10 mm spindle and 9.5 mm gap between the spindle and cup edges
- Parallel plate
 - + Base binder
 - High-temperature tests: 25 mm diameter plate with 1 mm gap
 - Intermediate-temperature tests: 8 mm diameter plate with 1 mm gap
 - + Asphalt rubber binder
 - High-temperature tests: 25 mm diameter plate with 3 mm gap
 - Intermediate-temperature tests: 8 mm diameter plate with 3 mm gap

Between three and five replicates, sampled from multiple cans of binder, were tested in each test to ensure that variability between samples was considered.

3.4 RHMA-G Mix Testing

Mix testing followed the same procedures used in the Phase 2f testing (3). The testing factorial is summarized in Table 3.1.

Table 3.1: Tests Performed on Plant-Produced Mixes

Test	Replicates	Air Voids (%) ^a	Test Variables
<u>Stiffness</u> <ul style="list-style-type: none"> • Dynamic modulus - AASHTO T 378 	3	7.0±1.0	<ul style="list-style-type: none"> • 1 temperature sequence (4, 20, 45°C) • 1 stress level^a • No confining pressure
<u>Stiffness</u> <ul style="list-style-type: none"> • Beam flexural frequency sweep - AASHTO T 321 	2	7.0±1.0	<ul style="list-style-type: none"> • 3 temperatures (10, 20, 30°C) • 2 strain levels (100 µstrain at 10 and 20°C; 200 µstrain at 30°C)
<u>Rutting Performance</u> <ul style="list-style-type: none"> • Flow number from repeated load triaxial results - AASHTO T 378 	3	7.0±1.0	<ul style="list-style-type: none"> • 1 temperature (52°C) • 1 deviator stress (600 kPa [87 psi])^b • 1 contact stress (30 kPa [4 psi]) • No confining pressure
<u>Cracking Performance</u> <ul style="list-style-type: none"> • Beam fatigue - AASHTO T 321 	3	7.0±1.0	<ul style="list-style-type: none"> • 1 temperature (20°C) • 3 strain ranges (high, medium, low) based on the mix stiffness • 1 frequency (10 Hz)
<u>Cracking Performance</u> <ul style="list-style-type: none"> • Semicircular Beam (SCB) test - AASHTO TP 124 	3	7.0±1.0	<ul style="list-style-type: none"> • 1 temperature (25°C)

^a Based on saturated surface-dry bulk specific gravity.

^b Deviator stress controlled by asphalt mix performance tester (AMPT) software to get 75 to 125 µstrain peak-to-peak axial strain.

3.4.1 Performance Testing Specimen Preparation

Specimen preparation details for the different tests were as follows:

- Asphalt mix performance tester (AMPT) tests were conducted on specimens with 100 mm (≈ 4 in.) diameter and 150 mm (≈ 6 in.) height, cored from 150 mm and 175 mm (≈ 7 in.) gyratory-compacted specimens.
- Beam fatigue specimens were cut from ingots compacted with a steel-wheel roller to target air-void contents of $7.0 \pm 1.0\%$. The beams were 380 mm (≈ 15 in.) in length, 50 mm (≈ 2 in.) in height, and 63 mm (≈ 2.5 in.) in width.
- Semicircular bend (SCB) specimens were cut from gyratory-compacted specimens with 150 mm diameter and 175 mm height. Two 50 mm (≈ 2 in.) thick discs were cut from the compacted specimen, from which four SCB specimens were cut. A 15 mm \times 1.5 mm notch was cut into each SCB specimen.

3.4.2 Mix Testing Details

Specimen Air Void Contents

Air-void contents were determined according to AASHTO T 269. Bulk specific gravity was determined using both saturated surface-dry (AASHTO T 166) and automatic vacuum sealing methods (AASHTO T 331).

Mix Stiffness: Dynamic Modulus

Tests to determine dynamic modulus (E^*) and phase angle of the RHMA-G mixes were performed using an AMPT at 10, 1, and 0.1 Hz when testing at 4°C and 20°C (39°F and 68°F) and at 10, 1, 0.1, and 0.01 Hz when testing at 45°C (113°F). In this test, the specimen is subjected to a haversine axial-compressive load with fixed amplitude under controlled-strain conditions. The axial deformation of the specimen during cyclic loading is measured using three linear variable displacement transducers (LVDTs) mounted around the specimen 120° apart. The dynamic modulus is calculated by dividing the peak stress (σ_{max}) by the peak strain (ϵ_{max}) during each loading cycle. Three replicate specimens from each mix were tested.

Dynamic modulus master curves were developed using Equation 3.1 through Equation 3.3. The measured modulus values were used to construct master curves at the reference temperature of 20°C by fitting the data to the sigmoidal function shown in Equation 3.1. The testing frequencies at any testing temperature were converted to the reduced frequency at the

reference temperature using the time-temperature superposition principle (Equation 3.2) with the aid of the Arrhenius shift factor (Equation 3.3).

$$\log(|G^*(f_r)|) = \delta + \frac{\alpha}{1+e^{\beta+\gamma \times \log(f_r)}} \quad (3.1)$$

where: $\delta, \alpha, \beta,$ and γ are sigmoidal function parameters
 f_r is the reduced frequency at reference temperature T_r

$$\log(f_r) = \log(a_T(T)) + \log(f) \quad (3.2)$$

where: f is the testing frequency at testing temperature T (°C)
 f_r is the reduced frequency at reference temperature T_r (°C)

$$\log(a_T(T)) = \frac{E_a}{\ln(10) \times R} \left(\frac{1}{T} - \frac{1}{T_r} \right) \quad (3.3)$$

where: $a_T(T)$ is the shift factor value for temperature T (°K)
 E_a is an activation energy term (Joules [J]/mol)
 R is the universal gas constant (J/(mol·K))
 T_r is the reference temperature (°K)

The parameters of the sigmoidal function as well as the activation energy term in the Arrhenius shift factor equation were estimated using the *Solver* feature in *Microsoft Excel* by minimizing the sum of square error between predicted and measured values.

Mix Stiffness: Flexural Modulus

Four-point-bending beam frequency sweep tests were conducted to measure the stiffness (flexural dynamic modulus) of the RHMA-G beams under different frequencies and various temperatures. Two replicates were tested at temperatures of 10°C, 20°C, and 30°C and over frequencies of 15, 10, 5, 2, 1, 0.5, 0.2, 0.1, 0.05, 0.02 and 0.01 Hz. Tests were performed in strain control mode (100 μ strain at 10°C and 20°C, and 200 μ strain at 30°C).

A sigmoidal function similar to that used to determine the dynamic modulus was used to construct the flexural dynamic modulus master curve at a reference temperature of 20°C. The shift factor equation used for generating the master curves is shown in Equation 3.4

$$\log(a_T(T)) = C \times (T - T_r) \quad (3.4)$$

where: C is a shift factor constant
 T_r is the reference temperature (°C)
 T is the testing temperature (°C)

Rutting Performance: Repeated Load Triaxial

The flow number test (AASHTO T 378) provides an indication of the resistance of an asphalt mix to permanent deformation (rutting). The accumulation of permanent deformation is assumed to occur in primary, secondary, and tertiary phases. Permanent strain typically accumulates rapidly in the primary phase, followed by a lower constant rate through the secondary phase, and then accumulates rapidly again in the tertiary phase. The flow number is defined as the number of cycles at which the tertiary phase starts. Higher flow number values imply that a mix has better rutting (permanent deformation) resistance. In this study, unconfined specimens were subjected to a repeated compressive deviator stress of 600 kPa (87 psi) and a 30 kPa (4.4 psi) contact stress. The resulting cumulative permanent deformation versus the number of loading cycles was recorded with flow number calculations performed automatically by the AMPT software. The numbers of cycles to 1%, 3%, and 5% permanent axial strain were also analyzed to obtain a better understanding of the likely rutting behavior of each of the mixes. According to the test method, the selected testing temperature should be based on the adjusted high PG temperature of the binder identified for the pavement location. Since testing for specific project locations was not included as part of the workplan, all tests were performed at 52°C to obtain a good understanding of how damage accumulated during the test. Running the test at higher temperatures (e.g., 64°C or the high PG temperatures determined in Chapter 4) could have resulted in accelerated evolution of permanent deformation, which would not provide a comprehensive indication of how damage accumulated with load repetition. Running the test at lower temperatures would extend the testing time but would probably not provide any additional useful information.

Cracking Performance: Four-Point Beam

The beam fatigue test (AASHTO T 321) provides an indication of the resistance of an asphalt mix to fatigue cracking at a constant deformation (strain). Beam specimens are subjected to four-point bending by applying sinusoidal loading at three different strain levels (high, intermediate, and low) at a frequency of 10 Hz and temperature of 20°C (68°F). The fatigue life for each strain level was selected by multiplying the maximum stiffness value for that strain level by the number of cycles at which that stiffness value occurred. Laboratory test results will generally correspond with field fatigue or reflection cracking performance for overlays thinner than about 75 mm (0.25 ft.) but may not correspond with expected field performance for thicker layers of asphalt.

For thicker layers, the interaction of the pavement structure, traffic loading, temperature, and mix stiffness with the controlled-strain beam fatigue results needs to be simulated using mechanistic analysis in order to rank mixes for expected field performance.

In this UCPRC study, the testing approach currently specified in AASHTO T 321 was modified to optimize the quantity and quality of the data collected. Replicate specimens were first tested at high- and medium-strain levels to develop an initial regression relationship between fatigue life and strain (Equation 3.5). Strain levels were selected, based on experience, to achieve fatigue lives between 10,000 and 100,000 load cycles and between 300,000 and 500,000 load cycles for high and medium strains, respectively. Additional specimens were then tested at lower-strain levels selected based on the results of the initial linear regression relationship to achieve a fatigue life of about 1 million load repetitions. The final regression relationship was then refined to accommodate the measured stiffness at the lower strain level.

$$\ln N = A + B \times \varepsilon \quad (3.5)$$

where: N is fatigue life (number of cycles)
 ε is the strain level (microstrain [μ strain])
 A and B are model parameters

Cracking Performance: Semicircular Bend

The semicircular bend (SCB) test can be used to determine the fracture resistance parameters of asphalt mixtures at intermediate temperature and to rank the cracking resistance of asphalt mixtures containing different binders, modifiers, aggregate gradations, and recycled asphalt pavement. The UCPRC is currently investigating the SCB and other simple cracking tests that relate to beam fatigue test results and can be used for mix design, quality control, and quality assurance purposes. The SCB fracture energy (G_f) and flexibility index (FI) test parameters were selected to compare the performance of mixes. Fracture energy is the area under the load-displacement curve and shows the overall resistance of the mix to crack-related damage. The flexibility index is calculated from the fracture energy and post-peak slope of the load-displacement curve that represents the average crack growth rate. Increasing fracture energy and flexibility index implies increasing cracking resistance that can be used to identify brittle mixes.

4. BINDER TESTING

4.1 Introduction

This chapter covers preliminary rheology testing to determine the high-, intermediate-, and low-temperature performance grades of five plant-produced asphalt rubber binders and the five virgin binders used to produce them.

4.2 Rubber Gradations

Rubber gradation results are summarized in Table 4.1. Although different across the different sieves, all gradations were considered reasonable. Maximum particle sizes met Caltrans specification requirements.

Table 4.1: Rubber Gradations Used in Plant-Produced Binders

Sieve Size (mm)	Sieve Size (US)	Percent Passing				
		BUT-162	MER-33	LAK-20	INY-395	IMP-111
2.36	#8	100.0	100.0	100.0	100.0	100.0
2.0	#10	100.0	99.9	100.0	99.5	100.0
1.18	#16	74.0	66.2	82.2	59.4	76.8
0.6	#30	45.8	40.2	40.2	31.7	42.2
0.3	#50	13.3	10.5	8.8	11.5	15.1
0.15	#100	1.9	1.6	0.9	2.8	4.3
0.075	#200	0.6	0.2	0.1	1.4	1.2
Max. particle size (mm)		1.6	2.0	2.0	2.3	1.6

4.3 High-Temperature Testing

Results of the high-temperature grade tests on the five asphalt rubber binders are listed in Table A.1 through Table A.10 in Appendix A. High temperature and true grade results for the base and asphalt rubber binders are summarized in Table 4.2.

Table 4.2: High-Temperature Grade and True Grade Results

Source	Base Binder		Asphalt Rubber Binder			
	High PG	True Grade	Concentric Cylinder (°C)		Parallel Plate (3 mm Gap [°C])	
			High PG	True Grade	High PG	True Grade
BUT-162	64	66.9	94	99.8	100	103.1
MER-33	64	65.4	82	84.8	82	86.0
LAK-20	64	67.6	94	99.8	100	101.9
INY-395	64	65.5	76	81.9	82	83.4
IMP-111	64	68.2	88	88.1	88	89.9

4.3.1 Base Binders

High-temperature PG and average true grade results for the five base binders are plotted in Figure 4.4. Test results ($G^*/\sin[\delta]$) for the unaged and RTFO-aged binders at 64°C and 70°C are plotted in Figure 4.2 and Figure 4.3, respectively. All of the binders had a high temperature PG of 64°C. True grades varied between 65.4 and 68.2, all higher than the PG.

4.3.2 Asphalt Rubber Binders

Performance grade and average true grade of the asphalt rubber binders are plotted in Figure 4.4. Results for the unaged and RTFO-aged binders tested with both concentric cylinder and parallel plate geometries are plotted in Figure 4.5 through Figure 4.8. Error bars on the results in these two plots indicate the range (highest and lowest) measured across the replicate samples tested. The percent difference in $G^*/\sin(\delta)$ between the concentric cylinder and parallel plate geometries, calculated using the formula in Equation 4.1, are shown in Figure 4.9 and Figure 4.10 for unaged and RTFO-aged samples, respectively. The differences in midpoint $G^*/\sin(\delta)$ for the two geometries are shown in Figure 4.11 and Figure 4.12 for the unaged and RTFO-aged binders, respectively.

$$\frac{PP[G^*/\sin(\delta)] - CC[G^*/\sin(\delta)]}{CC[G^*/\sin(\delta)]} \times 100 \quad (4.1)$$

A review of the data led to the following observations:

- All of the asphalt rubber binders had higher high-temperature PGs than their respective base binders, with two of the binders (BUT-162 and LAK-20) testing at five grades higher than their respective base binders using concentric cylinder geometry and six grades higher using parallel plate geometry. One binder (IMP-111) tested four grades higher (both geometries), one (MER-33) tested three grades higher (both geometries), and one tested two grades higher than the corresponding base binder. Grades higher than 82 (maximum in AASHTO M 320) are considered to be unrealistically high and probably not a true indication of likely high-temperature performance (i.e., rut resistance under heavy loads on hot days).
- True grades varied between 81.9 and 99.8 using concentric cylinder geometry and between 83.4 and 103.1 using parallel plate geometry. True grade rankings were the same for the two geometries. No clear reasons for the significant differences across the five binders were identified. However, the ranking of true grades tested with the concentric cylinder geometry was consistent with the ranking of those of the base binders and with the percent passing the #16 [1.18 mm] sieve (i.e., higher percent passing had higher PG).

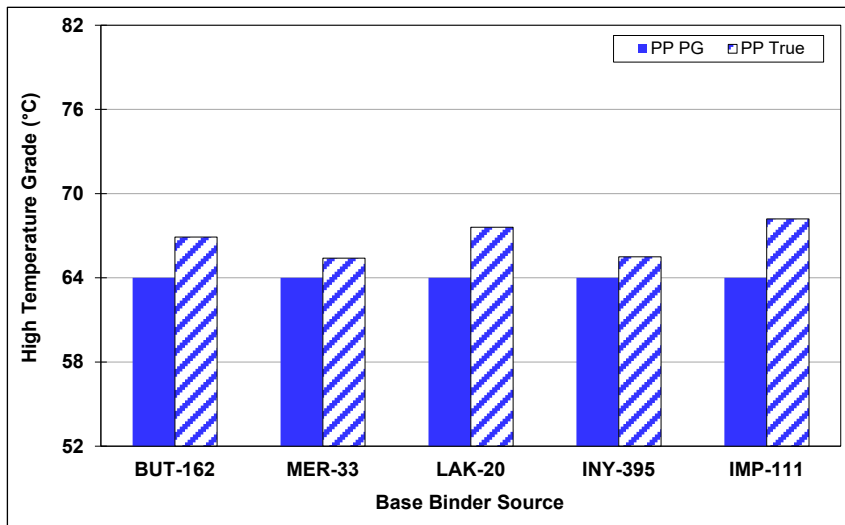


Figure 4.1: Base binder high-temperature grade and true grade.

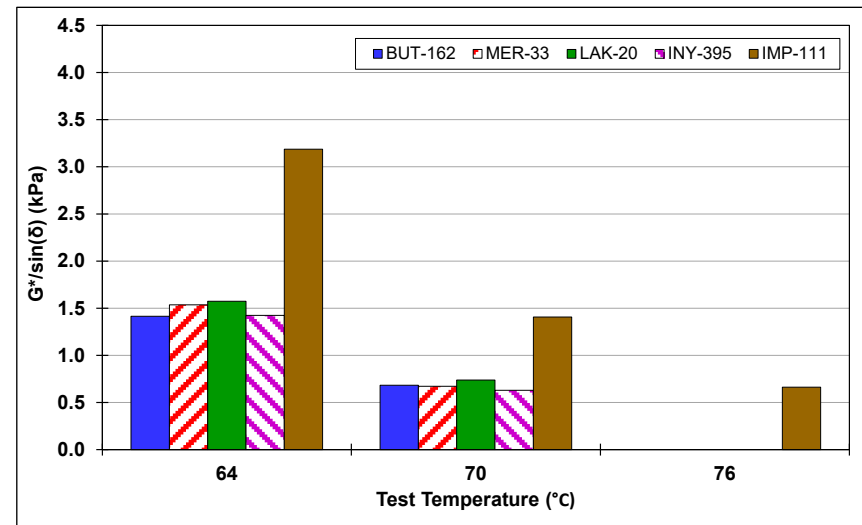


Figure 4.2: Base binder unaged high-temperature.

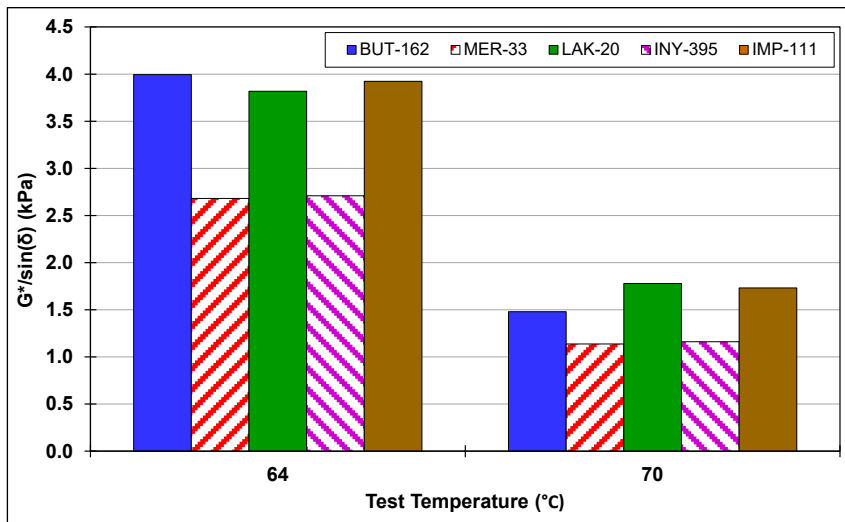


Figure 4.3: Base binder RTFO-aged high-temperature.

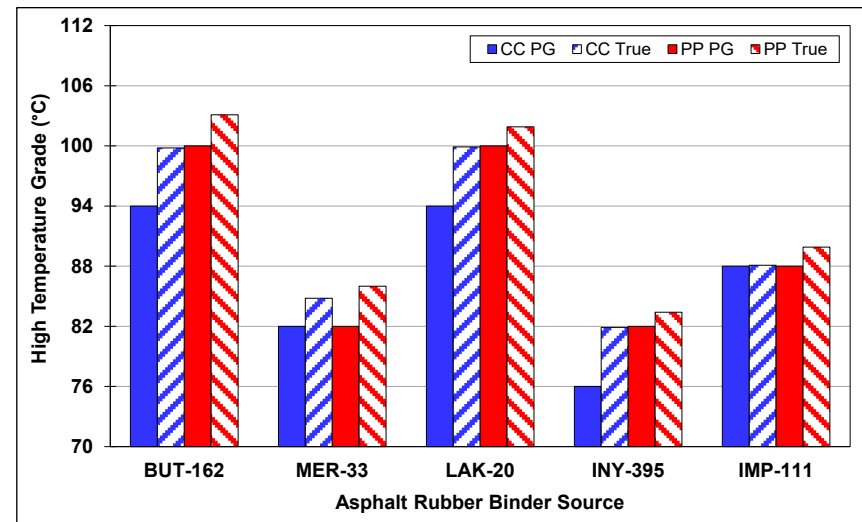


Figure 4.4: AR binder high-temperature grade and true grade.

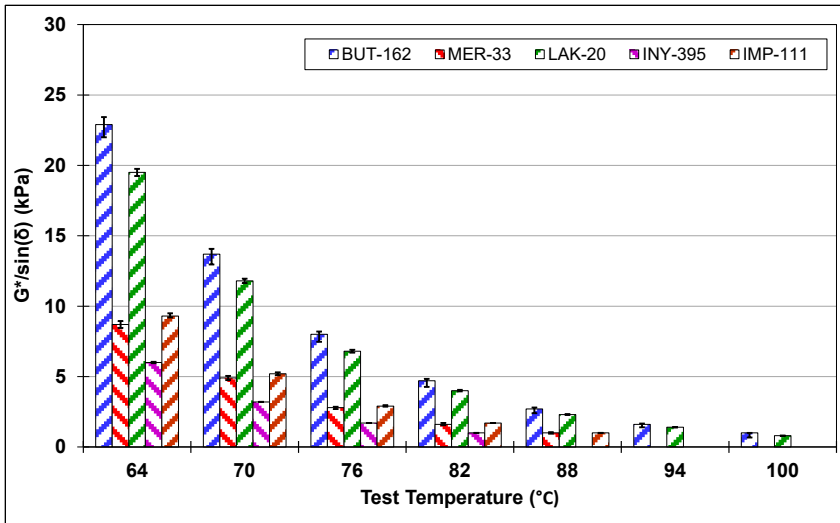


Figure 4.5: AR binder high temperature (unaged): Concentric cylinder.

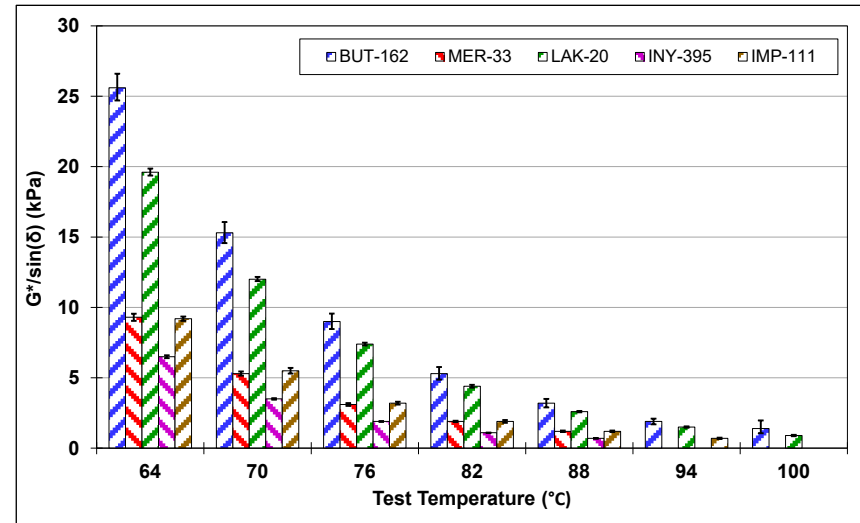


Figure 4.6: AR binder high temperature (unaged): Parallel plate.

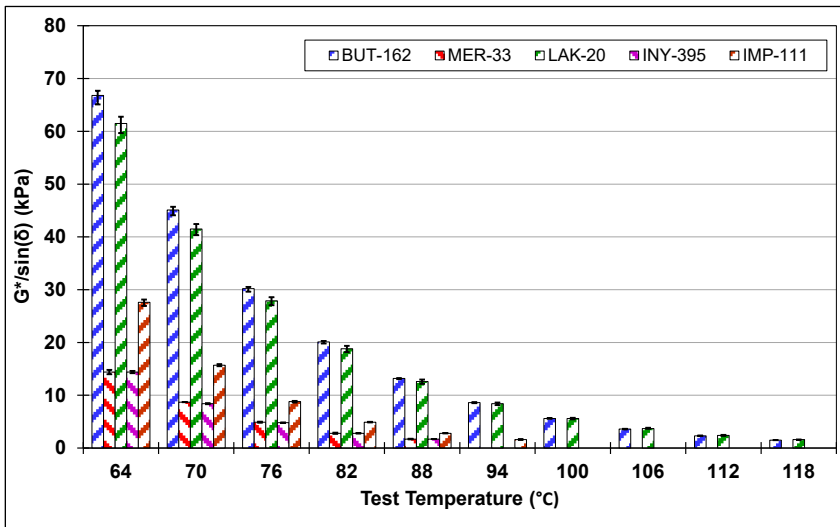


Figure 4.7: AR binder high temperature (RTFO-aged): Concentric cylinder.

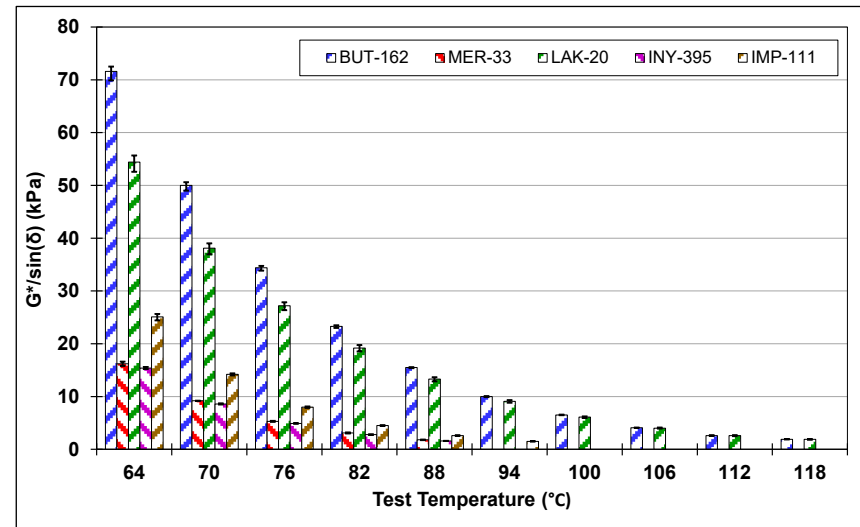


Figure 4.8: AR binder high temperature (RTFO-aged): Parallel plate.

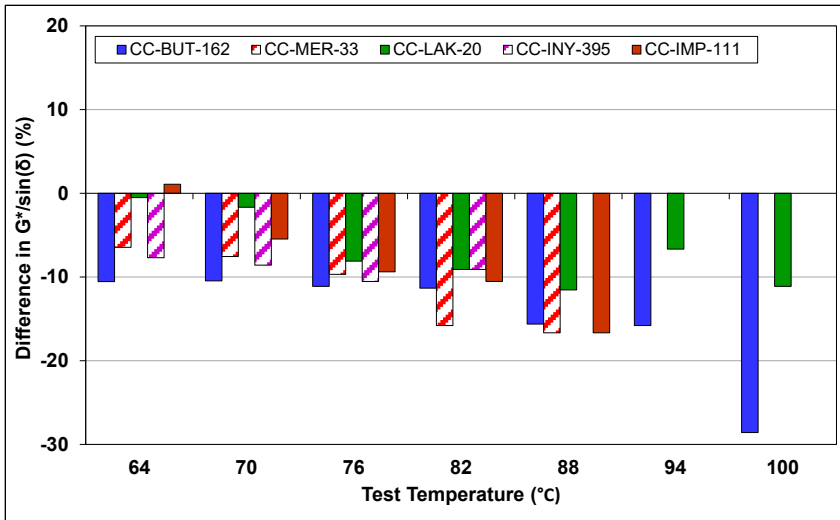


Figure 4.9: AR binder high temperature (unaged): Difference between DSR geometries.

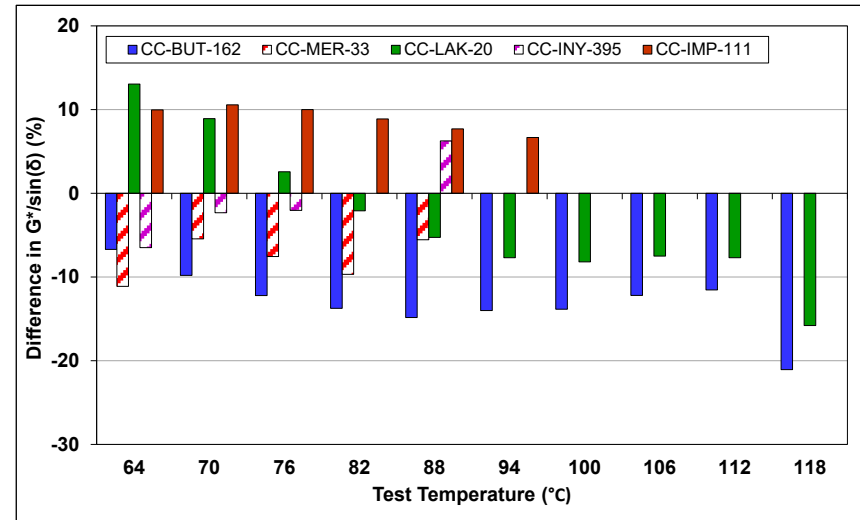


Figure 4.10: AR binder high temperature (RTFO-aged): Difference between DSR geometries.

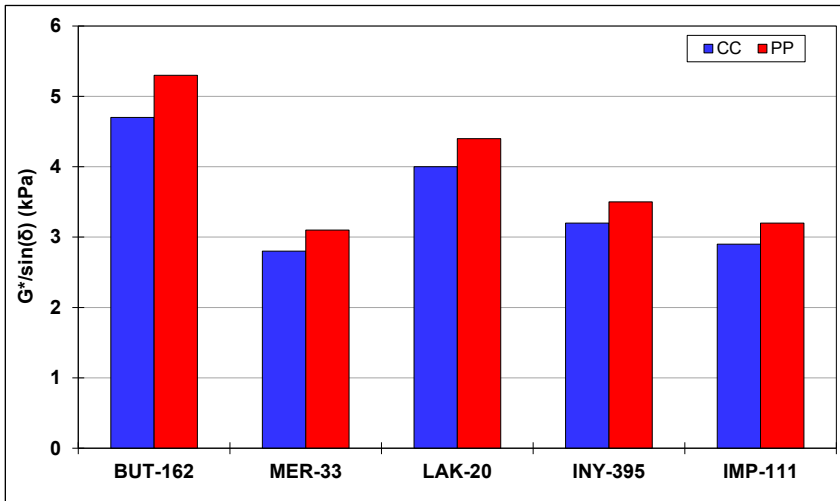


Figure 4.11: AR binder high temperature (unaged): Difference in mid-point $G^*/\sin(\delta)$.

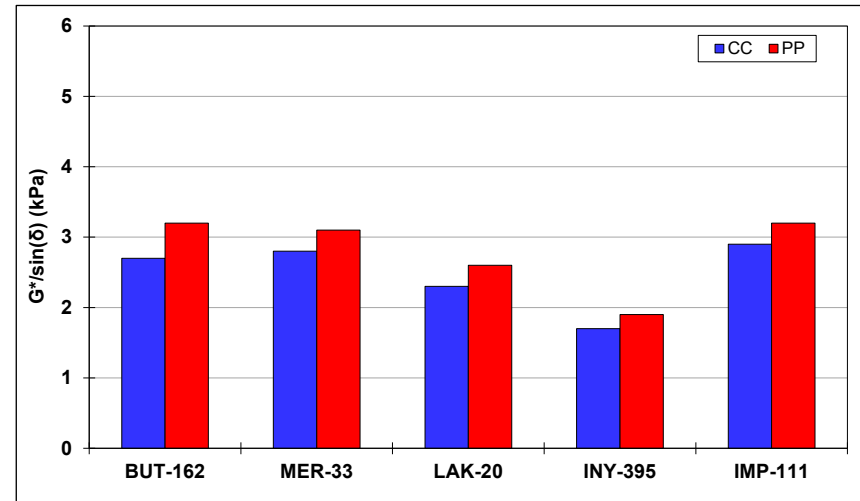


Figure 4.12: AR binder high temperature (RTFO-aged): Difference in mid-point $G^*/\sin(\delta)$.

- Testing with parallel plate geometry resulted in one grade higher high-temperature PGs on three of the five asphalt rubber binders when compared to results for testing with concentric cylinder geometry. When comparing true grades, testing with parallel plate geometry gave higher true grades for all five binders.
- Three of the five binders (BUT-162, LAK-20, and IMP-111) had PGs higher than the maximum grade of 82°C listed in the AASHTO M 320 standard.
- Stiffness/rut resistance ($G^*/\sin[\delta]$) decreased with increasing test temperature in all instances, as expected.
- Variability between replicate samples was considered to be acceptable for both geometries at both aging conditions. Variability generally decreased with increasing test temperature.
- When comparing the two geometries at individual testing temperatures on unaged binders, $G^*/\sin(\delta)$ values determined with concentric cylinder were lower than those determined with parallel plate. The difference between the two geometries increased with increasing test temperature. On RTFO-aged binders, the differences between the two geometries were inconsistent and no clear trends were apparent. Although precision and bias limits have not been determined for concentric cylinder and parallel plate with 3 mm gap geometries used for high temperature testing of asphalt rubber binders, the differences for both unaged and RTFO-aged binders are expected to be higher than the precision and bias for each geometry.
- When comparing the two geometries in terms of the midpoint testing temperature, $G^*/\sin(\delta)$ values determined with concentric cylinder were consistently lower than those determined with parallel plate, regardless of aging condition.
- Incompletely digested rubber particles likely had a considerable influence on the results for both geometries when compared to the base binders. Higher true grades measured with the parallel plate geometry were likely attributed to the effect of the incompletely digested rubber particles in the smaller gap (i.e., 3 mm versus 6 mm in the concentric cylinder).
- The results were consistent with those determined in Phase 2e (3).

4.4 Intermediate Temperature Testing

Results of the intermediate-temperature grade tests on the five asphalt rubber binders are listed in Table A.11 through Table A.15 in Appendix A. Intermediate temperature and true grade results for the base and asphalt rubber binders are summarized in Table 4.3.

Table 4.3: Intermediate-Temperature Grade and True Grade Results

Source	Base Binder		Asphalt Rubber Binder			
	Int. PG	True Grade	Concentric Cylinder (°C)		Parallel Plate (3 mm Gap [°C])	
			Int. PG	True Grade	Int. PG	True Grade
BUT-162	22	20.4	16	13.6	13	11.5
MER-33	31	29.1	22	21.2	22	19.7
LAK-20	25	22.3	22	19.9	19	17.7
INY-395	31	29.2	22	20.4	22	19.7
IMP-111	31	30.5	22	20.9	22	20.8

4.4.1 Base Binders

Intermediate-temperature PG and average true grade results for the five base binders are plotted in Figure 4.13. Test results ($G^* \times \sin[\delta]$) for the PAV-aged binders are plotted in Figure 4.14. Three of the binders had intermediate-temperature PGs of 31, one (LAK-20) had an intermediate-temperature PG of 25, and one (BUT-162) had an intermediate-temperature PG of 22. True grades varied between 20.4 and 30.5 and were all lower than the PG.

4.4.2 Asphalt Rubber Binders

Intermediate-temperature PG and average true grade of the asphalt rubber binders are plotted in Figure 4.15. Results ($G^* \times \sin[\delta]$) for the PAV-aged binders tested with both concentric cylinder and parallel plate geometries are plotted in Figure 4.16 and Figure 4.17. Error bars on the figures in these two plots indicate the minimum and maximum values of replicate tests. The percent difference in $G^* \times \sin(\delta)$ between the concentric cylinder and parallel plate geometries, calculated using the formula in Equation 4.1, are shown in Figure 4.18. The differences in midpoint $G^* \times \sin(\delta)$ for the two geometries are shown in Figure 4.19.

A review of the data led to the following observations:

- All of the asphalt rubber binders had intermediate-temperature PGs that were two or three grades lower than their respective base binders.
- Using concentric cylinder geometry, three of the binders (MER-33, INY-395, and IMP-111) tested at three grades lower than their respective base binders, one (BUT-162) tested at two grades lower, and one (LAK-20) tested at one grade lower. Using parallel plate geometry, four of the binders tested at three grades lower and one (LAK-20) tested at two grades lower. Lower intermediate temperature grades imply improved fatigue and reflective cracking resistance, which is expected when testing asphalt rubber binders.
- There were no apparent trends between intermediate PG and rubber gradation.

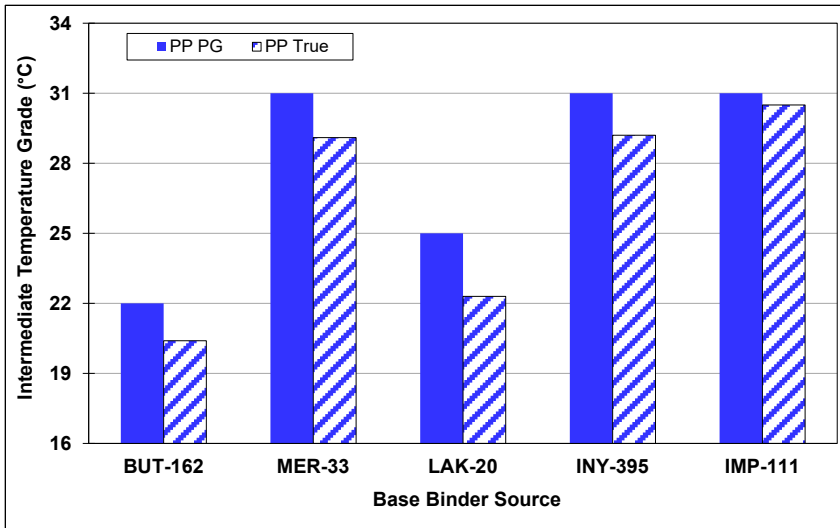


Figure 4.13: Base binder intermediate-temperature performance grade and true grade.

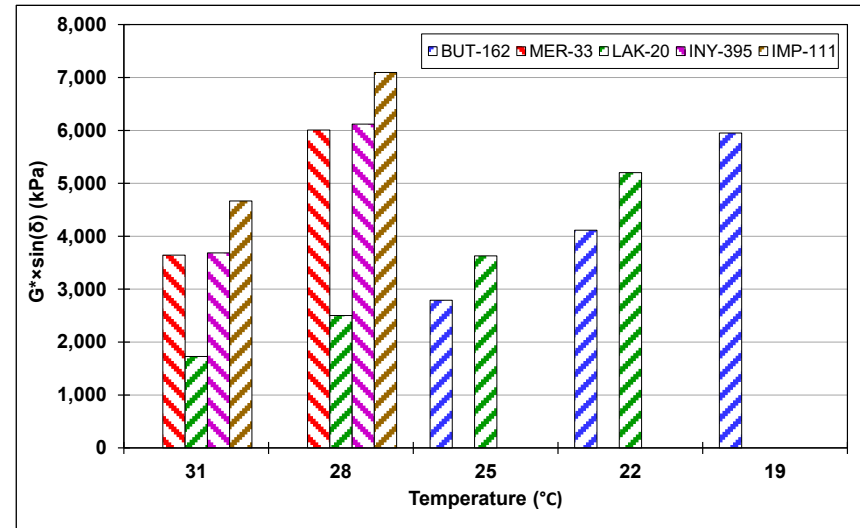


Figure 4.14: Base binder intermediate temperature.

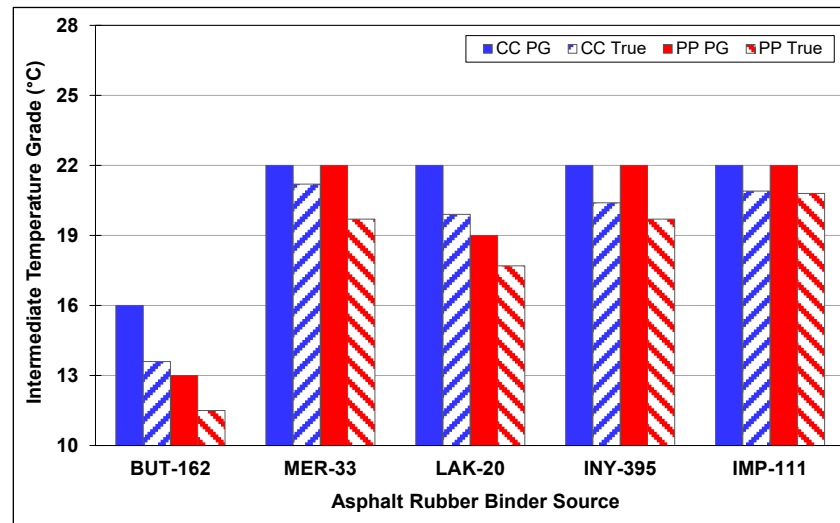


Figure 4.15: AR binder intermediate-temperature performance grade and true grade.

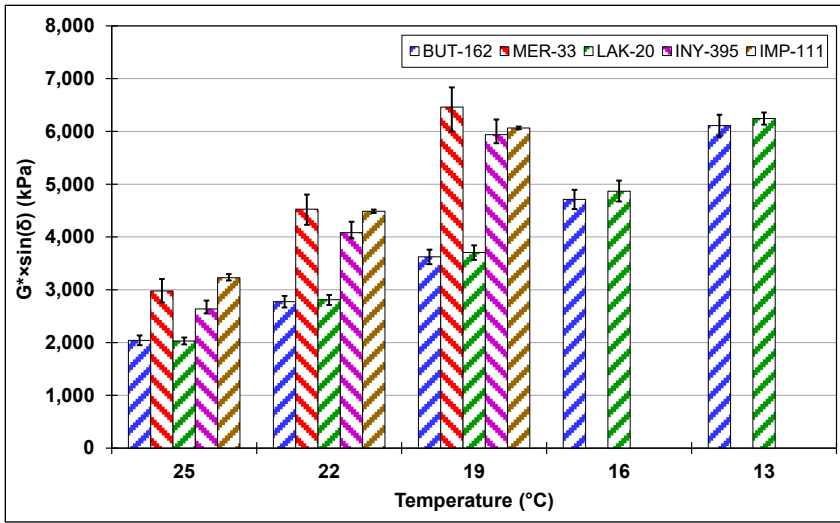


Figure 4.16: AR binder intermediate temperature: Concentric cylinder.

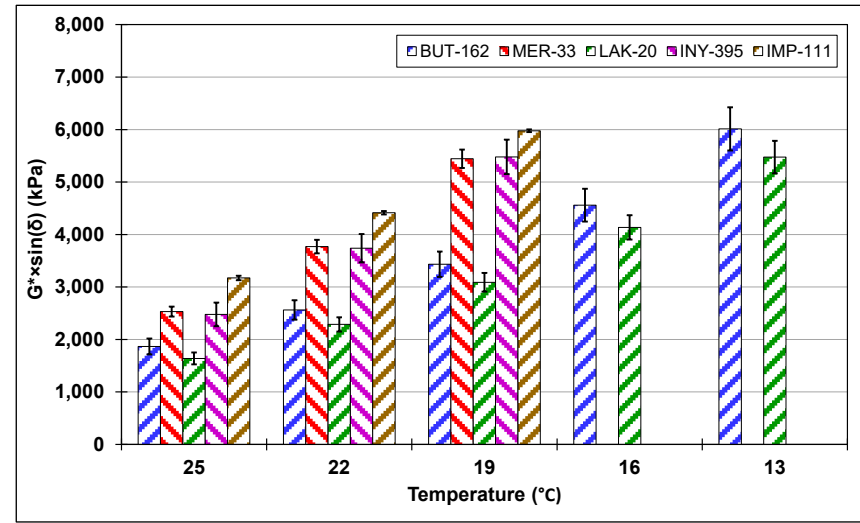


Figure 4.17: AR binder intermediate temperature: Parallel plate.

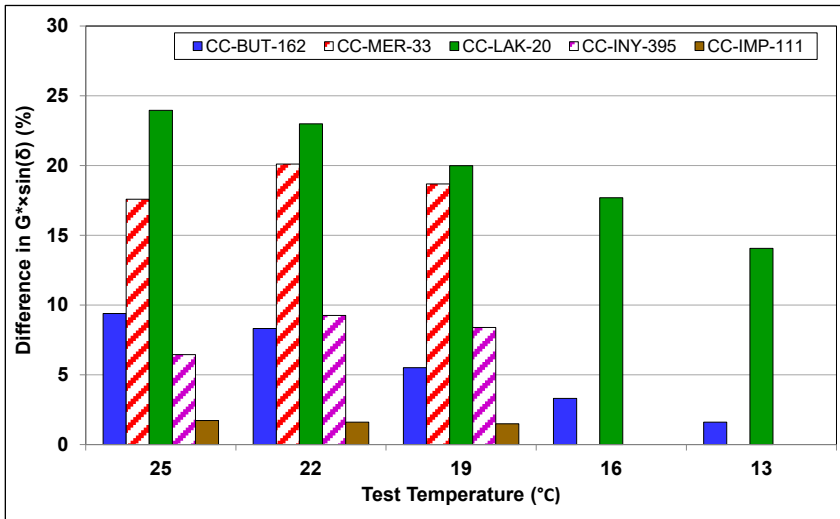


Figure 4.18: AR binder intermediate temperature: Difference between DSR geometries.

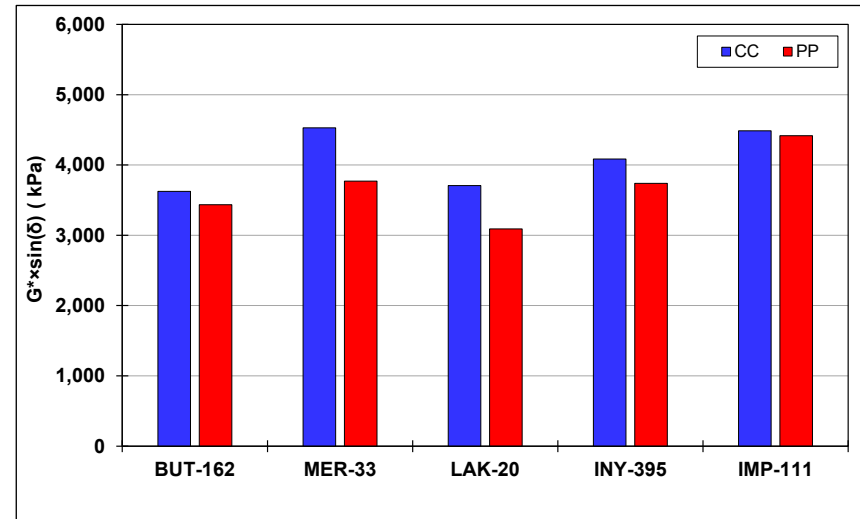


Figure 4.19: AR binder intermediate temperature: Difference in mid-point $G^* \times \sin(\delta)$.

- True grades varied between 13.6 and 21.2 using concentric cylinder geometry and between 11.5 and 20.8 using parallel plate geometry. Parallel plate true grade results were all lower than the concentric cylinder results. True grade rankings were not the same for the two geometries, and neither geometry had the same ranking as the respective base binder.
- No clear trends were observed when comparing high- and intermediate-temperature results.
- Variability between replicate samples was considered to be reasonable for both geometries.
- Fatigue resistance ($G^* \times \sin[\delta]$) decreased with decreasing test temperature in all instances, as expected.
- When comparing the two geometries at individual testing temperatures, $G^* \times \sin(\delta)$ values determined with concentric cylinder were consistently higher than those determined with parallel plate. The largest differences were recorded on the LAK-20 and MER-33 binders. The difference between the two geometries decreased with decreasing test temperature. Although precision and bias limits have not been determined for concentric cylinder and parallel plate with 3 mm gap geometries used for intermediate temperature testing of asphalt rubber binders, the differences are expected to be higher than the precision and bias for each geometry.
- When comparing the two geometries in terms of the midpoint testing temperature, $G^* \times \sin(\delta)$ values determined with concentric cylinder were consistently higher than those determined with parallel plate.
- Incompletely digested rubber particles likely had an influence on the results for both geometries when compared to the base binders. Lower values measured with the parallel plate geometry were likely attributed to the effect of the incompletely digested rubber particles in the smaller gap (i.e., 3 mm versus 9.5 mm in the concentric cylinder) and the ratio of the rubber particle size to plate diameter.

4.5 Low-Temperature Testing

Results of the low-temperature grade tests on the five asphalt rubber binders are listed in Table A.16 in Appendix A. Low-temperature and true grade results for the base and asphalt rubber binders are summarized in Table 4.4.

4.5.1 Base Binders

Low-temperature PG and average true grade results for the five base binders are plotted in Figure 4.20. Stiffness and m-value test results are plotted in Figure 4.21 and Figure 4.22, respectively. Three of the base binders (MER-33, INY-395, and IMP-111) had low-temperature

PGs of -16 and the other two graded at -22. True grades varied between -18.1 and -26.8, all lower than the PG. Grades were dictated by the m-value (i.e., ≥ 0.30) for all base binders.

Table 4.4: Low-Temperature Grade and True Grade Results

Source	Base Binder		Asphalt Rubber Binder	
	Low PG	True Grade	Low PG	True Grade
BUT-162	-22	-25.1	-22	-27.0
MER-33	-16	-18.1	-22	-23.8
LAK-20	-22	-26.8	-22	-26.7
INY-395	-16	-18.4	-22	-27.7
IMP-111	-16	-18.4	-22	-26.2

4.5.2 Asphalt Rubber Binders

Low-temperature PG and average true grade results for the five asphalt rubber binders are plotted in Figure 4.23. Stiffness and m-value test results are plotted in Figure 4.24 and Figure 4.25, respectively.

A review of the data led to the following observations:

- All of the asphalt rubber binders had the same low-temperature PGs (-22). Two of the binders (BUT-162 and LAK-20) had the same PG as their respective base binders; the other three binders tested one grade lower than their respective base binders.
- True grades varied between -23.8 and -27.7, all lower than the PG. True grade rankings of the asphalt rubber binders were not the same as the base binder rankings.
- Low-temperature cracking resistance decreased with decreasing test temperature in all instances, as expected.
- Stiffness values were well below the AASHTO M 320 criteria for determining the low-temperature grade ($S \leq 300$) and, consequently, grades were dictated by the m-value (≥ 0.30). The presence of incompletely digested rubber particles and potential phase separation between these particles and the asphalt binder probably contributed to the low stiffness values.
- There were no apparent trends between low-temperature PG and rubber gradation.
- Variability between replicate specimens was attributed in part to the rougher beam surfaces after trimming and to variation in the number, size, and degree of digestion of the rubber particles in each beam.
- The AASHTO M 320 procedure contains no recommendations for asphalt rubber binders. The minimum low-temperature grade in the standard table for conventional binders with a high-temperature grade equal to or greater than 76°C is -22°C, which was achieved for all five binders.

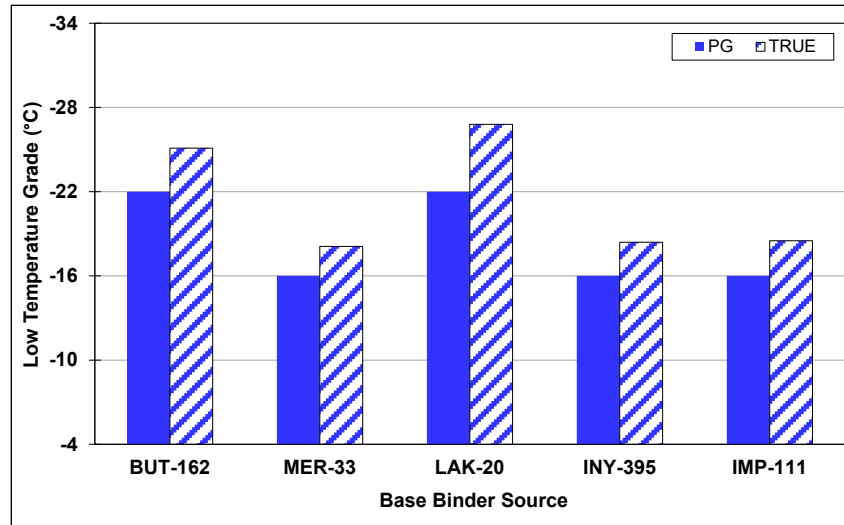


Figure 4.20: Base binder: Low-temperature performance grade and true grade.

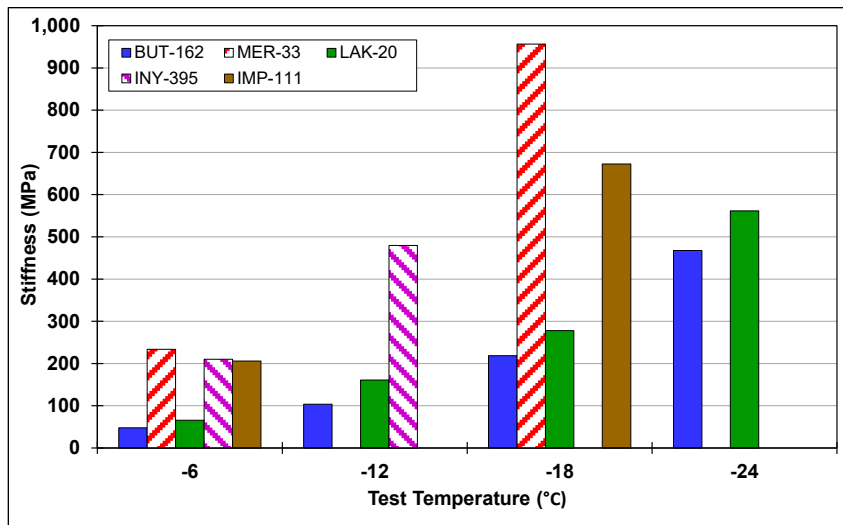


Figure 4.21: Base binder: Low-temperature stiffness.

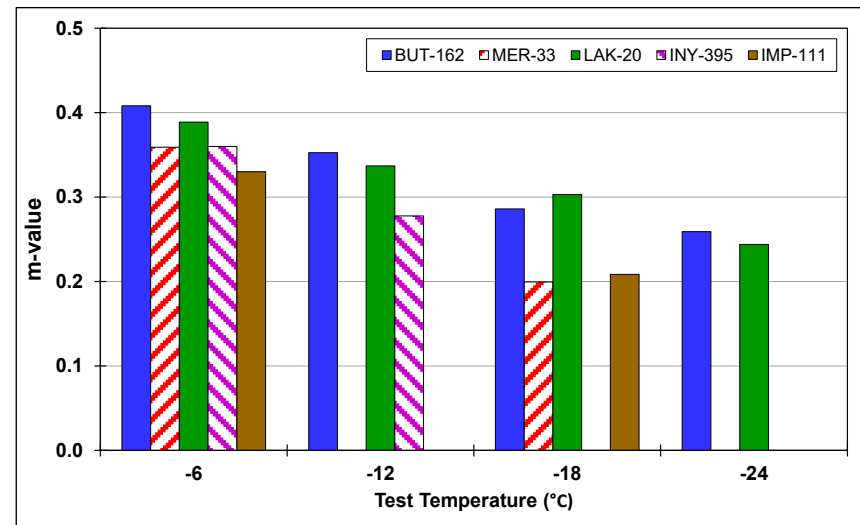


Figure 4.22: Base binder: Low-temperature m-value.

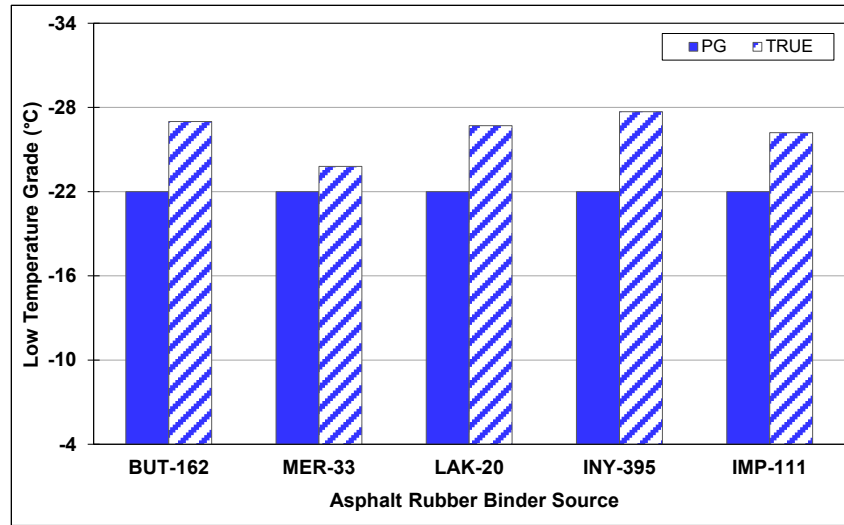


Figure 4.23: AR binder: Low-temperature performance grade and true grade.

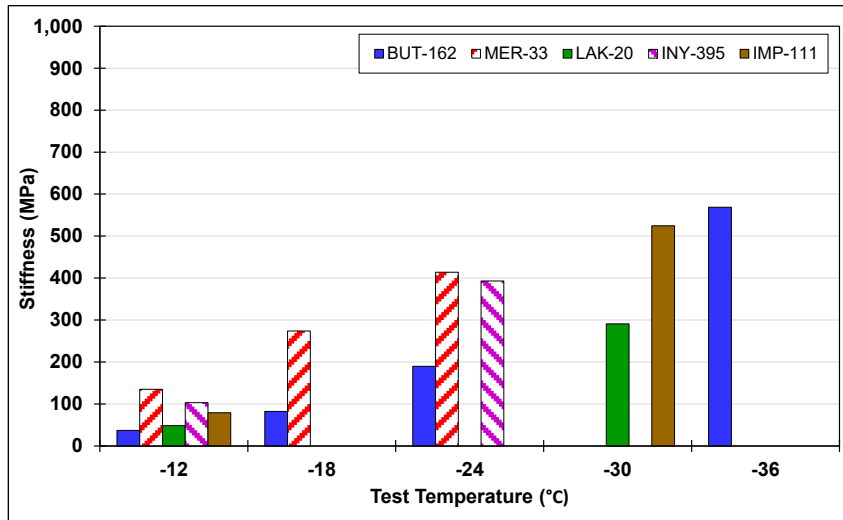


Figure 4.24: AR binder: Low-temperature stiffness.

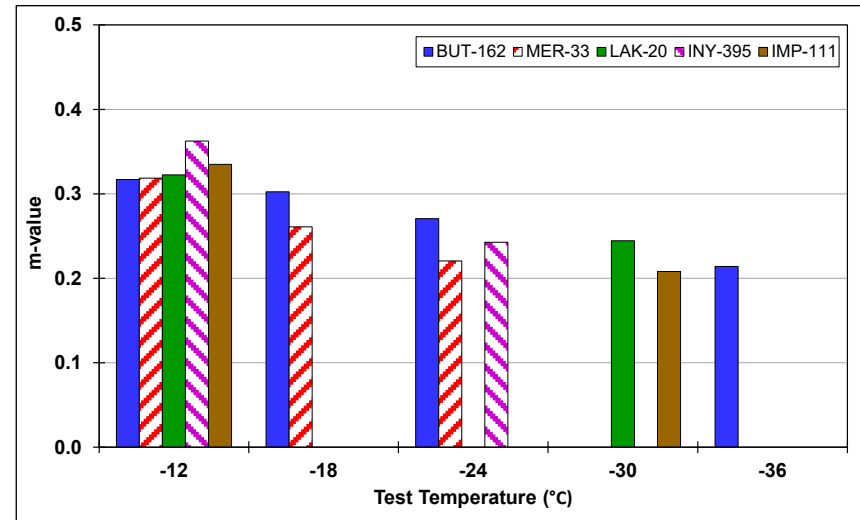


Figure 4.25: AR binder: Low-temperature m-value.

- Questions regarding other factors that may influence results, and specifically the variability between results, include:
 - + Whether changes in the properties of the incompletely digested rubber particles occur at very low temperatures (i.e., in the range of glass transition)
 - + Whether different rubber particles (e.g., synthetic versus natural rubber) have different coefficients of thermal expansion
 - + Whether the properties of the rubber particles are in any way effected by the type of temperature control medium used in the bending beam rheometer (i.e., ethanol for the testing discussed in this report).

Critical temperatures (ΔT_c) for the five base and asphalt rubber binders are plotted in Figure 4.26. The generally recommended minimum ΔT_c for unmodified binders is -5.0°C (7). No minimum ΔT_c has been recommended for asphalt rubber binders, but it is acknowledged that values determined for modified binders (polymer and rubber) may not be a true reflection of cracking performance.

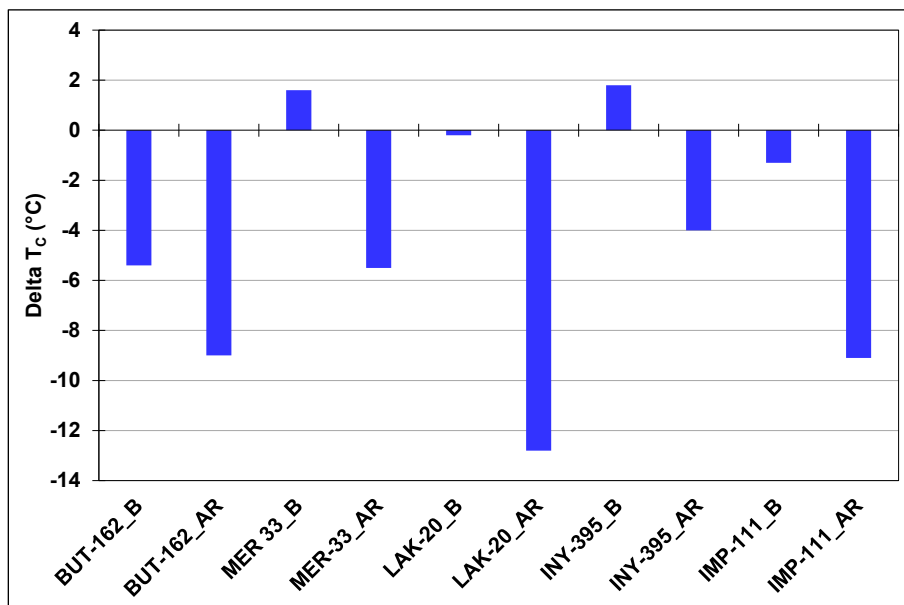


Figure 4.26: ΔT_c of base and asphalt rubber binders.

A review of the data led to the following observations:

- ΔT_c values for the base binders varied between $+1.8$ and -5.4 and between -4 and -12.8 for the asphalt rubber binders.
- Four of the base binders met the minimum recommended -5.0 value for unmodified binders, with one binder (BUT-162) slightly lower at -5.4 . Only one of the asphalt rubber binders met this criterion, suggesting that further studies relating ΔT_c to field-cracking

performance of RHMA-G mixes are required before any conclusions can be drawn with regard to whether -5.0 is an appropriate value for asphalt rubber binders.

- Delta T_C values for the asphalt rubber binders ranked the same as the high temperature true grade (highest to lowest).

4.6 Multiple Stress Creep Recovery Testing

Results of the multiple stress creep recovery (MSCR) tests on the five asphalt rubber binders are listed in Table A.17 in Appendix A.

4.6.1 Base Binders

Although the MSCR test was developed primarily for quantifying the benefits of modified binders (polymer and rubber), the base binders were also tested for comparative purposes. Average percent recovery and non-recoverable creep compliance (J_{nr}) for the base binders are plotted in Figure 4.27 and Figure 4.28, respectively. A review of the data led to the following observations:

- The average percent recoveries of three of the base binders tested at the low stress level (0.1 kPa) were generally consistent, but two (MER-33 and INY-395) had very low recoveries, consistent with unmodified binders.
- Variability in average percent recovery between replicates of the same base binder samples was small at both stress levels.
- The non-recoverable creep compliance showed some variation across the different base binders with little difference between the two stress levels. Creep compliance at 3.2 kPa was higher than that at 0.1 kPa for all binders, as expected.

4.6.2 Asphalt Rubber Binders

Average percent recovery and non-recoverable creep compliance (J_{nr}) for the asphalt rubber binders are plotted in Figure 4.29 and Figure 4.30, respectively. Error bars on the figures indicate the minimum and maximum values of replicate tests. A review of the data led to the following observations:

- Average percent recoveries of the asphalt rubber binders were generally consistent across four of the five binders, with the INY-395 binder about 20% lower than the other binders when tested with concentric cylinder geometry and about 10% lower when tested with parallel plate geometry.
- Average percent recoveries tested with parallel plate geometry were slightly higher than those tested with concentric cylinder geometry for both stress levels. Exceptions were the MER-33 binder tested at 0.1 kPa and the IMP-111 binder tested at both 0.1 and 3.2 kPa. However, these differences are probably within the precision and bias of the tests.

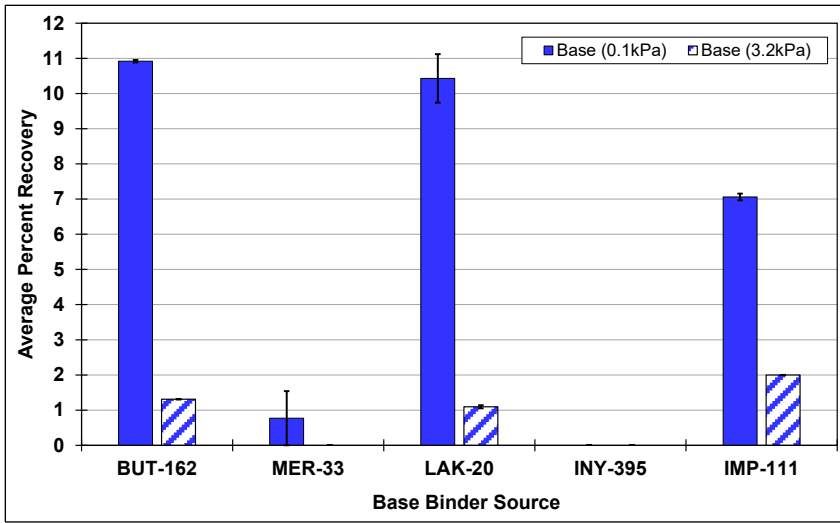


Figure 4.27: Base binder: Average percent recovery at 64°C.

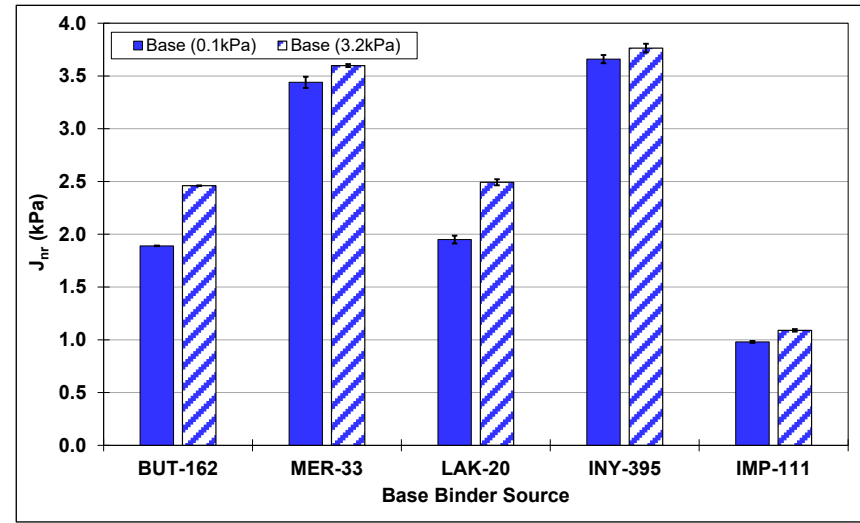


Figure 4.28: Base binder: Non-recoverable creep compliance at 64°C.

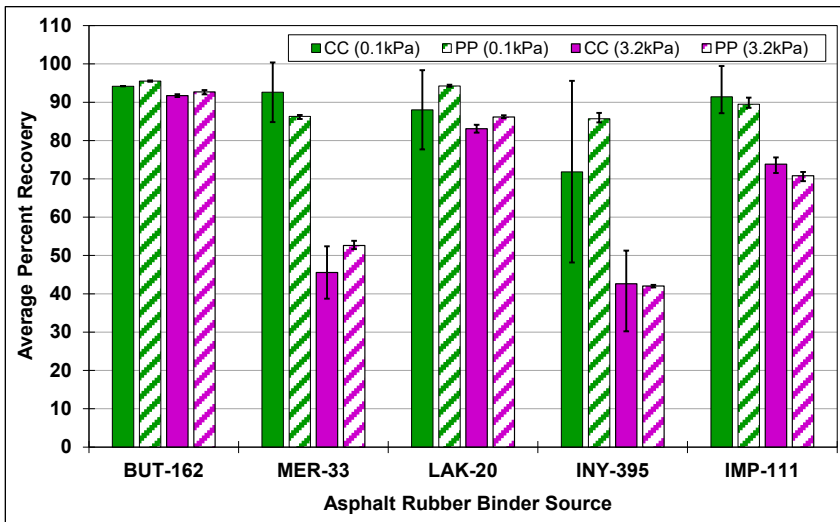


Figure 4.29: AR binder: Average percent recovery at 64°C.

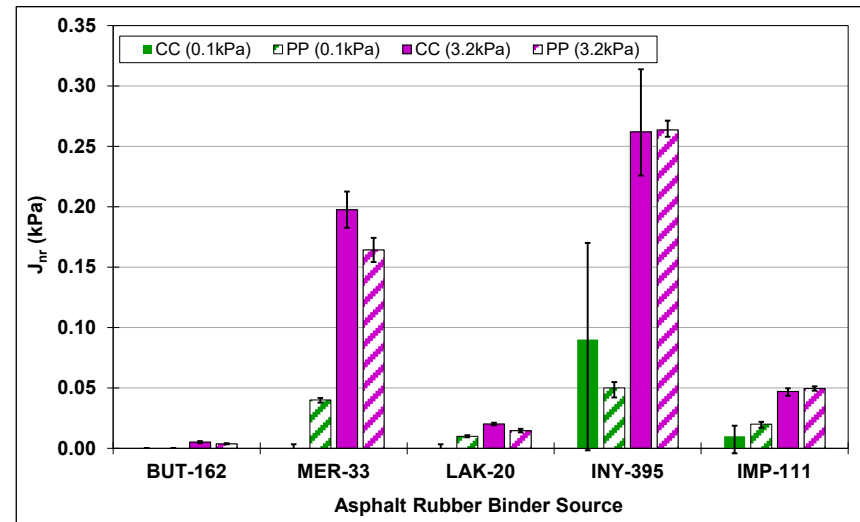


Figure 4.30: AR binder: Non-recoverable creep compliance at 64°C.

- Variability in average percent recovery of the asphalt rubber binders was higher than the base binders, with results tested with concentric cylinder geometry appearing to be more variable than those tested with parallel plate geometry. Compression of larger incompletely digested rubber particles between the parallel plates may have contributed to the lower variability.
- The asphalt rubber binders had significantly lower creep compliances than their respective base binders, as expected. When tested at 0.1 kPa, non-recoverable creep compliance was close to zero for all binders except INY-395.
- Rankings (highest to lowest) of non-recoverable creep compliance at 3.2 kPa were the same as the high temperature true grade (lowest to highest) and the same as Delta T_c (lowest to highest) for the INY-395, MER-33, and IMP-111 binders. The LAK-20 and BUT-162 binders changed places in this ranking.
- There were no apparent trends between MSCR and rubber gradation.
- Variability in non-recoverable creep compliance at 0.1 kPa was very low between replicates of the same sample. At 3.2 kPa, three of the binders had low variability, while the MER-33 and INY-395 had higher variability between replicates.
- The difference in non-recoverable creep compliance between the two geometries was generally small with no clear trends.
- None of the asphalt rubber binders passed the AASHTO M 322 grading criteria (these criteria were developed for modified binders with particles no larger than 500 μm), indicating that the presence of incompletely digested rubber particles likely influenced the results.

4.7 Discussion

Testing in this phase of the study provided results that were consistent with those obtained during preliminary testing in Phase 2e of the larger study investigating performance-based specifications for asphalt rubber binders (3). Although the low-temperature performance grades appeared to be reasonable, the high-temperature grades appeared to be unrealistically high, while the intermediate-temperature grades appeared to be potentially lower than anticipated, when compared to the base binders. A comparison of the concentric cylinder and parallel plate (3 mm gap) geometries indicate that the results between the two geometries are different and are likely to be higher than the precision and bias of the individual procedures. Precision and bias statements for these procedures had not been developed at the time of preparing this report.

Consistent trends in results were observed between high temperature PG/true grade, Delta T_c, and non-recoverable creep compliance at 3.2 kPa (Table 4.5).

Table 4.5: Rankings of Select Binder Testing Results

Rank	High True Grade	Int. True Grade	m-Value at -12°C	Delta T _c	Jnr at 3.2 kPa
1	LAK-20	MER-33	INY-395	INY-395	INY-395
2	BUT-162	IMP-111	IMP-111	MER-33	MER-33
3	IMP-111	INY-395	LAK-20	IMP-111	IMP-111
4	MER-33	LAK-20	MER-33	BUT-162	LAK-20
5	INY-395	BUT-162	BUT-162	LAK-20	BUT-162

Observations in Phase 2e and during this phase of the study indicated that incompletely digested rubber particles appeared to have a dominant influence on results and caused variability between results, regardless of the testing geometry used. Considering these incompletely digested particles as part of a homogenous binder may therefore not be appropriate when determining performance grades. Phase 3 of the study is therefore investigating the extent to which these incompletely digested particles might affect performance grading results along with testing procedures to overcome the problems. The study is focusing on removal of larger incompletely digested particles from the binder by sieving or centrifuging and then testing the binders following standard performance grading procedures using parallel plate geometry with either 1 mm or 2 mm gaps. Results after removal of particles larger than 250, 500, and 850 μm are being compared with unprocessed binders. The five asphalt rubber binders tested in this phase of the study are being retested in Phase 3 to assess the removal of larger incompletely digested rubber particles on performance grades.

5. MIX TESTING

5.1 Introduction

This chapter covers preliminary mix testing to develop a database of stiffness, permanent deformation, and cracking test results against which binder test results can be compared. These comparisons will be used in Phase 3 of the study to determine whether the performance grades (PGs) determined from the binder testing are representative of actual expected performance, or whether they need to be adjusted accordingly.

5.2 Specimen Air-Void Contents

Air-void contents (based on saturated surface-dry bulk specific gravity) for the specimens compacted in a Superpave gyratory compactor (cylindrical AMPT and SCB specimens) and with a rolling-wheel compactor (beam specimens) are listed in Table B.1, Table B.2, and Table B.3, respectively in Appendix B. Averages and standard deviations for the AMPT, SCB, and beam specimens are shown in Figure 5.1. Whiskers on the data show the lowest and highest air-void contents of the replicate specimens.

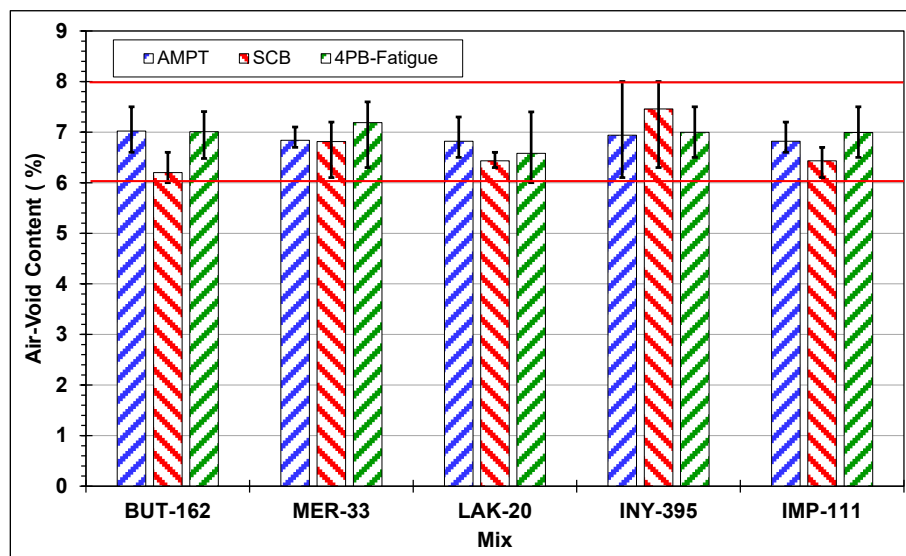


Figure 5.1: Specimen air-void contents.

All specimens were within the target limits ($7.0 \pm 1.0\%$), indicating that consistent compaction was achieved. However, some specimens had air-void contents close to the limits. Any potential influences of air-void content were considered during analysis of the results.

5.3 Mix Stiffness: AMPT Dynamic Modulus

Dynamic modulus test results are listed in Table B.4 and Table B.5 in Appendix B. Table 5.1 lists the function parameters (Equation 3.1) used in the Arrhenius shift factor equation (Equation 3.3) to determine the master curves for the evaluated mixes, which are shown in Figure 5.2.

Table 5.1: Dynamic Modulus Master Curve Parameters

Mix	Master Curve Parameters			
	δ (MPa)	α	β	γ
BUT-162	-2.00978	6.54885	-1.62476	-0.23620
MER-33	-2.98884	7.38279	-1.89871	-0.35582
LAK-20	+0.37438	3.91528	-1.32789	-0.33064
INY-395	-1.30564	5.67048	-1.54182	-0.39657
IMP-111	+0.38196	3.92519	-1.51476	-0.36474

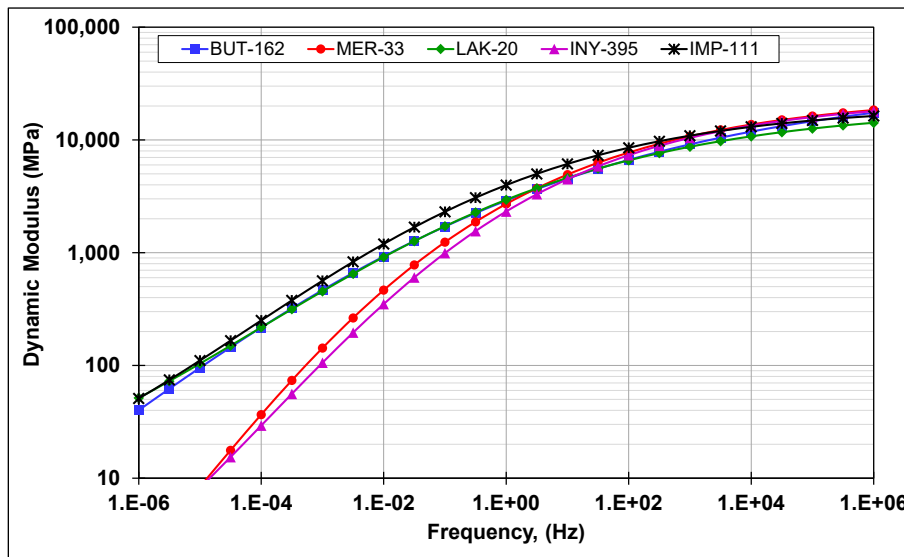


Figure 5.2: Dynamic shear modulus master curves.

The stiffness results for the BUT-162, LAK-20, and IMP-111 mixes were similar to each other and were consistent with those measured on typical RHMA-G mixes. The MER-33 and INY-395 mixes had similar stiffnesses to the other three mixes at the medium to higher frequencies, but notably lower stiffnesses at the medium to lower frequencies. This implies that the MER-33 and INY-395 mixes could be susceptible to rutting at higher temperatures.

5.4 Mix Stiffness: Flexural Modulus

Table 5.2 lists the sigmoidal function parameters (Equation 3.3) to determine the master curves for the evaluated mixes.

Table 5.2: Flexural Modulus Master Curve Parameters

Mix	Master Curve Parameters			
	δ (kPa)	α	β	γ
BUT-162	2.30103	1.62031	0.37267	0.69252
MER-33	2.30103	1.63938	0.40434	0.95376
LAK-20	2.30103	1.57744	0.12049	0.70529
INY-395	2.30103	1.53835	0.99232	1.06779
IMP-111	2.30103	1.60423	0.00868	0.69196

Flexural modulus test results are listed in Table B.6 in Appendix B. Figure 5.3 shows the flexural modulus master curves for the different RHMA-G mixes. Results for four of the mixes were similar to each other and were consistent with those measured on typical RHMA-G mixes. The INY-395 mix had marginally lower stiffnesses in the mid to lower frequencies indicating the potential for mix sensitivity at intermediate temperatures.

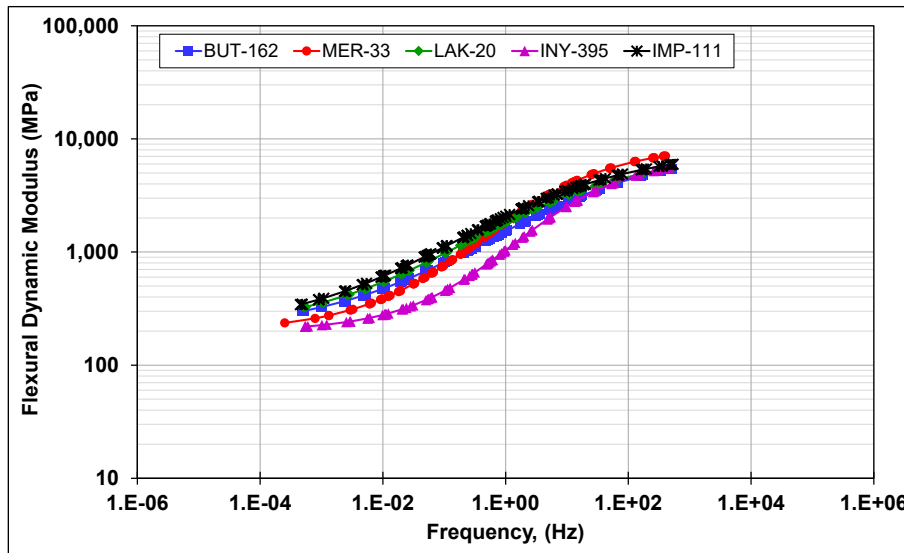


Figure 5.3: Flexural dynamic modulus master curves.

5.5 Rutting Performance: Unconfined Repeated Load Triaxial

Flow number test results are listed in Table B.7 in Appendix B. Figure 5.4 shows the relationship between cumulative permanent axial strains and the number of load cycles for all mixes evaluated. A review of the data led to the following observations:

- The repeatability of the test results met the single-operator precision specified in AASHTO T 378 for all mixes, but it showed some variability between the replicate specimens in each mix, which is consistent with repeated load testing.
- The evolution rate of cumulative permanent deformation with increasing loading cycles was initially similar for all mixes, but thereafter the MER-33 and INY-395 mixes appeared

to be more susceptible to rutting than the other three mixes, consistent with the dynamic modulus results.

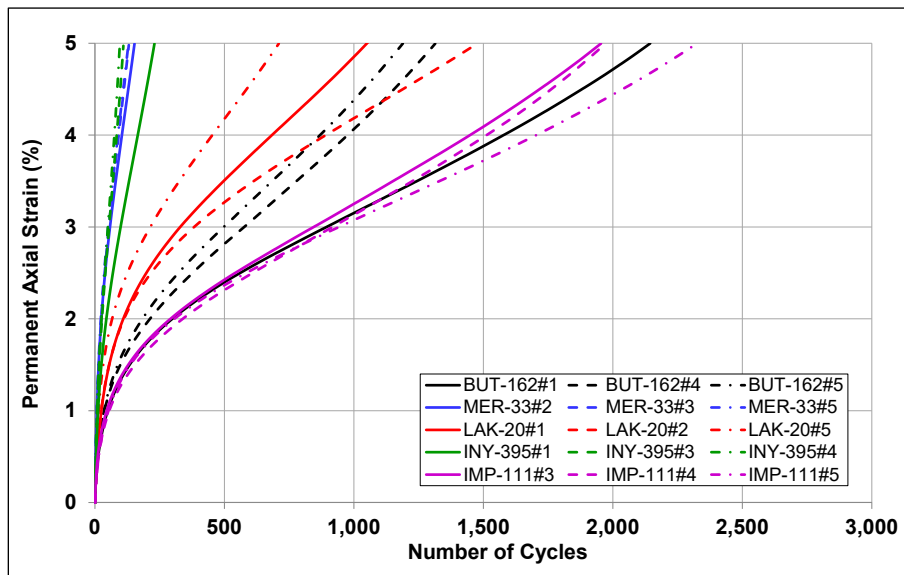


Figure 5.4: Cumulative permanent axial strain versus number of cycles (52°C).

Figure 5.5 shows the flow number values for the different mixes. Error bars on the data show the lowest and highest flow numbers of the three replicates in each mix. The MER-33 and INY-395 mixes had the lowest average flow numbers, considerably lower than the other three mixes and showing the same trends as the high-temperature PG results. Although there was considerable variability between the results of the three replicates in each mix, this ranking of average flow numbers was consistent with the true high-temperature grade results of the binders (Table 4.2).

Figure 5.6 shows the number of cycles to 1%, 3%, and 5% permanent axial strain (note that the y-axis is on a log scale). Trends observed for the number of cycles to 3% and 5% permanent axial strain were similar to those observed for the flow number results. At lower strain levels, the difference in the number of cycles required to reach the selected strain level was much closer between the mixes (also clearly shown in Figure 5.4), with the rankings of some of the mixes different from those for the higher strain levels.

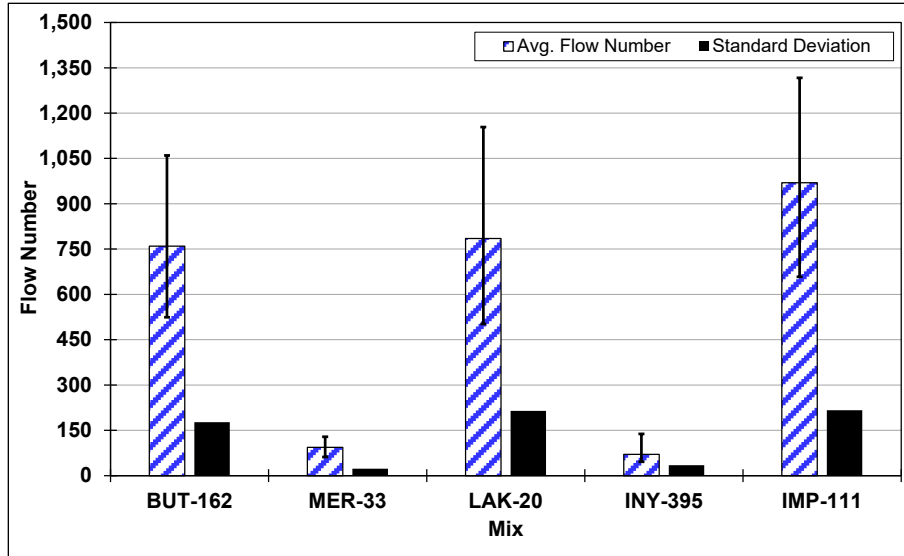


Figure 5.5: Average flow number (52°C).

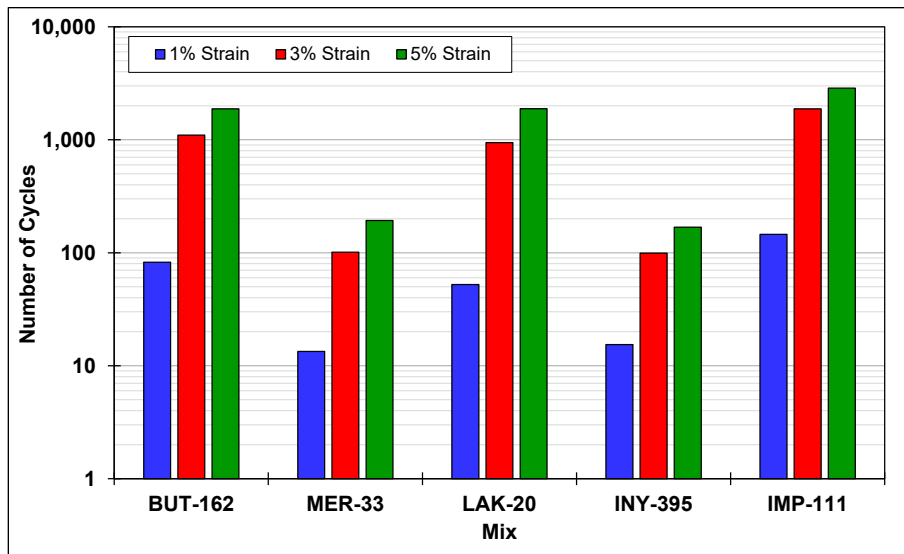


Figure 5.6: Number of cycles to 1%, 3%, and 5% permanent axial strain.

5.6 Cracking Performance: Four-Point Bending Beam Fatigue

Plots of the fatigue models for each mix are shown in Figure 5.7. The models were considered to be generally appropriate based on the reasonably high R-squared values of the model fitting and the repeatability of the test results at each strain level. The MER-33 mix beams had less variability than the other four mixes at low and high strains. Calculated fatigue lives at 200, 300, 400, and 600 μ strain of the five mixes are compared in Figure 5.8. Note that no mixes were tested at 200 μ strain and that fatigue life at this strain level was extrapolated.

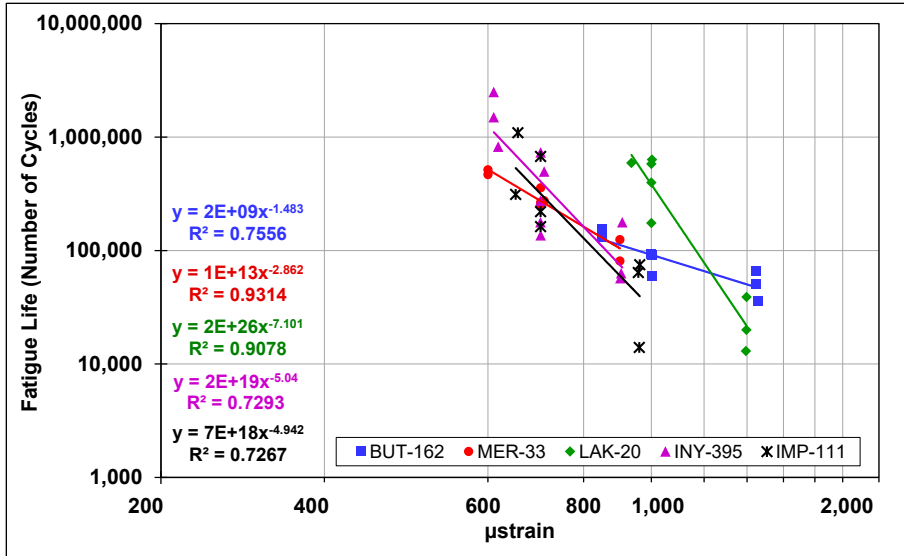


Figure 5.7: Fatigue regression models.

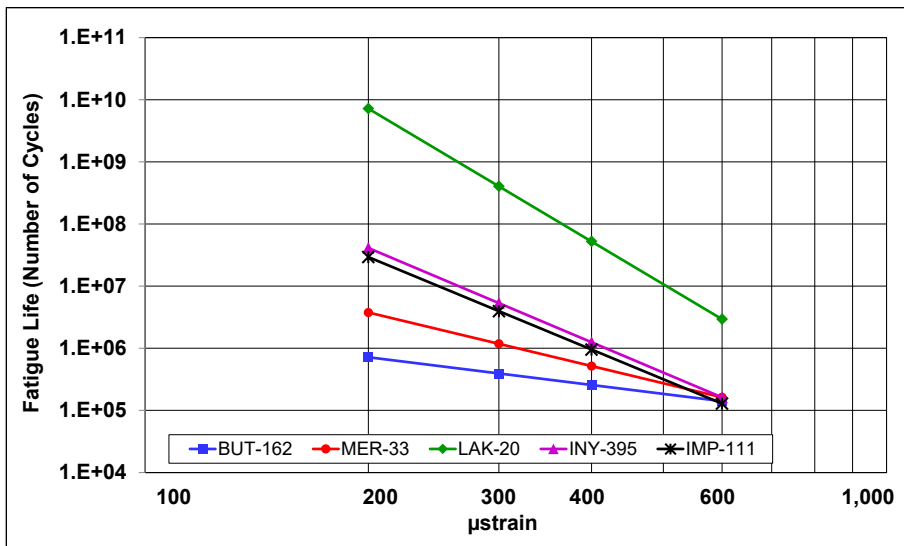


Figure 5.8: Calculated fatigue life at 200, 300, 400, and 600 μ strain.

A review of the data led to the following observations:

- Fatigue life decreased with increasing strain level, as expected.
- The LAK-20 mix indicated notably better fatigue performance than the other mixes at all strains. This mix also indicated similar fatigue performance to other RHMA-G mixes previously tested at the UCPRC. The other four mixes had lower fatigue performance than the LAK-20 mix and compared to mixes tested in other recent studies.
- There was considerable variation in fatigue performance among the mixes at low strain levels, with less variability with increasing strain. Fatigue life at 600 μ strain was essentially the same for all mixes except the LAK-20 mix.

- The results were not consistent with the flexural modulus test results, the intermediate temperature binder test results, or the Delta T_C results. However, if the LAK-20 binder is excluded from the rankings, the fatigue life and binder m-value rankings were the same for the other four binders.

5.7 Cracking Performance: Semicircular Bend

Semicircular bend test results are listed in Table B.8 in Appendix B. Average fracture energies and flexibility indices for the five mixes are shown in Figure 5.9 and Figure 5.10. Error bars on the data show the lowest and highest fracture energies and flexibility indices for the replicates tested.

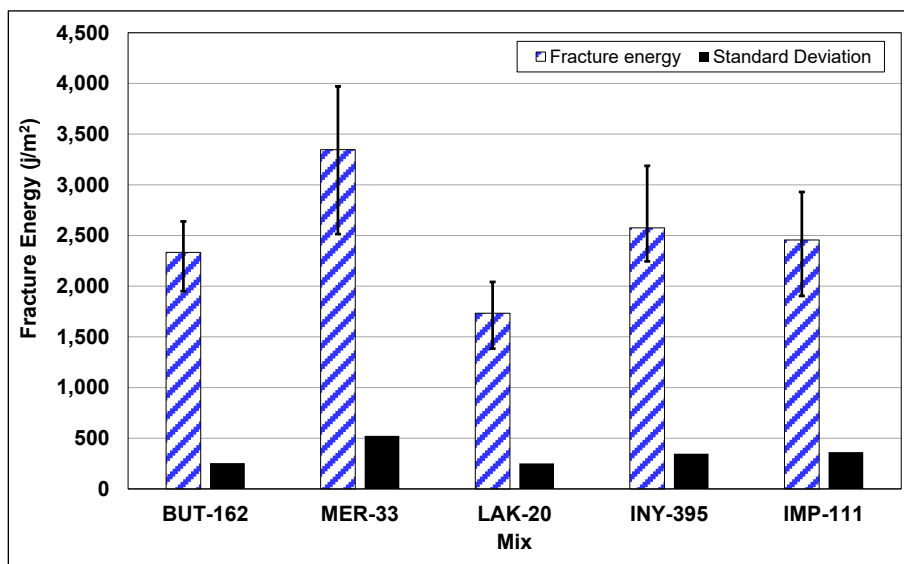


Figure 5.9: Semicircular bend fracture energy.

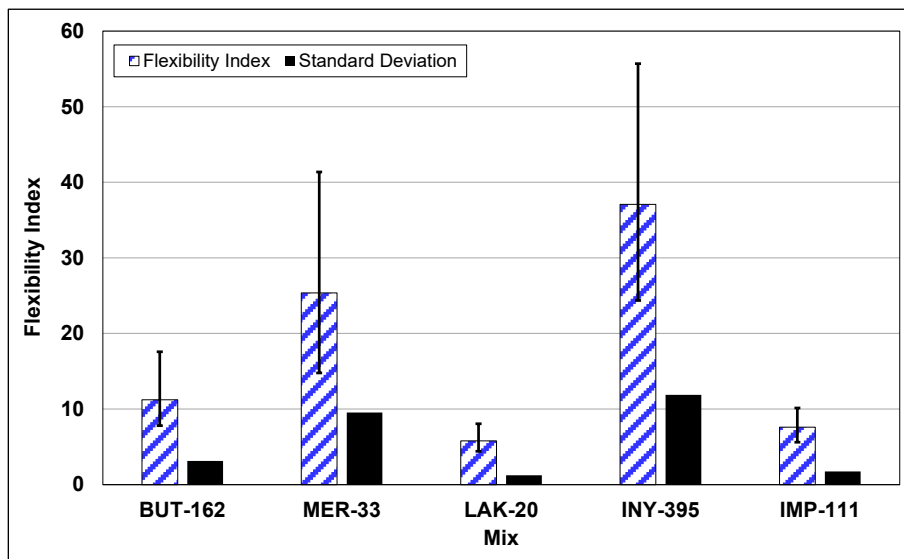


Figure 5.10: Semicircular bend flexibility index.

A review of the data led to the following observations:

- There was notable variability between mixes and between replicate specimens within each mix for both the fracture energy and flexibility index.
- The LAK-20 mix had the lowest fracture energy and flexibility index, but the highest fatigue life. Rankings of the three sets of cracking test results (calculated fatigue life, fracture energy, and flexibility index) are provided in Table 5.3 and do not indicate consistency across all mixes, although two mixes had similar rankings for the three tests (i.e., INY-395 and IMP-111, shaded in the table).

Table 5.3: Ranking of Cracking Test Results

Rank	Ranking		
	Fatigue Life	Fracture Energy	Flexibility Index
1	LAK-20	MER-33	INY-395
2	INY-395	INY-395	MER-33
3	IMP-111	IMP-111	BUT-162
4	MER-33	BUT-162	IMP-111
5	BUT-162	LAK-20	LAK-20

- The flexibility index of the INY-395 mix was notably higher than the other mixes, indicating that this mix would likely have better cracking resistance than the others. However, this mix also had the highest variability between replicate specimens.
- Flexibility index results showed the same trends and rankings to the Delta T_c results (i.e., the MER-33 and INY-395 binders had the highest flexibility indices and lowest Delta T_c values).
- Flexibility index results showed the same trends and similar rankings to the non-recoverable creep compliance results.

5.8 Discussion

A comparison of binder and mix test results did not show any consistent trends across all five binders (Table 5.4). However, the following trends between some results were observed:

- Rutting test result rankings (flow number and cycles to 5% permanent axial strain) were consistent with the binder high temperature PG result rankings.
- Flexibility index rankings (highest to lowest) were consistent with Delta T_c (lowest to highest) and non-recoverable creep compliance (highest to lowest). Flexibility index results (highest to lowest) also corresponded with mix rutting results (lowest to highest) as expected (i.e., cracking and rutting results are opposite).
- Beam fatigue rankings did not match any binder testing rankings, however, if the LAK-20 binder and mix results are excluded, the mix fatigue life and binder m-value rankings are the same for the other four binders.

Table 5.4: Rankings of Select Binder and Mix Testing Results

Rank	High True Grade	Int. True Grade	m-Value at -12°C	Delta T _c	Jnr at 3.2 kPa	Flow Number	Cycles to 5% PAS	Fatigue Life	Fracture Energy	Flexibility Index
1	LAK-20	MER-33	INY-395	INY-395	INY-395	IMP-111	IMP-111	LAK-20	MER-33	INY-395
2	BUT-162	IMP-111	IMP-111	MER-33	MER-33	LAK-20	LAK-20	INY-395	INY-395	MER-33
3	IMP-111	INY-395	LAK-20	IMP-111	IMP-111	BUT-162	BUT-162	IMP-111	IMP-111	BUT-162
4	MER-33	LAK-20	MER-33	BUT-162	LAK-20	MER-33	MER-33	MER-33	BUT-162	IMP-111
5	INY-395	BUT-162	BUT-162	LAK-20	BUT-162	INY-395	INY-395	BUT-162	LAK-20	LAK-20

Blank page

6. DETERMINATION OF RUBBER CONTENT IN ASPHALT RUBBER BINDERS

6.1 Introduction

Delays in the awarding of the contract for this project resulted in limited time and reduced funding to investigate methods of determining the presence of rubber and rubber content in modified asphalt binders, and potentially in recycled asphalt pavement (RAP) materials. However, limited exploratory testing was conducted on the topic using Fourier-transform infrared (FTIR) spectroscopy.

6.2 Methodology

One base binder (BUT-162) with eight different crumb rubber modifier (CRM) contents were tested in unaged and PAV-aged condition. Extender oil alone and base binder modified with extender oil only were also tested to determine the potential influence of extender oil on the results. A known styrene-butadiene rubber (SBR, 75% butadiene and 25% styrene) signature was used to identify the presence of CRM. The area under the curve in the SBR zone (965.1 cm^{-1} to 909.9 cm^{-1} [Figure 6.1]) was calculated to determine the quantity of rubber in the binder (8,9). The area calculated under the curve of the SBR signatures of the base binder and base binder with modifier was subtracted from those of the asphalt rubber binders to focus the results on the CRM only.

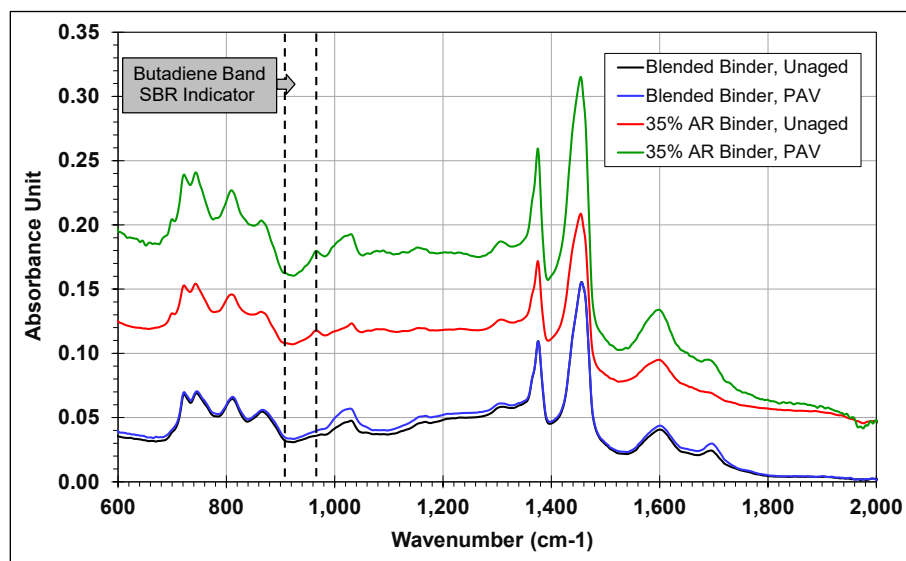


Figure 6.1: Typical wave form of FTIR data and butadiene band location.

The following were considered when identifying SBR as a baseline signature:

- SBR is a chemical compound present in synthetic rubber, it is a common blend elastomer used in approximately 40% of all synthetic rubber worldwide (8), and it is widely used in tires.
- Since synthetic rubber and asphalt are both derived from crude oil, an SBR signature may be present in some unmodified binders and in petroleum-based binder modifiers.

Figure 6.2 shows the area under-the-curve calculations of the SBR signatures of the seven CRM dosages (2.5% to 35% by weight of the binder) in both unaged and PAV-aged conditions. In both conditions, the SBR signature values increased with increasing rubber dosage. Values for the PAV-aged binders were notably higher than those for the unaged binders, indicating that aging will influence values over time. These results indicate that FTIR is a potentially valid method for quantifying rubber content in rubber modified binders.

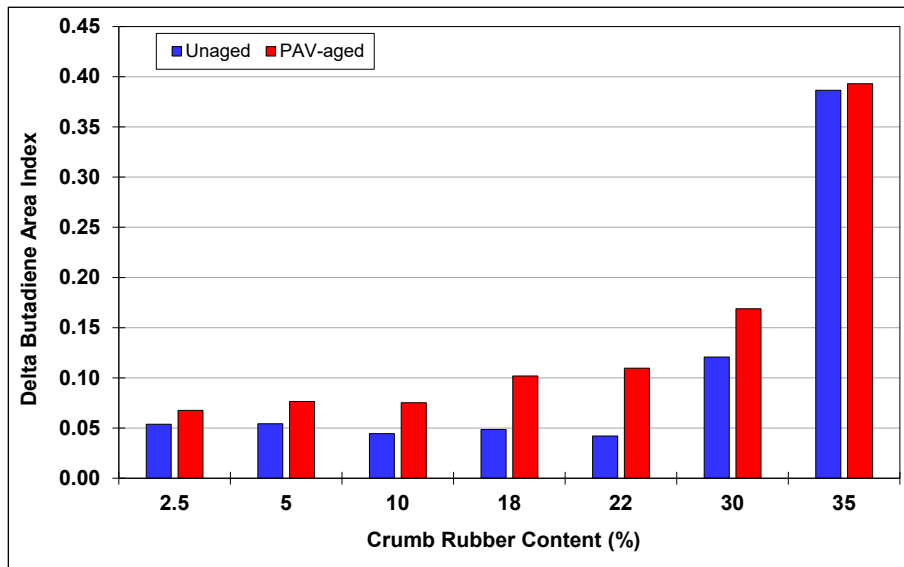


Figure 6.2: Area under the curve calculation for the butadiene signature of AR binders.

Mastics from an RHMA mix and from an HMA mix containing rubberized RAP were also tested. However, the results were inconclusive, which was attributed primarily to the size of the sample being larger than the measurement zone on the equipment used and to the potential influence of the fine aggregate in the mastic.

7. CONCLUSIONS AND RECOMMENDATIONS

7.1 Introduction

The work discussed in this interim report is part of a larger study, funded by the California Department of Transportation (Caltrans), with the objective of developing and recommending testing procedures and criteria for performance-based specifications of asphalt rubber binders used in gap- and open-graded mixes using current Superpave performance grading (PG) equipment. Work covered the testing of five plant-produced binders and the gap-graded rubberized hot mix asphalt mixes produced with them.

7.2 Testing Summary

7.2.1 Rheology Testing

Rheology testing to determine the high-, intermediate-, and low-temperature PGs and multiple stress creep recovery (MSCR) of five plant-produced asphalt rubber binders using the testing procedures developed in Phase 2 of a comprehensive study for Caltrans on the development of performance-based specifications for asphalt rubber binder was undertaken to test the procedures. The following important observations from the high-temperature tests were made:

- Testing in this phase of the study provided results that were consistent with those obtained during preliminary testing in Phase 2e of the larger study.
- Although the low-temperature performance grades appeared to be reasonable, the high-temperature grades appeared to be unrealistically high, while the intermediate-temperature grades appeared to be potentially lower than anticipated, when compared to the base binders.
- A comparison of the concentric cylinder and parallel plate (3 mm gap) geometries indicated that the results between the two geometries are different and are likely to be higher than the precision and bias of the individual procedures. Precision and bias statements for these procedures had not been developed at the time of preparing this report.
- Consistent trends in results were observed between high temperature PG/true grade, Delta T_C , and non-recoverable creep compliance at 3.2 kPa.
- Observations in Phase 2e and during this phase of the study indicated that incompletely digested rubber particles appeared to have a dominant influence on results and caused variability between results, regardless of the testing geometry used. Considering these incompletely digested particles as part of a homogenous binder may therefore not be appropriate when determining performance grades.

7.2.2 Mix Testing

Mix testing was undertaken to assess rutting and cracking performance in relation to performance grading to determine whether the rheology testing approaches provide properties that are representative of likely field performance. A comparison of binder and mix test results did not show any consistent trends across all five binders. However, the following trends between some results were observed:

- Rutting test result rankings (flow number and cycles to 5% permanent axial strain) were consistent with the binder high temperature PG result rankings.
- Flexibility index rankings (highest to lowest) were consistent with Delta T_c (lowest to highest), and non-recoverable creep compliance (highest to lowest). Flexibility index results (highest to lowest) also corresponded with mix rutting results (lowest to highest) as expected (i.e., cracking and rutting results are opposite).
- Beam fatigue rankings did not match any binder testing rankings. However, excluding the binder and mix results from one “outlier,” the mix fatigue life and binder m-value rankings were the same for the other four binders/mixes.

7.2.3 Rubber Content Determination

Limited exploratory testing was conducted to assess the use of Fourier-transform infrared (FTIR) spectroscopy to determine rubber content in rubber modified binders. One base binder with eight different crumb rubber modifier (CRM) contents, ranging from 2.5% to 35% by weight of the base binder, were tested in unaged and PAV-aged condition. Extender oil alone and base binder modified with extender oil only were also tested to determine the potential influence of extender oil on the results. A known styrene-butadiene rubber (SBR, 75% butadiene and 25% styrene) signature was used to identify the presence of CRM.

In both aging conditions, the SBR signature values increased with increasing rubber dosage. Values for the PAV-aged binders were notably higher than those for the unaged binders, indicating that aging will influence values over time. The results indicate that FTIR is a potentially valid method for quantifying rubber content in rubber modified binders.

7.3 Conclusions

Incompletely digested rubber particles—which have different sensitivities to temperature, aging, and applied stress and strain than the base asphalt binder—appear to dominate the binder

rheology test results, leading to what appears to be unrealistic performance grades. Work is continuing in Phase 3 of this study to adjust testing procedures to account for the influence that these incompletely digested particles have on results.

The proposed modifications to short- and long-term aging procedures (i.e., rolling thin film oven and pressure aging vessel) and to the bending beam rheometer specimen preparation procedures developed in Phase 2 are considered to be more aligned with the original intent of the tests and will likely reduce the variability between replicate specimens during testing.

7.4 Recommendations

No recommendations for implementation are warranted at this stage of the study. Phase 3 is investigating the extent to which incompletely digested rubber particles might affect PG results along with testing procedures to overcome the problems. This phase is focusing on removal of larger incompletely digested particles from the binder by sieving or centrifuging and then testing the binders following standard performance grading procedures using parallel plate geometry with either 1 mm or 2 mm gaps. Results after removal of particles larger than 250, 500, and 850 μm are being compared with unprocessed binders tested with concentric cylinder and parallel plate with 3 mm gap geometries. The five asphalt rubber binders tested in this phase of the study are being retested in Phase 3 to assess the removal of larger incompletely digested rubber particles on performance grades.

Blank page

REFERENCES

1. California Integrated Waste Management Board. 2005. *California Waste Tire Generation, Markets, and Disposal: 2003 Staff Report*. Sacramento, CA: California Integrated Waste Management Board.
2. Federal Highway Administration. 2006. *Status of the Nation's Highways, Bridges, and Transit: Conditions and Performance*. Washington, DC: Federal Highway Administration.
3. Jones, D., Rizvi, H., Liang, Y., Hung, S., Buscheck, J., Alavi, Z. and Hofko, B. 2017. *Development of Performance-Based Specifications for Asphalt Rubber Binder: Interim Report on Phase 1 and Phase 2 Testing* (Research Report: UCPRC-RR-2017-01). Davis and Berkeley, CA: University of California Pavement Research Center. doi.org/10.7922/G2T72FQQ.
4. Harvey, J. and Bejarano, M. 2001. "Performance of Two Overlay Strategies under Heavy Vehicle Simulator Trafficking." *Transportation Research Record* 1769: 123–133.
5. Jones, D., Tsai, B.W., Ullidtz, P., Wu, R., Harvey, J. and Monismith, C. 2008. *Reflective Cracking Study: Second-Level Analysis Report* (Research Report: UCPRC-RR-2007-09). Davis and Berkeley, CA: University of California Pavement Research Center. escholarship.org/uc/item/1rc624m9.
6. Jones, D. and Harvey, J. 2009. "Accelerated Pavement Testing Experiment to Assess the Use of Modified Binders to Limit Reflective Cracking in Thin Asphalt Concrete Overlays." In *Transportation Research Circular E-C139: Use of Accelerated Pavement Testing to Evaluate Maintenance and Pavement Preservation Treatments*, 11–31. Washington, DC: Transportation Research Board. onlinepubs.trb.org/onlinepubs/circulars/ec139.pdf.
7. Asphalt Institute. 2019. *Use of the Delta TC Parameter to Characterize Asphalt Binder Behavior* (IS-240). Lexington KY: Asphalt Institute. asphaltinstitute.org/download/1305/.
8. Azevedo, J.B., Murakami, L.M.S., Ferriera, A.C., Diniz, M.F., Silva, L.M. and Dutra, R.L. 2018. "Quantification by FT-IR (UATR/NIRA) of NBR/SBR Blends." *Polímeros* 28, no. 5.
9. Araujo, E.M., Siqueira, D.D., Morais, D.D.S., Filho, E.A.S., Filho, E.A. and Fook, M.V.L. 2019. "Incorporation of a Recycled Rubber Compound from the Shoe Industry in Polystyrene: Effect of SBS Compatibilizer Content." *Journal of Elastomers and Plastics* 52, no. 1: 1–26.

Blank page

APPENDIX A: BINDER TEST RESULTS

Binder test results are summarized in the following tables:

- Table A.1: High Temperature Test Results (Unaged) for BUT-162
- Table A.2: High Temperature Test Results (Unaged) for MER-33
- Table A.3: High Temperature Test Results (Unaged) for LAK-20
- Table A.4: High Temperature Test Results (Unaged) for INY-395
- Table A.5: High Temperature Test Results (Unaged) for IMP-111
- Table A.6: High Temperature Test Results (RTFO-Aged) for BUT-162
- Table A.7: High Temperature Test Results (RTFO-Aged) for MER-33
- Table A.8: High Temperature Test Results (RTFO-Aged) for LAK-20
- Table A.9: High Temperature Test Results (RTFO-Aged) for INY-395
- Table A.10: High Temperature Test Results (RTFO-Aged) for IMP-111
- Table A.11: Intermediate Temperature Test Results for BUT-162
- Table A.12: Intermediate Temperature Test Results for MER-33
- Table A.13: Intermediate Temperature Test Results for LAK-20
- Table A.14: Intermediate Temperature Test Results for INY-395
- Table A.15: Intermediate Temperature Test Results for IMP-111
- Table A.16: Low-Temperature Test Results
- Table A.17: Multiple Stress Creep Recovery Test Results (64°C)

Table A.1: High Temperature Test Results (Unaged) for BUT-162

Test Temp. (°C)	Concentric Cylinder			25 mm Parallel Plate with 3 mm Gap		
	G* (kPa)	Phase Angle (degrees)	G*/sin(δ) (kPa)	G* (kPa)	Phase Angle (degrees)	G*/sin(δ) (kPa)
64	17.7	49.1	23.4	19.9	48.4	26.6
	16.6	49.2	21.9	19.1	50.6	24.7
	17.7	49.3	23.3	19.4	49.6	25.5
Mean	17.3	49.2	22.9	19.5	49.5	25.6
Std. Dev.	0.5	0.10	0.7	0.3	0.87	0.8
Std. Err.	0.3	0.06	0.4	0.2	0.50	0.4
70	11.2	52.8	14.1	12.7	52.5	16.1
	10.6	53.1	13.2	12.0	55.0	14.6
	11.1	53.3	13.9	12.3	53.7	15.3
Mean	11.0	53.0	13.7	12.3	53.7	15.3
Std. Dev.	0.3	0.20	0.4	0.3	1.01	0.6
Std. Err.	0.2	0.11	0.2	0.2	0.58	0.3
76	6.9	57.5	8.2	8.1	57.4	9.6
	6.6	57.8	7.7	7.3	60.1	8.5
	6.9	58.1	8.1	7.7	58.6	9.0
Mean	6.8	57.8	8.0	7.7	58.7	9.0
Std. Dev.	0.2	0.25	0.2	0.3	1.08	0.4
Std. Err.	0.1	0.15	0.1	0.2	0.62	0.3
82	4.2	62.4	4.8	5.1	62.5	5.8
	4.0	62.8	4.5	4.4	65.2	4.9
	4.2	63.1	4.7	4.8	63.5	5.3
Mean	4.1	62.8	4.7	4.8	63.7	5.3
Std. Dev.	0.1	0.29	0.1	0.3	1.10	0.4
Std. Err.	0.1	0.17	0.1	0.2	0.64	0.2
88	2.6	67.3	2.8	3.2	67.2	3.5
	2.4	67.6	2.6	2.7	69.6	2.9
	2.5	67.9	2.7	2.9	68.0	3.2
Mean	2.5	67.6	2.7	3.0	68.3	3.2
Std. Dev.	0.1	0.27	0.1	0.2	1.01	0.3
Std. Err.	0.0	0.16	0.0	0.1	0.58	0.1
94	1.6	71.5	1.7	2.0	71.2	2.1
	1.5	71.8	1.6	1.6	73.5	1.7
	1.5	72.1	1.6	1.8	71.9	1.9
Mean	1.5	71.8	1.6	1.8	72.2	1.9
Std. Dev.	0.0	0.22	0.0	0.2	0.97	0.2
Std. Err.	0.0	0.13	0.0	0.1	0.56	0.1
100	—	—	—	1.8	67.6	2.0
	0.9	75.4	1.0	1.0	76.6	1.1
	1.0	75.5	1.0	1.2	75.1	1.2
Mean	0.9	75.4	1.0	1.3	73.1	1.4
Std. Dev.	0.0	0.04	0.0	0.4	3.95	0.4
Std. Err.	0.0	0.03	0.0	0.2	2.28	0.2

Table A.2: High Temperature Test Results (Unaged) for MER-33

Test Temp. (°C)	Concentric Cylinder			25 mm Parallel Plate with 3 mm Gap		
	G* (kPa)	Phase Angle (degrees)	G*/sin(δ) (kPa)	G* (kPa)	Phase Angle (degrees)	G*/sin(δ) (kPa)
64	7.5	62.5	8.5	7.8	58.9	9.1
	—	—	—	—	—	—
	7.9	61.4	9.0	8.2	58.8	9.6
Mean	7.7	62.0	8.7	8.0	58.9	9.3
Std. Dev.	0.2	0.55	0.2	0.2	0.05	0.2
Std. Err.	0.1	0.39	0.2	0.1	0.04	0.2
70	4.4	67.1	4.8	4.6	63.1	5.2
	—	—	—	—	—	—
	4.6	66.2	5.1	4.9	63.3	5.5
Mean	4.5	66.7	4.9	4.8	63.2	5.3
Std. Dev.	0.1	0.45	0.2	0.1	0.10	0.1
Std. Err.	0.1	0.32	0.1	0.1	0.07	0.1
76	2.5	71.3	2.7	2.8	66.8	3.0
	—	—	—	—	—	—
	2.7	70.4	2.9	3.0	67.5	3.2
Mean	2.6	70.9	2.8	2.9	67.2	3.1
Std. Dev.	0.1	0.45	0.1	0.1	0.35	0.1
Std. Err.	0.1	0.32	0.1	0.1	0.25	0.1
82	1.5	74.7	1.6	1.7	69.9	1.9
	—	—	—	—	—	—
	1.6	73.8	1.7	1.8	70.7	2.0
Mean	1.6	74.3	1.6	1.8	70.3	1.9
Std. Dev.	0.1	0.45	0.1	0.1	0.40	0.0
Std. Err.	0.0	0.32	0.0	0.0	0.28	0.0
88	0.9	77.5	0.9	1.1	72.2	1.2
	—	—	—	—	—	—
	1.0	76.5	1.0	1.2	72.6	1.3
Mean	1.0	77.0	1.0	1.2	72.4	1.2
Std. Dev.	0.0	0.50	0.1	0.0	0.20	0.0
Std. Err.	0.0	0.35	0.0	0.0	0.14	0.0

Table A.3: High Temperature Test Results (Unaged) for LAK-20

Test Temp. (°C)	Concentric Cylinder			25 mm Parallel Plate with 3 mm Gap		
	G* (kPa)	Phase Angle (degrees)	G*/sin(δ) (kPa)	G* (kPa)	Phase Angle (degrees)	G*/sin(δ) (kPa)
64	15.2	52.1	19.2	15.4	50.5	19.9
	—	—	—	15.0	50.1	19.6
	15.5	51.7	19.7	15.1	51.1	19.4
Mean	15.4	51.9	19.5	15.2	50.6	19.6
Std. Dev.	0.2	0.20	0.3	0.2	0.41	0.2
Std. Err.	0.1	0.14	0.2	0.1	0.24	0.1
70	9.5	55.3	11.6	9.6	54.1	11.9
	—	—	—	9.8	53.1	12.2
	9.8	55.1	11.9	9.8	54.2	12.0
Mean	9.6	55.2	11.8	9.7	53.8	12.0
Std. Dev.	0.1	0.10	0.2	0.1	0.50	0.1
Std. Err.	0.1	0.07	0.1	0.0	0.29	0.1
76	5.8	59.5	6.7	—	—	—
	—	—	—	6.3	57.3	7.5
	5.9	59.4	6.9	6.2	58.1	7.3
Mean	5.9	59.5	6.8	6.2	57.7	7.4
Std. Dev.	0.1	0.05	0.1	0.05	0.4	0.1
Std. Err.	0.0	0.04	0.1	0.04	0.3	0.1
82	3.5	64.0	3.9	—	—	—
	—	—	—	4.0	61.6	4.5
	3.6	64.0	4.0	3.8	62.3	4.3
Mean	3.6	64.0	4.0	3.9	62.0	4.4
Std. Dev.	0.0	0.00	0.0	0.08	0.3	0.1
Std. Err.	0.0	0.00	0.0	0.05	0.2	0.1
88	2.1	68.4	2.3	—	—	—
	—	—	—	2.5	65.6	2.7
	2.2	68.4	2.3	2.4	66.3	2.6
Mean	2.1	68.4	2.3	2.4	66.0	2.6
Std. Dev.	0.0	0.00	0.0	0.06	0.4	0.1
Std. Err.	0.0	0.00	0.0	0.05	0.2	0.1
94	1.3	72.4	1.4	1.4	70.7	1.5
	—	—	—	—	—	—
	1.3	72.4	1.4	1.5	69.6	1.6
Mean	1.3	72.4	1.4	1.4	70.2	1.5
Std. Dev.	0.0	0.00	0.0	0.0	0.55	0.1
Std. Err.	0.0	0.00	0.0	0.0	0.39	0.0
100	0.8	75.7	0.8	0.9	73.9	0.9
	—	—	—	—	—	—
	0.8	75.8	0.8	0.9	72.4	1.0
Mean	0.8	75.8	0.8	0.9	73.2	0.9
Std. Dev.	0.0	0.05	0.0	0.0	0.75	0.0
Std. Err.	0.0	0.04	0.0	0.0	0.53	0.0

Table A.4: High Temperature Test Results (Unaged) for INY-395

Test Temp. (°C)	Concentric Cylinder			25 mm Parallel Plate with 3 mm Gap		
	G* (kPa)	Phase Angle (degrees)	G*/sin(δ) (kPa)	G* (kPa)	Phase Angle (degrees)	G*/sin(δ) (kPa)
64	5.7	69.4	6.1	5.9	66.4	6.4
	5.6	69.4	6.0	—	—	—
	—	—	—	6.1	67.6	6.6
Mean	5.6	69.4	6.0	6.0	67.0	6.5
Std. Dev.	0.0	0.00	0.1	0.1	0.60	0.1
Std. Err.	0.0	0.00	0.0	0.1	0.42	0.0
70	3.1	74.0	3.2	3.3	71.3	3.4
	3.1	73.9	3.2	—	—	—
	—	—	—	3.3	72.7	3.5
Mean	3.1	74.0	3.2	3.3	72.0	3.5
Std. Dev.	0.0	0.05	0.0	0.04	0.7	0.0
Std. Err.	0.0	0.04	0.0	0.02	0.5	0.0
76	1.7	77.6	1.7	1.9	74.9	1.9
	1.7	77.5	1.7	—	—	—
	—	—	—	1.9	76.5	1.9
Mean	1.7	77.6	1.7	1.9	75.7	1.9
Std. Dev.	0.0	0.05	0.0	0.0	0.80	0.0
Std. Err.	0.0	0.04	0.0	0.0	0.57	0.0
82	1.0	80.1	1.0	1.1	77.6	1.1
	1.0	80.2	1.0	—	—	—
	—	—	—	1.1	79.1	1.1
Mean	1.0	80.2	1.0	1.1	78.4	1.1
Std. Dev.	0.0	0.05	0.0	0.0	0.75	0.0
Std. Err.	0.0	0.04	0.0	0.0	0.53	0.0
88	—	—	—	0.7	79.7	0.7
	—	—	—	—	—	—
	—	—	—	0.7	81.1	0.7
Mean	—	—	—	0.7	80.4	0.7
Std. Dev.	—	—	—	0.0	0.70	0.0
Std. Err.	—	—	—	0.0	0.49	0.0

Table A.5: High Temperature Test Results (Unaged) for IMP-111

Test Temp. (°C)	Concentric Cylinder			25 mm Parallel Plate with 3 mm Gap		
	G* (kPa)	Phase Angle (degrees)	G*/sin(δ) (kPa)	G* (kPa)	Phase Angle (degrees)	G*/sin(δ) (kPa)
64	8.3	63.7	9.2	—	—	—
	8.3	64.0	9.2	8.2	64.0	9.1
	8.5	63.5	9.5	8.3	62.2	9.4
Mean	8.3	63.7	9.3	8.2	63.1	9.2
Std. Dev.	0.1	0.21	0.1	0.1	0.90	0.1
Std. Err.	0.1	0.12	0.1	0.0	0.63	0.1
70	4.7	67.9	5.1	5.3	67.7	5.7
	4.8	68.2	5.2	—	—	—
	4.9	67.7	5.3	4.9	66.3	5.3
Mean	4.8	67.9	5.2	5.1	67.0	5.5
Std. Dev.	0.1	0.22	0.1	0.2	0.69	0.2
Std. Err.	0.0	0.12	0.0	0.2	0.49	0.1
76	2.7	71.8	2.9	3.1	71.4	3.3
	2.8	72.1	2.9	—	—	—
	2.8	71.6	3.0	2.9	70.3	3.1
Mean	2.8	71.8	2.9	3.0	70.9	3.2
Std. Dev.	0.0	0.18	0.0	0.1	0.56	0.1
Std. Err.	0.0	0.10	0.0	0.1	0.39	0.1
82	1.6	75.2	1.7	1.9	74.4	2.0
	1.6	75.4	1.7	—	—	—
	1.7	75.1	1.7	1.7	73.7	1.8
Mean	1.6	75.2	1.7	1.8	74.0	1.9
Std. Dev.	0.0	0.13	0.0	0.1	0.34	0.1
Std. Err.	0.0	0.07	0.0	0.1	0.24	0.1
88	1.0	78.1	1.0	1.2	76.7	1.2
	1.0	77.9	1.0	—	—	—
	1.0	77.8	1.0	1.0	76.8	1.1
Mean	1.0	77.9	1.0	1.1	76.8	1.2
Std. Dev.	0.0	0.09	0.0	0.1	0.08	0.1
Std. Err.	0.0	0.05	0.0	0.1	0.06	0.1
94	—	—	—	0.8	78.7	0.8
	—	—	—	—	—	—
	—	—	—	0.7	79.1	0.7
Mean	—	—	—	0.7	78.9	0.7
Std. Dev.	—	—	—	0.1	0.20	0.1
Std. Err.	—	—	—	0.0	0.14	0.0

Table A.6: High Temperature Test Results (RTFO-Aged) for BUT-162

Test Temp. (°C)	Concentric Cylinder			25 mm Parallel Plate with 3 mm Gap		
	G* (kPa)	Phase Angle (degrees)	G*/sin(δ) (kPa)	G* (kPa)	Phase Angle (degrees)	G*/sin(δ) (kPa)
64	41.2	39.3	65.1	44.8	39.9	69.9
	42.6	38.9	67.7	46.9	40.0	72.9
	42.8	39.3	67.6	44.5	38.1	72.2
Mean	42.2	39.2	66.8	45.4	39.3	71.6
Std. Dev.	0.7	0.16	1.2	1.0	0.90	1.3
Std. Err.	0.4	0.09	0.7	0.6	0.52	0.8
70	28.3	39.8	44.1	31.4	40.4	48.5
	29.1	39.6	45.7	32.9	40.3	50.9
	29.1	39.8	45.5	31.5	38.4	50.7
Mean	28.8	39.7	45.1	32.0	39.7	50.0
Std. Dev.	0.4	0.11	0.7	0.7	0.92	1.1
Std. Err.	0.2	0.06	0.4	0.4	0.53	0.6
76	19.5	41.1	29.6	22.1	41.8	33.1
	20.0	40.9	30.5	23.2	41.5	34.9
	19.9	41.0	30.4	22.5	39.6	35.3
Mean	19.8	41.0	30.2	22.6	41.0	34.4
Std. Dev.	0.2	0.06	0.4	0.4	0.99	0.9
Std. Err.	0.1	0.03	0.2	0.3	0.57	0.5
82	13.5	43.0	19.8	15.4	44.0	22.2
	13.8	43.0	20.3	16.3	43.5	23.6
	13.7	42.9	20.2	16.0	41.6	24.2
Mean	13.7	42.9	20.1	15.9	43.0	23.3
Std. Dev.	0.1	0.05	0.2	0.3	1.05	0.8
Std. Err.	0.1	0.03	0.1	0.2	0.61	0.5
88	9.3	45.6	13.1	10.7	46.9	14.7
	9.5	45.6	13.3	11.3	46.5	15.6
	9.5	45.5	13.3	11.4	44.5	16.2
Mean	9.4	45.6	13.2	11.1	46.0	15.5
Std. Dev.	0.1	0.08	0.1	0.3	1.03	0.6
Std. Err.	0.0	0.04	0.1	0.2	0.59	0.4
94	6.4	48.8	8.5	7.4	50.5	9.5
	6.5	48.9	8.7	7.7	50.1	10.1
	6.5	48.7	8.6	7.9	48.4	10.5
Mean	6.5	48.8	8.6	7.7	49.7	10.0
Std. Dev.	0.1	0.10	0.1	0.2	0.87	0.4
Std. Err.	0.0	0.06	0.0	0.1	0.50	0.2
100	4.4	52.5	5.5	5.0	54.4	6.2
	4.5	52.6	5.6	5.2	54.0	6.4
	4.4	52.3	5.5	5.4	52.7	6.8
Mean	4.4	52.5	5.6	5.2	53.7	6.5
Std. Dev.	0.0	0.11	0.1	0.1	0.70	0.2
Std. Err.	0.0	0.06	0.0	0.1	0.41	0.1
106	2.9	56.5	3.5	3.4	58.6	4.0
	3.0	56.5	3.6	3.5	58.0	4.1
	3.0	56.3	3.6	3.6	57.3	4.3
Mean	3.0	56.4	3.6	3.5	57.9	4.1
Std. Dev.	0.0	0.11	0.0	0.1	0.5	0.15
Std. Err.	0.0	0.06	0.0	0.1	0.3	0.08

Test Temp. (°C)	Concentric Cylinder			25 mm Parallel Plate with 3 mm Gap		
	G* (kPa)	Phase Angle (degrees)	G*/sin(δ) (kPa)	G* (kPa)	Phase Angle (degrees)	G*/sin(δ) (kPa)
112	2.0	60.6	2.3	2.3	62.7	2.6
	2.0	60.5	2.4	2.3	62.1	2.6
	2.0	60.3	2.3	2.4	61.7	2.8
Mean	2.0	60.4	2.3	2.3	62.1	2.6
Std. Dev.	0.0	0.12	0.0	0.1	0.40	0.1
Std. Err.	0.0	0.07	0.0	0.0	0.23	0.0
118	1.3	64.1	1.5	1.7	65.5	1.9
	1.4	64.3	1.5	1.7	64.8	1.9
	1.3	64.1	1.5	1.8	64.7	2.0
Mean	1.4	64.1	1.5	1.7	65.0	1.9
Std. Dev.	0.0	0.09	0.0	0.1	0.35	0.1
Std. Err.	0.0	0.05	0.0	0.0	0.20	0.0

Table A.7: High Temperature Test Results (RTFO-Aged) for MER-33

Test Temp. (°C)	Concentric Cylinder			25 mm Parallel Plate with 3 mm Gap		
	G* (kPa)	Phase Angle (degrees)	G*/sin(δ) (kPa)	G* (kPa)	Phase Angle (degrees)	G*/sin(δ) (kPa)
64	—	—	—	14.0	57.3	16.6
	12.4	62.4	14.0	13.2	57.5	15.7
	12.3	56.2	14.8	—	—	—
Mean	12.3	59.3	14.4	13.6	57.4	16.2
Std. Dev.	0.1	3.12	0.4	0.4	0.10	0.5
Std. Err.	0.0	2.21	0.3	0.3	0.07	0.3
70	7.7	62.6	8.7	8.2	60.3	9.4
	—	—	—	7.9	60.2	9.1
	7.4	59.2	8.7	—	—	—
Mean	7.6	60.9	8.7	8.0	60.3	9.2
Std. Dev.	0.2	1.72	0.0	0.2	0.05	0.2
Std. Err.	0.1	1.21	0.0	0.1	0.04	0.1
76	4.4	66.5	4.8	4.9	63.8	5.4
	—	—	—	4.7	63.6	5.2
	4.5	63.0	5.0	—	—	—
Mean	4.5	64.8	4.9	4.8	63.7	5.3
Std. Dev.	0.0	1.75	0.1	0.1	0.10	0.1
Std. Err.	0.0	1.23	0.1	0.1	0.07	0.1
82	2.6	70.6	2.7	2.9	67.5	3.1
	—	—	—	2.8	67.0	3.1
	2.7	67.0	2.9	—	—	—
Mean	2.6	68.8	2.8	2.9	67.3	3.1
Std. Dev.	0.1	1.81	0.1	0.0	0.25	0.0
Std. Err.	0.0	1.28	0.1	0.0	0.18	0.0
88	1.5	74.1	1.6	1.7	70.7	1.8
	—	—	—	1.7	69.9	1.9
	1.6	70.6	1.7	—	—	—
Mean	1.6	72.3	1.7	1.7	70.3	1.8
Std. Dev.	0.1	1.8	0.1	0.0	0.40	0.0
Std. Err.	0.0	1.2	0.1	0.0	0.28	0.0

Table A.8: High Temperature Test Results (RTFO-Aged) for LAK-20

Test Temp. (°C)	Concentric Cylinder			25 mm Parallel Plate with 3 mm Gap		
	G* (kPa)	Phase Angle (degrees)	G*/sin(δ) (kPa)	G* (kPa)	Phase Angle (degrees)	G*/sin(δ) (kPa)
64	40.3	40.4	62.1	34.9	40.9	53.3
	38.8	40.6	59.7	34.4	41.0	52.5
	40.4	40.1	62.8	38.4	42.0	57.4
Mean	39.8	40.3	61.5	35.9	41.3	54.4
Std. Dev.	0.7	0.21	1.4	1.8	0.49	2.1
Std. Err.	0.4	0.12	0.8	1.0	0.28	1.2
70	27.0	40.3	41.7	24.5	40.5	37.8
	26.1	40.5	40.3	24.3	40.6	37.3
	27.2	40.0	42.4	26.3	41.9	39.4
Mean	26.8	40.3	41.5	25.0	41.0	38.1
Std. Dev.	0.5	0.22	0.9	0.9	0.62	0.9
Std. Err.	0.3	0.13	0.5	0.5	0.36	0.5
76	18.4	40.9	28.1	17.8	40.8	27.2
	17.8	41.1	27.1	17.5	40.9	26.8
	18.6	40.6	28.6	18.6	42.4	27.7
Mean	18.3	40.8	27.9	18.0	41.3	27.2
Std. Dev.	0.3	0.23	0.6	0.5	0.72	0.4
Std. Err.	0.2	0.13	0.4	0.3	0.42	0.2
82	12.7	42.1	18.9	12.9	41.9	19.3
	12.3	42.4	18.2	12.7	41.9	19.1
	12.9	41.8	19.4	13.3	43.6	19.3
Mean	12.6	42.1	18.8	13.0	42.5	19.2
Std. Dev.	0.3	0.25	0.5	0.2	0.79	0.1
Std. Err.	0.2	0.14	0.3	0.1	0.46	0.1
88	8.8	44.1	12.7	9.3	43.8	13.5
	8.5	44.4	12.2	9.2	43.8	13.3
	9.0	43.8	13.0	9.5	45.5	13.2
Mean	8.8	44.1	12.6	9.3	44.4	13.3
Std. Dev.	0.2	0.25	0.3	0.1	0.81	0.1
Std. Err.	0.1	0.14	0.2	0.1	0.47	0.1
94	6.1	46.7	8.4	6.7	46.6	9.2
	5.9	47.0	8.1	6.6	46.5	9.1
	6.3	46.4	8.6	6.7	48.2	9.0
Mean	6.1	46.7	8.4	6.7	47.1	9.1
Std. Dev.	0.1	0.23	0.2	0.0	0.79	0.1
Std. Err.	0.1	0.13	0.1	0.0	0.46	0.1
100	4.2	49.8	5.6	4.7	50.0	6.2
	4.1	50.1	5.4	4.7	49.9	6.1
	4.4	49.6	5.7	4.6	51.6	5.9
Mean	4.2	49.8	5.6	4.7	50.5	6.1
Std. Dev.	0.1	0.19	0.1	0.0	0.79	0.1
Std. Err.	0.1	0.11	0.1	0.0	0.45	0.1
106	2.9	53.4	3.6	3.3	53.9	4.1
	2.9	53.6	3.6	3.3	53.7	4.1
	3.0	53.2	3.8	3.2	55.4	3.9
Mean	2.9	53.4	3.7	3.3	54.3	4.0
Std. Dev.	0.1	0.14	0.1	0.0	0.76	0.1
Std. Err.	0.0	0.08	0.0	0.0	0.44	0.1

Test Temp. (°C)	Concentric Cylinder			25 mm Parallel Plate with 3 mm Gap		
	G* (kPa)	Phase Angle (degrees)	G*/sin(δ) (kPa)	G* (kPa)	Phase Angle (degrees)	G*/sin(δ) (kPa)
112	2.0	57.2	2.4	2.3	57.9	2.7
	2.0	57.3	2.3	2.3	57.7	2.7
	2.1	57.1	2.5	2.2	59.2	2.5
Mean	2.0	57.2	2.4	2.3	58.3	2.6
Std. Dev.	0.0	0.10	0.0	0.1	0.69	0.1
Std. Err.	0.0	0.06	0.0	0.0	0.40	0.1
118	1.4	60.9	1.6	1.7	61.0	2.0
	1.4	61.0	1.5	1.7	60.5	2.0
	1.4	60.9	1.6	1.6	61.8	1.9
Mean	1.4	60.9	1.6	1.7	61.1	1.9
Std. Dev.	0.0	0.06	0.0	0.0	0.54	0.1
Std. Err.	0.0	0.03	0.0	0.0	0.31	0.0

Table A.9: High Temperature Test Results (RTFO-Aged) for INY-395

Test Temp. (°C)	Concentric Cylinder			25 mm Parallel Plate with 3 mm Gap		
	G* (kPa)	Phase Angle (degrees)	G*/sin(δ) (kPa)	G* (kPa)	Phase Angle (degrees)	G*/sin(δ) (kPa)
64	12.2	57.1	14.6	12.9	58.0	15.2
	—	—	—	12.8	56.0	15.5
	11.9	57.1	14.2	13.1	57.6	15.5
Mean	12.1	57.1	14.4	12.9	57.2	15.4
Std. Dev.	0.2	0.05	0.2	0.1	0.90	0.2
Std. Err.	0.1	0.03	0.1	0.1	0.52	0.1
70	7.4	60.7	8.5	7.5	62.5	8.4
	—	—	—	7.7	60.0	8.9
	7.2	60.3	8.3	7.6	61.8	8.7
Mean	7.3	60.5	8.4	7.6	61.4	8.6
Std. Dev.	0.1	0.19	0.1	0.1	1.06	0.2
Std. Err.	0.1	0.13	0.1	0.0	0.61	0.1
76	4.4	64.8	4.9	4.4	66.8	4.8
	—	—	—	4.6	64.4	5.1
	4.3	64.1	4.8	4.5	66.4	4.9
Mean	4.4	64.4	4.8	4.5	65.9	4.9
Std. Dev.	0.0	0.34	0.0	0.1	1.04	0.1
Std. Err.	0.0	0.24	0.0	0.0	0.60	0.1
82	2.7	68.6	2.9	2.6	70.8	2.7
	—	—	—	—	—	—
	2.6	67.6	2.8	2.6	70.4	2.8
Mean	2.6	68.1	2.8	2.6	70.6	2.8
Std. Dev.	0.0	0.48	0.0	0.0	0.24	0.0
Std. Err.	0.0	0.34	0.0	0.0	0.17	0.0
88	1.6	71.8	1.7	1.6	74.1	1.6
	—	—	—	—	—	—
	1.6	70.6	1.7	1.6	73.6	1.7
Mean	1.6	71.2	1.7	1.6	73.8	1.6
Std. Dev.	0.0	0.62	0.0	0.0	0.22	0.0
Std. Err.	0.0	0.44	0.0	0.0	0.15	0.0

Table A.10: High Temperature Test Results (RTFO-Aged) for IMP-111

Test Temp. (°C)	Concentric Cylinder			25 mm Parallel Plate with 3 mm Gap		
	G* (kPa)	Phase Angle (degrees)	G*/sin(δ) (kPa)	G* (kPa)	Phase Angle (degrees)	G*/sin(δ) (kPa)
64	23.0	58.5	26.9	21.3	57.9	25.2
	23.8	58.0	28.1	21.4	57.7	25.3
	23.5	58.0	27.7	21.2	59.0	24.8
Mean	23.4	58.2	27.6	21.3	58.2	25.1
Std. Dev.	0.4	0.23	0.5	0.1	0.59	0.2
Std. Err.	0.2	0.13	0.3	0.0	0.34	0.1
70	13.5	60.4	15.5	12.3	59.7	14.2
	13.6	60.0	15.7	12.4	59.7	14.4
	13.8	60.0	15.9	12.2	61.0	13.9
Mean	13.6	60.1	15.7	12.3	60.1	14.2
Std. Dev.	0.1	0.19	0.2	0.1	0.61	0.2
Std. Err.	0.1	0.11	0.1	0.1	0.35	0.1
76	7.7	63.2	8.6	7.2	62.7	8.0
	7.8	62.9	8.8	7.3	62.6	8.2
	7.9	62.5	8.9	7.0	64.0	7.7
Mean	7.8	62.9	8.8	7.1	63.1	8.0
Std. Dev.	0.1	0.27	0.1	0.1	0.65	0.2
Std. Err.	0.0	0.16	0.1	0.1	0.38	0.1
82	4.5	66.5	4.9	4.2	66.2	4.6
	4.5	66.2	4.9	4.3	66.1	4.7
	4.6	65.6	5.0	4.0	67.6	4.3
Mean	4.5	66.1	4.9	4.2	66.6	4.5
Std. Dev.	0.0	0.39	0.1	0.1	0.66	0.2
Std. Err.	0.0	0.22	0.0	0.1	0.38	0.1
88	2.6	70.0	2.8	2.4	69.9	2.6
	2.6	69.7	2.8	2.5	69.7	2.7
	2.7	69.0	2.9	—	—	—
Mean	2.6	69.6	2.8	2.5	69.8	2.6
Std. Dev.	0.0	0.38	0.1	0.0	0.11	0.1
Std. Err.	0.0	0.22	0.0	0.0	0.08	0.0
94	1.5	73.2	1.6	1.4	73.1	1.5
	1.6	73.0	1.6	1.5	72.9	1.6
	1.6	72.5	1.7	—	—	—
Mean	1.6	72.9	1.6	1.5	73.0	1.5
Std. Dev.	0.0	0.33	0.0	0.0	0.09	0.0
Std. Err.	0.0	0.19	0.0	0.0	0.06	0.0

Table A.11: Intermediate Temperature Test Results for BUT-162

Test Temp. (°C)	Concentric Cylinder			25 mm Parallel Plate with 3 mm Gap		
	G* (kPa)	Phase Angle (degrees)	G* \times sin(δ) (kPa)	G* (kPa)	Phase Angle (degrees)	G* \times sin(δ) (kPa)
25	3,873	33	2,135	3,374	37	2,018
	3,509	34	1,950	2863	37	1,716
	—	—	—	—	—	—
Mean	3,691	34	2,042	3,118	37	1,867
Std. Dev.	182	0.16	92	255	0.05	151
Std. Err.	105	0.09	53	147	0.05	87
22	5,416	32	2,884	4,733	35	2,747
	4,968	32	2,665	4,097	35	2,376
	—	—	—	—	—	—
Mean	5,192	32	2,774	4,415	35	2,561
Std. Dev.	224	0.13	109	318	0.01	185
Std. Err.	129	0.08	63	183	0.01	107
19	7,251	31	3,762	6,526	34	3,676
	6,661	32	3,486	5,680	34	3,193
	—	—	—	—	—	—
Mean	6,956	31	3,624	6,103	34	3,435
Std. Dev.	295	0.15	138	423	0.04	242
Std. Err.	209	0.11	98	299	0.03	171
16	9,775	30	4,895	8,912	33	4,873
	8,892	31	4,528	7,801	33	4,248
	—	—	—	—	—	—
Mean	9,333	30	4,712	8,356	33	4,560
Std. Dev.	442	0.28	183	555	0.08	312
Std. Err.	312	0.20	130	393	0.05	221
13	13,072	29	6,317	12,118	32	6,425
	12,073	29	5,902	10,622	32	5,601
	—	—	—	—	—	—
Mean	12,573	29	6,110	11,370	32	6,013
Std. Dev.	500	0.19	207	748	0.10	412
Std. Err.	289	0.11	120	432	0.06	238

Table A.12: Intermediate Temperature Test Results for MER-33

Test Temp. (°C)	Concentric Cylinder			25 mm Parallel Plate with 3 mm Gap		
	G* (kPa)	Phase Angle (degrees)	G* \times sin(δ) (kPa)	G* (kPa)	Phase Angle (degrees)	G* \times sin(δ) (kPa)
25	3,901	49	2,964	3,456	49	2,626
	3,648	49	2,761	3,138	51	2,437
	4,274	49	3,205	—	—	—
Mean	3,941	49	2,977	3,297	50	2,531
Std. Dev.	257	0.36	181	159	0.74	95
Std. Err.	149	0.21	105	112	0.53	67
22	6,337	46	4,547	5,337	47	3,898
	5,883	46	4,230	4,878	48	3,641
	6,754	45	4,805	—	—	—
Mean	6,325	46	4,528	5,108	48	3,770
Std. Dev.	356	0.27	235	229	0.68	128
Std. Err.	205	0.15	136	162	0.48	91
19	9,672	43	6,544	8,047	44	5,619
	8,764	43	6,003	7,381	46	5,268
	10,142	42	6,834	—	—	—
Mean	95,26	43	6,460	7,714	45	5,444
Std. Dev.	572	0.37	344	333	0.63	176
Std. Err.	330	0.21	199	236	0.44	124

Table A.13: Intermediate Temperature Test Results for LAK-20

Test Temp. (°C)	Concentric Cylinder			25 mm Parallel Plate with 3 mm Gap		
	G* (kPa)	Phase Angle (degrees)	G* \times sin(δ) (kPa)	G* (kPa)	Phase Angle (degrees)	G* \times sin(δ) (kPa)
25	3,471	36	2,033	—	—	—
	3,351	36	1,963	2,450	39	1,525
	3,562	36	2,097	2,844	38	1,752
Mean	3,461	36	2,031	2,647	38	1,639
Std. Dev.	87	0.10	55	197	0.23	114
Std. Err.	50	0.06	32	139	0.16	80
22	5,038	34	2,822	—	—	—
	4,836	34	2,712	3,588	37	2,151
	5,139	34	2,904	4,067	37	2,423
Mean	5,005	34	2,812	3,828	37	2,287
Std. Dev.	126	0.16	79	239	0.13	136
Std. Err.	73	0.09	46	169	0.09	96
19	6,829	33	3,712	—	—	—
	6,547	33	3,567	5,030	35	2,912
	6,988	33	3,842	5,663	35	3,267
Mean	6,788	33	3,707	5,347	35	3,089
Std. Dev.	183	0.18	112	317	0.07	178
Std. Err.	105	0.11	65	224	0.05	126
16	9,279	32	4,860	—	—	—
	8,832	32	4,672	6,987	34	3,903
	9,551	32	5,068	7,822	34	4,367
Mean	9,221	32	4,867	7,405	34	4,135
Std. Dev.	297	0.20	162	418	0.01	232
Std. Err.	171	0.11	93	295	0.01	164
13	12,599	30	6,360	—	—	—
	12,102	30	6,129	9,590	33	5,165
	—	—	—	10,713	33	5,784
Mean	12,351	30	6,244	10,152	33	5,475
Std. Dev.	249	0.06	116	561	0.04	309
Std. Err.	176	0.04	82	397	0.03	219

Table A.14: Intermediate Temperature Test Results for INY-395

Test Temp. (°C)	Concentric Cylinder			25 mm Parallel Plate with 3 mm Gap		
	G* (kPa)	Phase Angle (degrees)	G* \times sin(δ) (kPa)	G* (kPa)	Phase Angle (degrees)	G* \times sin(δ) (kPa)
25	3,574	51	2,795	—	—	—
	3,286	51	2,553	3,395	53	2,703
	3,291	51	2,565	2,826	53	2,253
Mean	3,383	51	2,637	3,110	53	2,478
Std. Dev.	135	0.09	111	285	0.05	225
Std. Err.	79	0.11	64	201	0.04	159
22	5,740	48	4,289	—	—	—
	5,362	48	3,974	5,217	50	4,008
	5,367	48	3,989	4,516	50	3,468
Mean	5,489	48.1	4,084	4,867	50.2	3,738
Std. Dev.	177	0.22	145	351	0.02	270
Std. Err.	102	0.12	84	248	0.01	191
19	8,744	45	6,226	—	—	—
	8,150	45	5,778	7,888	47,	5,807
	8,202	45	5,815	7,010	47,	5,152
Mean	8,365	45	5,940	7,449	47,	5,479
Std. Dev.	269	0.11	203	439	0.05	328
Std. Err.	155	0.07	117	310	0.04	232

Table A.15: Intermediate Temperature Test Results for IMP-111

Test Temp. (°C)	Concentric Cylinder			25 mm Parallel Plate with 3 mm Gap		
	G* (kPa)	Phase Angle (degrees)	G* \times sin(δ) (kPa)	G* (kPa)	Phase Angle (degrees)	G* \times sin(δ) (kPa)
25	5,290	39	3,297	4,819	41	3,130
	5,139	39	3,209	—	—	—
	5,070	39	3,176	4,980	40	3,215
Mean	5,166	39	3,227	4,900	40	3,173
Std. Dev.	92	0.10	51	81	0.15	43
Std. Err.	53	0.06	30	57	0.10	30
22	7,660	37	4,573	7,072	38	4,383
	7,474	37	4,466	—	—	—
	7,362	37	4,421	7,187	38	4,448
Mean	7,499	37	4,487	7,129	38	4,415
Std. Dev.	123	0.11	64	57	0.03	32
Std. Err.	71	0.06	37	41	0.02	23
19	10,885	35	6,183	10,062	36	5,952
	10,601	35	6,028	—	—	—
	10,454	35	5,987	10,115	36	6,002
Mean	10,646	35	6,066	10,088	36	5,977
Std. Dev.	179	0.14	84	27	0.06	25
Std. Err.	103	0.08	49	19	0.05	18

Table A.16: Low-Temperature Test Results (PAV-Aged)

Test Temp. (°C)	BUT-162		MER-33		LAK-20		INY-395		IMP-111	
	S (MPa)	m-Value	S (MPa)	m-Value	S (MPa)	m-Value	S (MPa)	m-Value	S (MPa)	m-Value
-12	38.5	0.315	136	0.318	47.1	0.326	97.1	0.360	78.6	0.33
	37.5	0.319	134	0.319	49.3	0.319	109.0	0.365	—	—
	35.5	0.317	—	—	—	—	—	—	79.7	0.34
Mean	37.2	0.317	135	0.319	48.2	0.323	103.1	0.363	79.2	0.34
Std. Dev.	1.3	0.002	1.0	0.001	1.1	0.004	6.0	0.003	0.6	0.00
Std. Err.	0.7	0.001	0.7	0.000	0.8	0.002	4.2	0.002	0.4	0.00
-18	85.7	0.307	283	0.259	—	—	—	—	—	—
	78.8	0.298	265	0.263	—	—	—	—	—	—
	—	—	—	—	—	—	—	—	—	—
Mean	82.3	0.303	274	0.261	—	—	—	—	—	—
Std. Dev.	3.5	0.005	9.0	0.002	—	—	—	—	—	—
Std. Err.	2.4	0.003	6.4	0.001	—	—	—	—	—	—
-24	192	0.275	432	0.221	—	—	402	0.241	—	—
	180	0.268	396	0.220	—	—	404	0.239	—	—
	197	0.269	—	—	—	—	373	0.248	—	—
Mean	189.7	0.271	414	0.221	—	—	393	0.243	—	—
Std. Dev.	7.1	0.003	18.0	0.001	—	—	14.2	0.004	—	—
Std. Err.	4.1	0.000	12.7	0.000	—	—	8.2	0.002	—	—
-30	—	—	—	—	274	0.242	—	—	494	0.206
	—	—	—	—	308	0.247	—	—	555	0.210
	—	—	—	—	400	0.242	—	—	—	—
Mean	—	—	—	—	327	0.244	—	—	525	0.208
Std. Dev.	—	—	—	—	53.0	0.002	—	—	30.5	0.002
Std. Err.	—	—	—	—	31.0	0.001	—	—	21.6	0.001

Table A.17: Multiple Stress Creep Recovery Test Results (64°C)

Geometry	Binder Source	0.1 kPa			3.2 kPa			Percent Difference		
		Rep. 1	Rep. 2	Average	Rep. 1	Rep. 2	Average	Rep. 1	Rep. 2	Average
		Average Percent Recovery (Apr)								
Concentric Cylinder	BUT-162	94.2	—	94.2	91.3	92.1	91.7	1.4	—	1.4
	MER-33	84.8	100.4	92.6	52.4	38.7	45.6	38.2	61.4	50
	LAK-20	98.4	77.7	88.0	82.1	84.1	83.1	16.6	-8.3	4.1
	INY-395	71.7	48.2	60.0	51.3	46.4	48.9	28.5	3.7	16
	IMP-111	87.1	87.7	87.4	74.4	75.6	75.0	14.7	13.8	14
Parallel Plate	BUT-162	95.4	95.7	95.5	92.1	92.9	92.7	3.4	3.0	3.2
	MER-33	86.7	85.6	86.3	52.4	51.7	52.6	39.6	39.7	40
	LAK-20	94.6	94.0	94.3	86.0	85.8	86.0	9.1	8.8	8.9
	INY-395	87.3	84.7	85.7	41.7	42.4	42.0	50.5	52.2	51
	IMP-111	88.5	88.7	88.6	71.3	69.4	70.4	19.5	21.7	21
Non-Recoverable Creep Compliance (Jnr) (kPa)										
Concentric Cylinder	BUT-162	0.003	—	0.003	0.006	0.004	0.005	43.4	—	43
	MER-33	0.007	—	0.006	0.183	0.213	0.198	—	—	—
	LAK-20	0.004	0.007	0.006	0.021	0.019	0.020	—	168	168
	INY-395	0.105	0.174	0.140	0.226	0.314	0.270	114.3	41.7	78
	IMP-111	0.023	0.020	0.022	0.048	0.044	0.046	107	122	115
Parallel Plate	BUT-162	0.003	0.002	0.002	0.004	0.004	0.004	74.0	70.0	72
	MER-33	0.041	0.042	0.041	0.174	0.164	0.017	330	293	312
	LAK-20	0.005	0.007	0.006	0.013	0.016	0.015	171	143	157
	INY-395	0.057	0.044	0.051	0.271	0.262	0.267	377	374	376
	IMP-111	0.018	0.017	0.018	0.050	0.051	0.051	174	198	186

APPENDIX B: MIX TEST RESULTS

Mix test results are summarized in the following tables:

- Table B.1: Air-Void Contents of Gyrotory-Compacted AMPT Specimens
- Table B.2: Air-Void Contents of Gyrotory-Compacted SCB Specimens
- Table B.3: Air-Void Contents of Rolling Wheel-Compacted Beam Specimens
- Table B.4: Dynamic Modulus Test Results
- Table B.5: Phase Angle Test Results for Dynamic Modulus
- Table B.6: Flexural Modulus Test Results at 10°C
- Table B.7: Flexural Modulus Test Results at 20°C
- Table B.8: Flexural Modulus Test Results at 30°C
- Table B.9: Repeated Load Triaxial Test Results
- Table B.10: Semicircular Bend Test Results

Table B.1: Air-Void Contents of Gyrotory-Compacted AMPT Specimens

Specimen Number	Air-Void Content (%)				
	BUT-162	MER-33	LAK-20	INY-395	IMP-111
1	6.8	6.7	7.3	8.0	6.7
2	7.2	6.7	6.6	6.1	6.6
3	7.0	7.1	6.5	6.4	7.2
4	7.5	6.9	7.1	6.6	6.9
5	6.6	6.8	6.6	7.6	6.7
Mean	7.0	6.8	6.8	6.9	6.8
Std. Deviation	0.31	0.15	0.32	0.73	0.21
Std. Error	0.14	0.07	0.14	0.33	0.10

Table B.2: Air-Void Contents of Gyrotory-Compacted SCB Specimens

Specimen Number	Air-Void Content (%)				
	BUT-162	MER-33	LAK-20	INY-395	IMP-111
1	6.6	7.0	6.4	8	6.7
2	6.6	7.0	6.4	8	6.7
3	6.0	6.6	6.3	8	6.1
4	6.0	6.6	6.3	6.3	6.3
5	6.0	7.2	6.6	7.8	6.1
6	6.0	7.2	6.6	7.8	6.7
Mean	6.2	6.9	6.4	7.7	6.4
Std. Deviation	0.28	0.25	0.12	0.61	0.27
Std. Error	0.11	0.09	0.05	0.23	0.11

Table B.3: Air-Void Contents of Rolling Wheel-Compacted Beam Specimens

Specimen Number	Air-Void Content (%)				
	BUT-162	MER-33	LAK-20	INY-395	IMP-111
1	6.8	7.2	6.0	6.8	6.6
2	7.4	6.7	7.4	6.9	7.3
3	7.0	7.6	6.4	7.3	6.6
4	6.9	6.3	6.8	6.8	6.6
5	7.2	7.5	6.4	7.1	7.0
6	6.7	7.4	6.2	6.8	7.3
7	7.2	7.6	6.3	6.7	7.4
8	7.1	7.3	6.3	7.2	6.5
9	6.7	7.1	6.7	7.0	6.9
10	7.4	7.4	7.0	7.3	7.5
11	7.4	7.0	7.0	7.0	6.7
12	7.1	7.2	6.5	7.2	7.5
Mean	7.1	7.2	6.6	7.0	7.0
Std. Deviation	0.23	0.37	0.38	0.21	0.38
Std. Error	0.06	0.11	0.11	0.05	0.10

Table B.4: Dynamic Modulus Test Results

Mix	Specimen ID	Dynamic Modulus (MPa)								
		Temperature (°C)								
		4			20			45		
		Frequency (Hz)								
		0.1	1	10	0.1	1	10	0.1	1	10
BUT-162	21	5,257	7,261	9,469	1,758	2,906	4,544	215	437	911
	25	3,821	5,388	7,251	1,472	2,472	3,881	214	457	948
	28	4,767	6,732	8,987	1,714	2,892	4,583	283	600	1,207
	32	4,175	5,848	7,850	1,546	2,577	4,057	253	503	1,009
	36	5,095	7,259	9,784	1,845	3,148	5,005	261	561	1,182
Mean		4,623	6,498	8,668	1,667	2,799	4,414	245	512	1,051
Std. Dev		546	758	966	138	244	402	27	61	121
Std. Err		315	437	558	80	141	232	16	35	70
MER-33	04	5,376	7,605	9,843	1,320	2,730	4,780	75	269	840
	08	4,561	6,816	9,152	952	2,113	3,965	87	320	952
	12	4,865	6,995	9,100	1,097	2,341	4,247	49	206	703
	17	5,417	7,866	10,344	1,250	2,688	4,928	90	312	931
	18	4,665	6,719	8,868	1,093	2,286	4,087	106	371	1,050
Mean		4,977	7,200	9,461	1,142	2,432	4,401	81	296	895
Std. Dev		357	454	548	130	239	383	19	55	117
Std. Err		206	262	317	75	138	221	11	32	68
LAK-20	06	4,139	5,598	7,172	1,465	2,462	3,808	269	594	1,206
	07	4,670	6,376	8,294	1,802	2,946	4,516	383	827	1,617
	13	4,910	6,617	8,471	2,192	3,539	5,358	525	1,046	1,949
	16	4,469	6,161	7,992	1,492	2,554	4,055	270	589	1,210
	17	3,716	5,242	6,967	1,373	2,390	3,878	257	568	1,150
Mean		4,381	5,999	7,779	1,665	2,778	4,323	341	725	1,426
Std. Dev		418	507	603	301	426	573	103	186	310
Std. Err		241	293	348	174	246	331	59	108	179
INY-395	07	6,300	8,843	11,500	1,629	3,175	5,365	130	361	985
	16	4,460	6,754	9,247	932	2,133	4,038	42	138	472
	25	4,066	6,516	9,359	928	2,180	4,245	42	158	538
	30	3,438	5,542	8,017	561	1,433	2,975	29	122	454
Mean		4,566	6,914	9,531	1,013	2,230	4,155	61	195	612
Std. Dev		1,065	1,203	1,253	387	620	848	40	97	217
Std. Err		615	695	723	223	358	490	23	56	125
IMP-111	11	6,559	8,559	10,582	2,261	3,730	5,650	241	594	1,349
	19	5,828	7,733	9,711	2,060	3,463	5,290	279	681	1,470
	22	6,231	8,190	10,222	2,409	3,865	5,752	346	799	1,645
	23	6,577	8,596	10,713	2,433	3,891	5,785	394	869	1,749
	27	6,351	8,331	10,353	2,211	3,638	5,518	314	752	1,607
Mean		6,309	8,282	10,316	2,275	3,717	5,599	315	739	1,564
Std. Dev		273	312	348	137	157	180	53	95	140
Std. Err		158	180	201	79	91	104	30	55	81

Table B.5: Phase Angle Test Results for Dynamic Modulus

Mix	Specimen ID	Phase Angle (δ) (Degrees)								
		Temperature ($^{\circ}$ C)								
		4			20			45		
		Frequency (Hz)								
		0.1	1	10	0.1	1	10	0.1	1	10
BUT-162	21	14.4	11.9	9.9	23.1	20.4	17.3	30.5	30.9	30.1
	25	15.7	13.1	23.3	20.2	17.5	30.1	30.9	30.6	29.0
	28	16.4	13.3	10.9	24.4	21.4	18.4	30.9	30.8	29.4
	32	16.4	13.6	11.3	23.8	21.0	18.2	29.3	29.8	29.0
	36	16.9	13.8	11.2	24.9	21.7	18.5	31.0	31.2	30.0
Mean		16.0	13.1	13.3	23.3	20.4	20.5	30.5	30.7	29.5
Std. Dev		0.9	0.7	5.0	1.7	1.5	4.8	0.6	0.5	0.5
Std. Err		0.5	0.4	2.9	1.0	0.9	2.8	0.4	0.3	0.3
MER-33	04	16.9	12.2	9.1	34.6	27.1	20.0	41.4	41.2	40.0
	08	19.5	14.0	10.3	37.8	30.3	22.5	40.5	39.9	38.0
	12	18.0	12.9	9.5	35.5	28.6	21.4	45.2	44.9	42.6
	17	18.4	13.0	9.5	35.9	28.6	21.5	40.6	41.9	39.3
	18	18.0	13.0	9.6	35.0	28.1	21.2	39.0	39.0	36.5
Mean		18.2	13.0	9.6	35.8	28.5	21.3	41.3	41.4	39.3
Std. Dev		0.8	0.6	0.4	1.1	1.0	0.8	2.1	2.0	2.0
Std. Err		0.5	0.3	0.2	0.6	0.6	0.5	1.2	1.2	1.2
LAK-20	06	14.3	11.4	9.2	24.4	20.4	16.6	33.1	31.6	28.5
	07	15.0	12.1	9.9	24.7	20.5	16.7	33.1	30.6	27.1
	13	13.9	11.2	9.2	23.2	19.8	16.5	30.1	28.5	26.2
	16	15.5	12.2	9.9	25.3	21.7	17.9	32.9	31.7	29.1
	17	16.4	13.1	10.6	25.9	22.4	18.9	31.6	30.3	28.4
Mean		15.0	12.0	9.7	24.7	21.0	17.3	32.2	30.6	27.9
Std. Dev		0.9	0.7	0.5	0.9	1.0	0.9	1.2	1.2	1.1
Std. Err		0.5	0.4	0.3	0.5	0.5	0.5	0.7	0.7	0.6
INY-395	07	16.2	12.2	9.3	31.3	25.2	19.5	38.0	40.1	38.4
	16	20.6	15.1	11.2	36.6	30.3	23.4	41.3	43.0	43.0
	25	23.3	17.0	12.4	38.3	31.0	23.6	45.6	44.2	43.1
	30	23.8	17.5	12.7	42.0	35.1	26.9	48.2	46.4	45.3
Mean		21.0	15.5	11.4	37.1	30.4	23.3	43.3	43.4	42.4
Std. Dev		3.0	2.1	1.3	3.9	3.5	2.6	3.9	2.3	2.5
Std. Err		1.7	1.2	0.8	2.2	2.0	1.5	2.3	1.3	1.5
IMP-111	11	13.1	10.5	8.4	24.8	20.1	15.9	36.4	35.2	31.7
	19	13.8	10.7	8.5	25.3	20.4	16.1	35.2	33.4	29.9
	22	13.0	10.3	8.3	23.3	18.9	15.1	31.9	30.4	27.7
	23	12.8	10.1	8.1	23.3	19.0	15.0	32.6	31.5	28.3
	27	13.0	10.1	8.1	24.3	19.7	15.6	35.0	33.3	29.5
Mean		13.1	10.3	8.3	24.2	19.6	15.5	34.2	32.7	29.4
Std. Dev		0.3	0.2	0.2	0.8	0.6	0.4	1.7	1.7	1.4
Std. Err		0.2	0.1	0.1	0.5	0.3	0.2	1.0	1.0	0.8

Table B.6: Flexural Modulus Test Results at 10°C

Mix	Specimen ID	Flexural Modulus (E*) (MPa) at 10°C										
		Frequency (Hz)										
		0.01	0.02	0.05	0.1	0.2	0.5	1	2	5	10	15
BUT-162	1	1,102	1,293	1,584	1,877	2,270	2,775	3,209	3,653	4,309	4,829	5,105
	2	1,230	1,447	1,803	2,123	2,625	3,203	3,679	4,200	4,936	5,515	5,832
	3	1,340	1,564	1,898	2,287	2,665	3,198	3,620	4,138	4,790	5,338	5,615
	Mean	1,224	1,435	1,762	2,096	2,520	3,058	3,502	3,997	4,678	5,227	5,518
Std. Dev	97	111	131	169	177	201	209	245	268	291	305	
Std. Err	56	64	76	97	102	116	121	141	155	168	176	
MER-33	1	1,020	1,318	1,812	2,267	2,888	3,656	4,272	4,927	5,795	6,413	6,791
	2	1,324	1,674	2,255	2,787	3,524	4,377	5,070	5,769	6,678	7,358	7,693
	3	1,162	1,523	2,063	2,553	3,252	4,061	4,689	5,365	6,231	6,791	7,164
	Mean	1,169	1,505	2,044	2,535	3,221	4,031	4,677	5,354	6,235	6,854	7,216
Std. Dev	124	146	182	213	261	295	326	344	360	388	370	
Std. Err	72	84	105	123	151	170	188	199	208	224	213	
LAK-20	1	1,384	1,614	1,949	2,236	2,719	3,227	3,623	4,088	4,667	5,131	5,371
	2	1,320	1,580	1,892	2,204	2,625	3,136	3,544	3,994	4,588	5,014	5,275
	3	1,623	1,878	2,281	2,623	3,095	3,681	4,127	4,621	5,317	5,823	6,117
	Mean	1,442	1,691	2,041	2,354	2,813	3,348	3,765	4,234	4,857	5,323	5,587
Std. Dev	130	133	171	190	203	239	258	276	327	357	376	
Std. Err	75	77	99	110	117	138	149	160	189	206	217	
INY-395	1	682	912	1,306	1,762	2,215	2,900	3,464	4,072	4,873	5,484	5,851
	2	607	796	1,148	1,483	2,012	2,660	3,186	3,771	4,577	5,183	5,498
	3	643	844	1,224	1,572	2,127	2,764	3,311	3,865	4,647	5,200	5,534
	Mean	644	851	1,226	1,606	2,118	2,775	3,320	3,903	4,699	5,289	5,628
Std. Dev	31	48	64	117	83	98	114	126	126	138	159	
Std. Err	18	28	37	67	48	57	66	73	73	79	92	
IMP-111	1	1,721	2,000	2,408	2,790	3,283	3,857	4,300	4,777	5,407	5,910	6,148
	2	1,496	1,743	2,105	2,430	2,862	3,371	3,775	4,203	4,749	5,155	5,396
	3	1,841	2,155	2,625	3,048	3,569	4,181	4,680	5,179	5,842	6,344	6,601
	Mean	1,686	1,966	2,379	2,756	3,238	3,803	4,251	4,720	5,333	5,803	6,048
Std. Dev	143	170	213	253	290	333	371	400	449	491	497	
Std. Err	83	98	123	146	168	192	214	231	259	284	287	

Table B.7: Flexural Modulus Test Results at 20°C

Mix	Specimen ID	Flexural Modulus (E*) (MPa) at 20°C										
		Frequency (Hz)										
		0.01	0.02	0.05	0.1	0.2	0.5	1	2	5	10	15
BUT-162	1	398	473	612	762	958	1,234	1,491	1,786	2,224	2,597	2,804
	2	417	518	671	836	1,085	1,401	1,693	2,042	2,576	3,003	3,273
	3	471	577	716	896	1,124	1,440	1,720	2,052	2,539	2,930	3,162
Mean		429	523	666	832	1,056	1,358	1,635	1,960	2,446	2,844	3,079
Std. Dev		31	43	42	55	71	90	102	123	158	177	200
Std. Err		18	25	25	32	41	52	59	71	91	102	116
MER-33	1	227	319	505	683	969	1,394	1,798	2,274	3,004	3,600	3,908
	2	294	402	613	834	1,197	1,719	2,206	2,767	3,580	4,193	4,609
	3	253	340	548	744	1,073	1,568	2,022	2,546	3,344	3,917	4,325
Mean		258	354	555	754	1,080	1,560	2,009	2,529	3,309	3,903	4,281
Std. Dev		28	35	44	62	93	133	167	202	237	242	288
Std. Err		16	20	26	36	54	77	96	116	137	140	166
LAK-20	1	517	631	812	988	1,230	1,572	1,862	2,194	2,673	3,089	3,284
	2	548	571	714	1,011	1,019	1,526	1,691	1,953	2,566	3,185	3,089
	3	632	749	957	1,157	1,474	1,858	2,194	2,582	3,153	3,554	3,844
Mean		566	650	828	1,052	1,241	1,652	1,916	2,243	2,797	3,276	3,406
Std. Dev		49	74	100	75	186	147	209	259	255	200	320
Std. Err		28	43	58	43	107	85	121	150	147	116	185
INY-395	1	137	185	303	407	610	915	1,224	1,597	2,190	2,693	2,984
	2	107	172	275	366	535	806	1,112	1,460	2,025	2,523	2,797
	3	114	162	264	363	558	837	1,127	1,464	2,003	2,448	2,728
Mean		120	173	281	379	568	853	1,154	1,507	2,073	2,555	2,836
Std. Dev		13	9	16	20	31	46	50	64	83	103	108
Std. Err		7	5	9	11	18	26	29	37	48	59	63
IMP-111	1	570	714	943	1,227	1,478	1,890	2,232	2,642	3,183	3,619	3,851
	2	501	619	822	1,024	1,298	1,670	1,968	2,322	2,801	3,162	3,401
	3	632	789	1,031	1,332	1,621	2,050	2,432	2,830	3,432	3,877	4,108
Mean		568	707	932	1,195	1,466	1,870	2,211	2,598	3,139	3,553	3,787
Std. Dev		54	69	86	128	132	156	190	209	259	296	292
Std. Err		31	40	50	74	76	90	110	121	150	171	169

Table B.8: Flexural Modulus Test Results at 30°C

Mix	Specimen ID	Flexural Modulus (E*) (MPa) at 30°C										
		Frequency (Hz)										
		0.01	0.02	0.05	0.1	0.2	0.5	1	2	5	10	15
BUT-162	1	131	155	214	255	338	458	580	714	951	1,144	1,242
	2	135	175	247	284	381	522	664	820	1,083	1,324	1,454
	3	147	180	264	313	405	540	674	829	1,102	1,313	1,427
	Mean	138	170	242	284	375	507	639	788	1,045	1,261	1,374
Std. Dev	7	11	21	24	28	35	42	52	67	82	94	
Std. Err	4	6	12	14	16	20	24	30	39	48	55	
MER-33	1	-	-	107	147	215	340	480	667	1,000	1,298	1,525
	2	45	86	128	179	265	413	582	809	1,214	1,570	1,831
	3	26	52	102	138	204	347	496	710	1,091	1,404	1,663
	Mean	35	69	112	155	228	367	519	729	1,102	1,424	1,673
Std. Dev	10	17	11	18	27	33	45	59	88	112	125	
Std. Err	6	10	6	10	15	19	26	34	51	65	72	
LAK-20	1	156	202	277	354	458	612	757	937	1,213	1,456	1,587
	2	147	189	260	335	441	589	731	904	1,181	1,408	1,540
	3	176	222	308	385	501	667	823	1,025	1,323	1,601	1,750
	Mean	160	204	282	358	467	622	770	955	1,239	1,488	1,626
Std. Dev	12	13	20	21	26	33	39	51	61	82	90	
Std. Err	7	8	11	12	15	19	22	29	35	47	52	
INY-395	1	80	40	71	86	122	196	277	401	636	851	994
	2	38	96	67	82	118	189	268	386	601	805	950
	3	27	33	47	69	94	150	218	320	513	672	789
	Mean	48	56	61	79	112	178	255	369	583	776	911
Std. Dev	23	28	11	7	12	20	26	35	52	76	88	
Std. Err	13	16	6	4	7	12	15	20	30	44	51	
IMP-111	1	145	187	259	364	487	675	864	1,080	1,420	1,692	1,862
	2	137	181	250	333	429	587	750	936	1,226	1,455	1,582
	3	148	209	314	390	533	754	955	1,208	1,589	1,914	2,095
	Mean	143	192	274	363	483	672	856	1,075	1,412	1,687	1,846
Std. Dev	5	12	28	23	43	68	84	111	149	188	210	
Std. Err	3	7	16	13	25	39	48	64	86	108	121	

Table B.9: Repeated Load Triaxial Test Results

Mix	Specimen ID	Flow Number (Cycles)	μ strain at Flow Point	Cycles at 1% PAS	Cycles at 3% PAS	Cycles at 5% PAS
BUT-162	21	1,060	21,627	135	1,879	2,963
	25	718	29,200	46	766	1,681
	28	680	30,988	41	641	1,288
	32	817	23,943	100	1,160	1,822
	36	524	20,403	90	1,047	1,628
Mean		760	25,232	82	1,099	1,876
Std. Dev		177	4,168	35	433	571
Std. Err		102	2,406	20	250	330
MER-33	4	77	28,561	12	87	155
	8	129	30,313	15	130	253
	12	98	27,938	16	114	216
	17	62	30,685	10	63	123
	18	102	29,127	14	111	219
Mean		94	29,325	13	101	193
Std. Dev		23	1,037	2	23	47
Std. Err		13	598	1	14	27
LAK-20	6	720	27,282	56	878	1,654
	7	1,154	29,387	57	1,212	2,528
	13	843	25,233	85	1,366	2,648
	16	706	30,395	32	689	1,468
	17	502	28,166	32	578	1,135
Mean		785	28,093	52	945	1,887
Std. Dev		215	1,779	20	301	598
Std. Err		124	1,027	11	174	345
INY-395	7	138	24,614	25	195	349
	16	48	31,257	8	48	92
	25	66	23,296	17	98	156
	29	54	22,008	16	86	133
	30	46	23,713	11	69	113
Mean		70	24,978	15	99	169
Std. Dev		35	3,250	6	51	93
Std. Err		20	1,876	3	29	53
IMP-111	11	1,030	16,737	239	2,904	4,143
	19	658	24,707	63	940	1,647
	22	855	20,139	130	1,717	2,708
	23	989	20,728	156	1,770	2,627
	27	1,317	23,144	139	2,049	3,201
Mean		970	21,091	145	1,876	2,865
Std. Dev		217	2,731	56	632	814
Std. Err		125	1,577	33	365	470

Table B.10: Semicircular Bend Test Results

Mix	Specimen ID	Strength (psi)	Slope	Fracture Energy (J/m ²)	Flexibility Index
BUT-162	5T-1	53.7	-1.82	2,202	12.11
	5T-2	56.7	-1.50	2,635	17.57
	6T-1	60.1	-2.33	2,149	9.22
	6T-2	57.5	-2.50	1,951	7.80
	8T-1	61.2	-2.59	2,639	10.19
	8T-2	62.9	-2.33	2,425	10.41
MER-33	1-B2	82.0	-2.95	3,780	12.81
	2-B1	70.4	-2.42	2,830	11.69
	3T-1	58.5	-0.96	3,971	41.36
	3T-2	64.8	-1.77	3,394	19.17
	4B-1	70.8	-1.69	3,789	22.42
	4B-2	58.2	-1.03	3,610	35.05
	5B-1	70.7	-1.90	2,807	14.78
	5B-2	50.0	-1.30	2,513	19.33
LAK-20	3-B1	58.7	-3.12	1,811	5.80
	3-B2	53.9	-2.52	2,032	8.06
	3-T1	61.2	-3.10	2,042	6.59
	3-T2	53.7	-3.05	1,486	4.87
	2-T1	53.2	-3.14	1,384	4.41
	2-T2	60.2	-3.28	1,641	5.00
INY-395	12B-1	44.8	-0.63	3,187	50.58
	12B-2	44.3	-0.98	2,783	28.39
	3B-1	45.3	-0.93	2,264	24.35
	11-B1	33.5	-0.43	2,694	62.66
	11-B2	31.3	-0.41	2,283	55.68
	15-B1	41.4	-0.77	2,693	34.98
	15-B2	37.6	-0.79	2,245	28.41
IMP-111	1-T1	72.2	-3.19	2,930	9.18
	1-T2	65.6	-2.36	2,394	10.14
	2-B1	73.5	-3.19	2,653	8.32
	2-T1	75.3	-3.71	2,099	5.66
	2-T2	66.8	-3.40	1,903	5.60
	3-B1	80.3	-4.12	2,759	6.70